ABSTRACT

Title of Document: RELIABILITY EVALUATION OF LIQUID AND POLYMER ALUMINUM ELECTROLYTIC CAPACITORS

Anshul Shrivastava,
Doctor of Philosophy (Ph.D.), 2014

Directed By: Professor Michael Pecht,
Department of Mechanical Engineering

Liquid aluminum electrolytic capacitors are known for their reliability problems. They are considered as the weakest link in the power electronics system. The liquid electrolyte of these capacitors is the single most important component which affects the reliability of these capacitors. The principal ingredients of the liquid electrolyte are solvent, water, solute and additives such as corrosion inhibitors and hydrogen absorbers. Usually, the primary solvent used in liquid electrolyte of aluminum electrolytic capacitors is ethylene glycol or γ-butyrolactone. The effect of liquid electrolyte solvent on the failure mechanisms observed in liquid aluminum electrolytic capacitors is missing. Effect of ripple current on the observed failure mechanisms is unknown.

Polymer aluminum (PA) capacitors were introduced as the polymer electrolyte is conductive and solid therefore, it does not evaporate and the equivalent series resistance (ESR) of the PA capacitors is low. Manufacturers advise not to use PA

capacitors in elevated temperature-humidity environments. But, the Failure modes and mechanisms of polymer aluminum electrolytic capacitors in elevated temperature-humidity are unknown.

In this study, life testing of liquid aluminum electrolytic capacitors chosen based on primary solvent of the electrolyte was performed. For γ-butyrolactone solvent based capacitors, the failure mechanisms observed causing decrease in capacitance were evaporation of electrolyte and decrease in surface area of the aluminum oxide dielectric layer. The observed ESR increase was due to evaporation of electrolyte. For ethylene glycol solvent based capacitors, ESR increase was observed due to ester and amide formation, along with decrease in concentration of the carboxylic acid salts in the electrolyte and evaporation of electrolyte. The failure mechanisms observed in life tests with and without ripple current were the same.

PA capacitors were tested at elevated temperature-humidity of 85ºC, 85%RH and Highly Accelerated Stress Test (HAST) condition of 110ºC, 85%RH. PA capacitors failed due to increase in ESR and increase in leakage current. Iron particles in dielectric layer from the manufacturing process of PA capacitors caused the high leakage current failure. This is a new failure mechanism which has not been reported in the literature. Failure modes observed in 85ºC, 85%RH and HAST tests were same therefore, HAST tests can be used as rapid assessment test for PA capacitors in elevated temperature-humidity environment.

RELIABILITY EVALUATION OF LIQUID AND POLYMER ALUMINUM ELECTROLYTIC CAPACITORS

By

Anshul Shrivastava

Dissertation submitted to the Faculty of the Graduate School of the
University of Maryland, College Park, in partial fulfillment
of the requirements for the degree of
Doctor of Philosophy
2014

Advisory Committee:
Professor Michael Pecht, Chair
Assistant Research Scientist Michael H. Azarian
Associate Professor Isabel Lloyd
Professor Abhijit Dasgupta
Professor F. Patrick McCluskey

Dedication

Dedicated to, my wife Shweta and son Advik. Thank you, Shweta for supporting me, standing by my side and putting up with my crazy work schedules. You were and are my pillar of strength and it would not have been possible for me to pursue my Ph.D. without you as a constant in my life.

Dedicated to, my parents. Thank you mom and dad for believing in me and constantly encouraging and supporting me in whatever I did. Without your constant support and believe, I could not have come this far.

Acknowledgements

Acknowledgements are in order starting with my advisor Professor Michael Pecht for giving me an opportunity to do my Ph.D. under his guidance. I would like to thank Dr. Michael H. Azarian, my Ph.D. co-advisor for helping me with his technical acumen and constantly giving me new ideas and encouragement.

I would like to thank Prof. Patrick McCluskey, Prof. Isabel Lloyd and Prof. Abhijit Dasgupta for their valuable guidance in the need of time and agreeing to become my dissertation committee members. I would specially like to thank Prof. Lloyd to let me use her thermo-gravimetric analysis (TGA) equipment. I would like to thank Dr. Carlos Morillo for his constant help during my degree. I would also like to thank my first boss Dr. Keith Rogers for his constant support and encouragement during my Ph.D. days.

Thanks are in order for the “Pecht group” faculty and students for their help and invaluable suggestions during the morning meeting presentations. Thanks to the members of our stress buster coffee sessions specially Sony Matthew, Swapnesh, Lakshmi, Ahmed Amin, Nikhil Lakhkar, Ranjith Kumar S.R., Bhanu Sood and many more.

Table of Contents

1: Introduction

1.1 Capacitors

Capacitor is a passive electronic component that consists of a pair of conductors separated by a dielectric material, such as air, vacuum, or any material of suitably high resistivity [1]. Capacitors are widely used in electronic circuits for blocking direct current while allowing alternating current to pass, in filter networks, for smoothing the output of power supplies, in the resonant circuits that tune radios to particular frequencies and for many other purposes.

This high diversity of useful properties makes the capacitor the most widely used electrical device in the electrical industry. They come in a variety of sizes, shapes, materials and types and each type has its advantages and disadvantages in different applications.

1.2 Liquid Aluminum Electrolytic Capacitor

Aluminum electrolytic capacitors which are also called “electrolytics” assume a special position among the various types of capacitors since their principle of operation relies, in part, on electrochemical processes.

The advantages of aluminum electrolytic capacitors that have led to their wide application range are their high volumetric efficiency (i.e. capacitance per unit volume), which enables the production of capacitors with up to one Farad capacitance, and the fact that an aluminum electrolytic capacitor provides a high

ripple current capability together with a high reliability and an excellent price/performance ratio.

An aluminum electrolytic capacitor comprises two electrically conductive material layers that are separated by a dielectric layer. The anode is formed by an aluminum foil with an enlarged surface area. The oxide layer (Al_2O_3) that is electrochemically grown on the anode foil is used as the dielectric layer. In contrast to other capacitors, the cathode of Al electrolytic capacitors is a conductive liquid, the operating electrolyte. A second aluminum foil, serves as a large-surfaced contact area for passing current to the operating electrolyte. In summary, the element is comprised of an anode foil, paper separators saturated with electrolyte and a cathode foil. The foils are high-purity aluminum and are etched with billions of microscopic tunnels to increase the surface area in contact with the electrolyte [2]. Figure 1 below shows the winding construction of Aluminum electrolytic capacitor. The cross-section capacitor element material is shown in Figure 2.

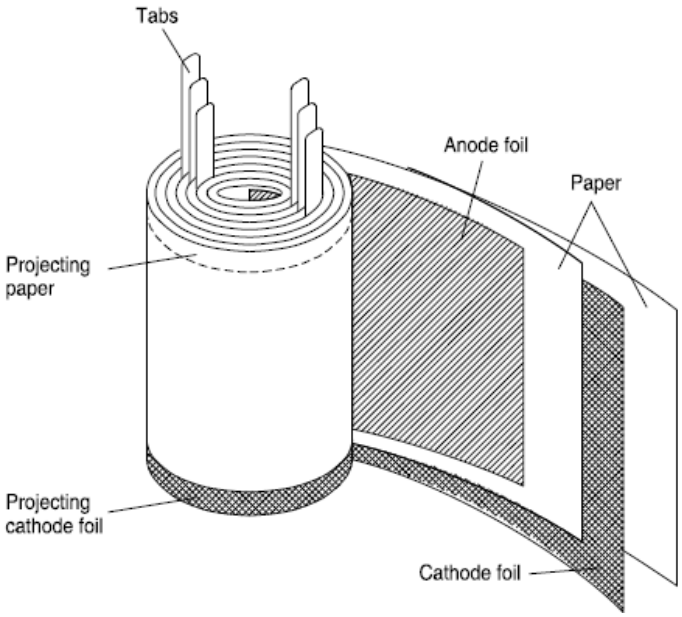

Figure 1: Construction of Al Electrolytic Capacitor [3]

The anode of an Al electrolytic capacitor is an aluminum foil of extreme purity. The effective surface area of this foil is greatly enlarged (by a factor of up to 200) by electrochemical etching in order to achieve the maximum possible capacitance values. The type of etch pattern and the degree of etching is matched to the respective requirements by applying specific etching processes.

Etched foils enable very compact aluminum electrolytic capacitor dimensions to be achieved and are the form used almost exclusively nowadays. The electrical characteristics of aluminum electrolytic capacitors with plain (not etched) foils are, in part, better, but these capacitors are considerably larger and are only used for special applications nowadays.

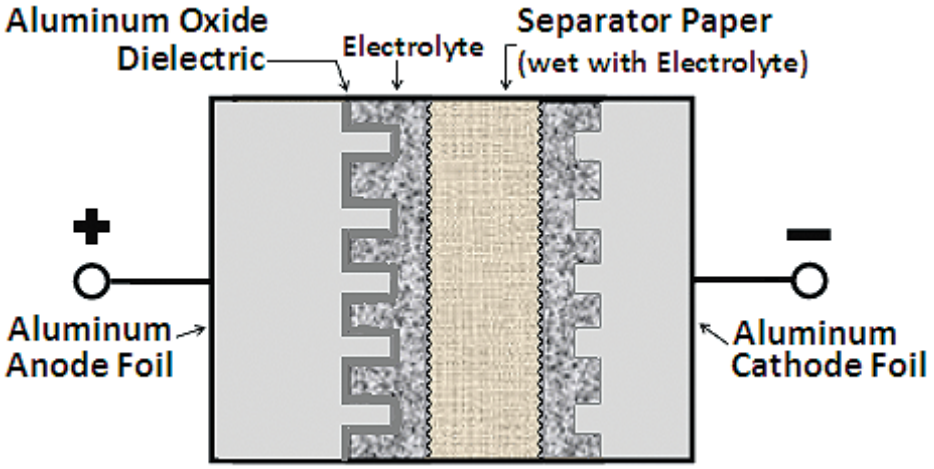

Figure 2: Capacitor Element Materials [2]

1.3 Reliability of Aluminum Electrolytic Capacitors

Liquid aluminum electrolytic capacitor technology is a century old but still there are reliability problems. Liquid aluminum electrolytic capacitors are considered as the weakest link in the power electronics systems. It is known that application of ripple current to liquid aluminum electrolytic capacitors causes a core temperature rise due

to joule heating. Ripple current is known to cause additional reliability problems for the liquid aluminum electrolytic capacitors. Common failure modes for liquid aluminum electrolytic capacitors are short circuit, open circuit and parametric failures. Parametric failures include increase in equivalent series resistance (ESR), decrease in capacitance and increase in leakage current. The failure mechanisms due to application of ripple current are not known. Similar failure modes are observed when liquid aluminum electrolytic capacitors are stressed with ripple current/temperature and DC voltage/temperature stress. But it is not known if the failure mechanism changes with the application of ripple current.

The requirements of a liquid electrolyte used in the capacitors are good ionic conductivity for low ESR, chemical stability at working voltages, working temperature range from lowest to highest rated temperature, optimum pH value, does not react with aluminum foil, tabs, paper separator, rubber seal and vent, low viscosity/surface tension, good wettability to paper separator, low vapor pressure, good anodizing capability and cost effective.

The composition of the liquid electrolyte inside various liquid aluminum electrolytic capacitors is proprietary, and manufacturers usually do not disclose their formulas. Typically, a liquid electrolyte consists of solvent and some solutes [4], less than 5 % water by weight [5], as well as some additives such as corrosion inhibitors and depolarizers or hydrogen absorbers. Ethylene glycol and gamma butyrolactone are common examples of solvents. A conductive salt, which usually is a resultant of the chemical reaction between an acid and a base, is used as a solute. Some of the acids commonly used are benzoic acid, adipic acid, and salicylic acid. Commonly used

bases include ammonium hydroxide and triethylamine. Picric acid is an example of a hydrogen absorber or depolarizer that is used in some electrolytes [6]. Weak organic acids are added in electrolytes and used as inhibitors to suppress corrosion. For example an acidic ester of an alkyl diphosphonic acid or an acidic derivative of a sulfonic acid has been added to some electrolytes as corrosion inhibitors [7].

Faulty electrolyte has caused a lot of reliability problems and financial losses in the past. Big original equipment manufacturers like Dell, Apple, Samsung and HP have suffered due to liquid aluminum electrolytic capacitors made from faulty electrolyte.

Counterfeiting of electronic components is a big problem in electronics industry. Original equipment manufacturers (OEMs) are concerned about counterfeiting because counterfeit parts can compromise the reliability of their final products [8]-[10]. In the past, concern about counterfeiting has generally focused on high-cost components, such as integrated circuits. However, less expensive passive components, such as capacitors and resistors, can also cause serious system reliability problems. In the past, counterfeit electrolytic capacitors have resulted in failures of electronic equipments of OEMs [11]. Failure modes and probable causes of failure for liquid aluminum electrolytic capacitors are listed in Table 1 below.

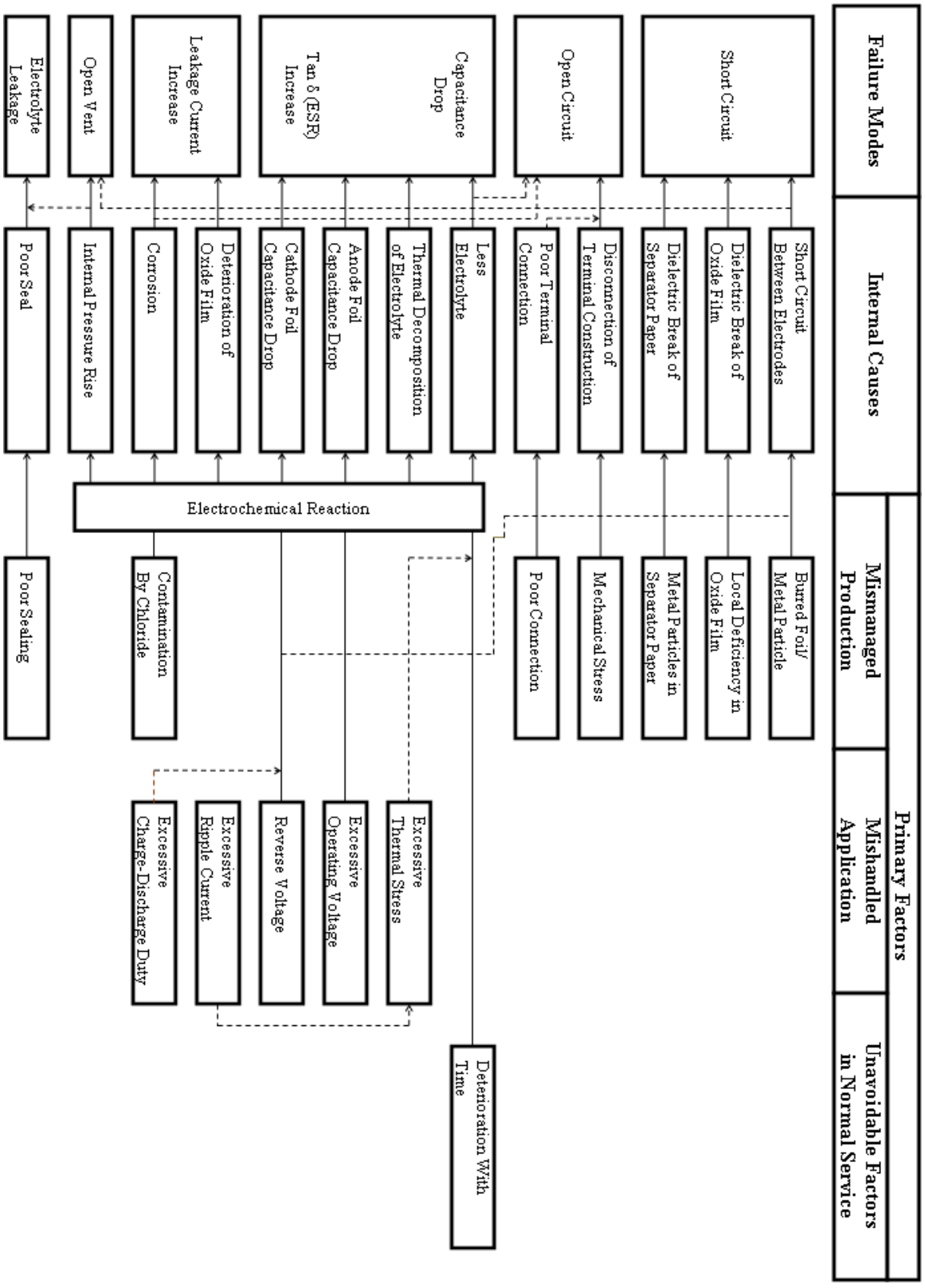

Table 1: Failure Modes and causes

1.4 Polymer Aluminum Electrolytic Capacitors

Polymer aluminum (PA) electrolytic capacitors were introduced as an alternative to liquid aluminum electrolytic capacitors. The liquid electrolyte was replaced by a solid conductive polymer electrolyte in polymer aluminum (PA) capacitors. The only difference in construction between the liquid aluminum electrolytic capacitors and PA electrolytic capacitors is the electrolyte. In liquid electrolytic capacitors, the electrolyte is liquid and is soaked in a paper layer between cathode and anode foil. In PA electrolytic capacitors, the electrolyte is a solid conductive polymer and is also soaked in the paper layer which is located between cathode and anode foil. Both electrolytes are part of cathode in the electrolytic capacitors. Figure 3 below shows comparison of construction between the liquid and polymer aluminum electrolytic capacitors. A drawback of liquid electrolytic capacitor is the low conductivity of the liquid electrolyte of about 0.01 S/cm [12]. Solid polymer electrolyte overcame the tendency of liquid electrolytes to evaporate over time and as the polymer used were conductive, the ESR of polymer aluminum capacitors was much lower than the liquid electrolytic capacitors. Some common polymers used in the capacitors are tetracyano-quinodimethane (TCNQ), polypyrole (PPY) and poly (3, 4-ethylenedioxythiophene) also known as PEDOT [13-14]. Conductivity of these polymers is shown in Figure 4. PEDOT has higher conductivity than other electrolytes as shown in Figure 4. During lead-free soldering, conducting polymers in electrolytic capacitors have to withstand a peak temperature of about 260°C. The elevated temperature stability of PEDOT is much better than other polymers [15-16].

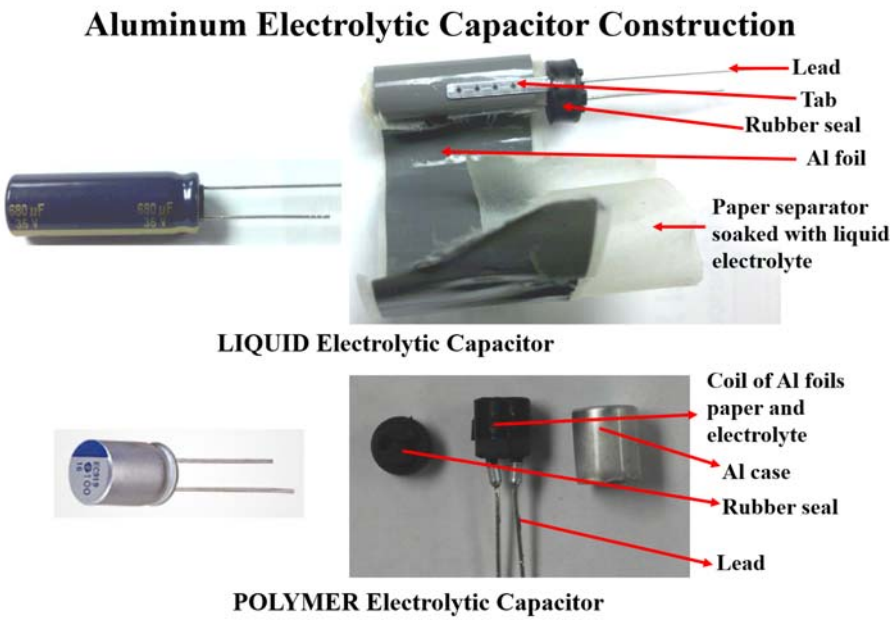

Figure 3: Aluminum electrolytic capacitor construction

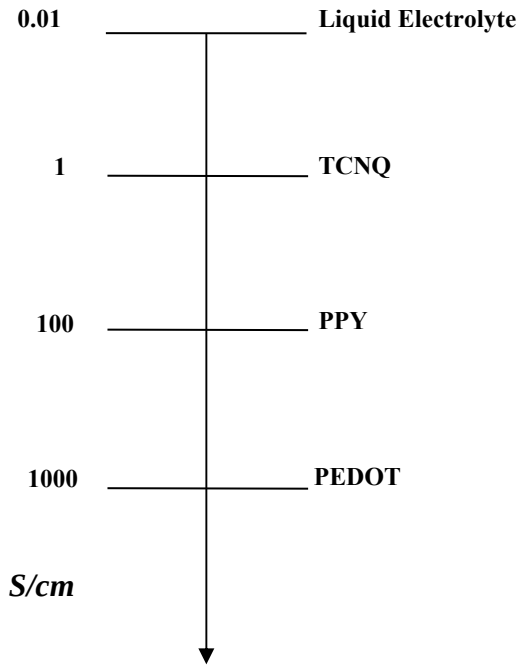

Figure 4: Conductivities of different electrolytes

1.5 Literature Review

Liquid electrolytic capacitors are known for their reliability problems and are often the weakest link in the reliability of power electronics systems [17-18]. Due to relatively high ESR of liquid aluminum electrolytic capacitors, ripple current causes additional core temperature rise causing reliability problems [19-20]. The most important factors affecting liquid electrolytic capacitors life are temperature, voltage and ripple current. Usually, these capacitors are used at high temperature, high temperature with DC voltage and high temperature, voltage and ripple current environments. The life testing of liquid aluminum electrolytic capacitors are typically performed at rated temperature, rated temperature plus DC bias and rated temperature rated ripple current plus maximum rated voltage (DC plus AC). Currently, there are no uniform standards that the liquid aluminum electrolytic capacitor manufacturers use to report the lifetimes.

There are some reliability studies performed on liquid aluminum electrolytic capacitors. In elevated temperature exposure studies on electrolytic capacitors, increase in equivalent series resistance (ESR) [21-23], leakage current (LC) [22] and decrease in capacitance [22-23] were reported. Elevated temperature and voltage exposure tests on electrolytic capacitors resulted in increase in dissipation factor [24], equivalent series resistance (ESR) [24-25] and decrease in capacitance [24-25]. Elevated temperature, voltage and ripple current exposure tests resulting in increase in ESR [26-27] and decrease in capacitance have been reported [26]. The exact electrolyte formula for liquid aluminum electrolytic capacitors is a trade secret which manufacturers do not disclose. Typically, a liquid electrolyte consists of solvent,

water, solutes, as well as additives such as corrosion inhibitors and hydrogen absorbers. The main solvents used are ethylene glycol and γ-butyrolactone.

Conductive salt, which usually is a product of the chemical reaction between an acid and a base, is used as a solute. Some of the commonly used acids are benzoic acid, adipic acid, salicylic acid and succinic acid. Commonly used bases include ammonium hydroxide and triethylamine. Picric acid and Nitrophenol are examples of a hydrogen absorber or depolarizer that is used in electrolytes. Phosphoric acid is an example of a corrosion inhibitor. In a study, ESR increase and capacitance decrease was observed in temperature, voltage and ripple current exposure tests with γ-butyrolactone (solvent) based electrolyte but the failure mechanisms were not determined [26]. Elevated temperature study of γ-butyrolactone based electrolyte was performed at 115°C. The conductivity decreased due to loss of acid components in the electrolyte [28]. This study was performed on just the electrolyte not on the whole capacitor system. Elevated temperature study of ethylene glycol based electrolyte was performed. Ester formation in the electrolyte was reported at 105°C and 145°C [29]. This study was also performed just on the electrolyte. There are no relevant studies which are performed on the whole capacitor which will include the interaction between all the subsystems. The effect of electrolyte solvent on the failure mechanisms observed in liquid aluminum electrolytic capacitors is missing. The effect of ripple current on the failure mechanisms observed in liquid aluminum electrolytic capacitors is not known.

Polymer aluminum (PA) capacitors have a conductive polymer electrolyte to overcome the tendency for liquid electrolytes to evaporate over time leading to failure

[30-35]. Polymer electrolytic capacitors have low ESR [30-37]. A NASA reliability study evaluated polymer aluminum electrolytic capacitors [30]. The results were:

- PA capacitors demonstrated low ESR and stability of capacitance versus frequency and temperature
- PA capacitors exhibited ignition free, non-flammable failure mode during application of reverse voltage that was twice the rated voltage
- No degradation of electrical performance was revealed before and after thermal vacuum test of 12 cycles, between -44ºC to 105ºC, at 10-5 Torr.

This study recommended high temperature-humidity testing as the future work that was needed. Manufacturers advise not to use PA capacitors in elevated temperature-humidity environments. But, there are no available studies which evaluates elevated temperature-humidity performance of PA capacitors. The failure modes and mechanisms of polymer aluminum electrolytic capacitors in elevated temperature-humidity are unknown. There are no established tests to perform rapid assessment of polymer aluminum electrolytic capacitors in elevated temperature-humidity environment to quickly assess their elevated temperature-humidity performance.

1.6 Research Objectives

- Determine if ripple current has an effect on the failure mechanisms observed in liquid aluminum electrolytic capacitors.
- Determine how the electrolyte solvent affects the failure mechanisms observed in liquid aluminum electrolytic capacitors.

- Determine failure modes and mechanisms of polymer aluminum electrolytic capacitors in elevated temperature humidity environment.
- Develop rapid assessment method for polymer aluminum electrolytic capacitors for elevated temperature and humidity environment.

2: Life Testing of Aluminum Electrolytic Capacitors

2.1 Objectives

- Determine if ripple current has an effect on the failure mechanisms observed in liquid aluminum electrolytic capacitors.
- Determine how the electrolyte solvent affects the failure mechanisms observed in liquid aluminum electrolytic capacitors.

2.2 Approach

- The approach used to achieve the above stated objectives was:
- Liquid aluminum electrolytic capacitors with γ-butyrolactone and ethylene glycol based electrolyte were chosen. The details of the capacitors used for life testing is shown in Table 2.
- Capacitance, dissipation factor, ESR and insulation resistance was measured before starting the life tests. Weight of the capacitors was also measured.
- Life testing was performed on the chosen liquid aluminum electrolytic capacitors by applying temperature/DC voltage/ripple current (with ripple current) and temperature/DC voltage (without ripple current) stresses.
- Capacitance, dissipation factor, ESR, insulation resistance and weight measurements were performed after stopping the test at room temperature at regular intervals.
- After failure, analysis of the failure data from life tests was performed to obtain failure distributions.

- Develop technique to analyze the liquid electrolyte which can be used in failure analysis and counterfeit detection.
- Performed failure analysis on the failed capacitors to determine the failure mechanisms.
- Apply techniques developed to analyze the electrolyte to detect counterfeit liquid aluminum electrolytic capacitors.

2.3 Life Testing of Liquid Aluminum Electrolytic Capacitors

Three liquid aluminum electrolytic capacitors C1, C2 and C3 were life tested. The liquid electrolyte of C1 and C2 had γ-butyrolactone as the solvent and the liquid electrolyte of C3 had ethylene glycol as solvent. Table 2 shows specifications of liquid electrolytic capacitor used for the life tests. Life test plan for liquid electrolytic capacitors is shown in Table 3.

	C1	**C2**	**C3**
Capacitance	680µF (±20%)	470µF (±20%)	220µF (±20%)
Rated Voltage	35V	6.3V	10V
Ripple Current (120 Hz)	1.36A	0.23A	0.12A
Dimensions	Diameter: 10mm, Length: 30mm	Diameter: 6.3mm, Length: 11mm	Diameter: 8mm, Length: 7mm
Electrolyte	**γ -Butyrolactone** (Main solvent)	**γ -Butyrolactone** (Main Solvent)	**Ethylene Glycol** (Main Solvent)

Table 2: Specifications of Capacitor Used in Life Tests

	Test 1 (Ripple Current)	**Test 2 (Voltage)**	**Test 3 (Temperature)**
Number of Samples	C1 (16) C2 (10) C3 (10)	C1 (10) C2 (10) C3 (10)	C1 (10)
Test Conditions	Rated ripple current plus DC voltage, in oven set at rated maximum temperature (105C).	Rated DC voltage, in oven set at core temperature measured in Test 1 (110C).	In oven set at core temperature (110C) measured in Test 1. No applied voltage.

Table 3: Life Test Plan

Ripple current causes additional core temperature rise for the capacitor due to joule healing. Core temperature rise was measured by a thermocouple that was inserted inside the capacitor core and was instantly sealed with an epoxy. The electrical properties like capacitance, ESR, dissipation factor and leakage current were measured before and after the thermocouple insertion to make sure that the capacitor did not get damaged during the thermocouple insertion process. Ripple current temperature rise was measured by exposing the capacitors to rated temperature, rated ripple current plus DC voltage. The measured core temperature for the capacitors was 110ºC. Three different life tests were run for C1 as shown in Table 3. For C2 and C3, two life tests were run which are shown in Table 3. The three tests were, 1) Rated ripple current plus DC voltage, along with rated maximum temperature (105°C) exposure. 2) Rated DC voltage, along with core temperature measured in Test 1

(110°C). 3) Core temperature measured in Test 1 (110°C). The electrical properties like capacitance, dissipation factor, equivalent series resistance (ESR) and insulation resistance was measured before and during the life tests at regular intervals. The weight measurement of capacitors was also performed to monitor the changes in weight during the life tests. The parametric failure criteria was 20% drop is capacitance from the rated capacitance value, 50% increase in ESR, 200% increase in dissipation factor and leakage current increasing above 0.01CV. Once the capacitors failed, analysis of the data from life tests was performed to obtain failure distributions. Failure analysis was performed on the failed capacitors including analysis on the anode, cathode foil, dielectric layer and the liquid electrolyte from inside the electrolytic capacitors.

2.4 Life Test Results

For capacitor C1, the capacitance plot for the individual C1 capacitors is shown in Figure 5. For C1, there was one early life/infant mortality failure in the ripple current test (Test 1) which is marked in red color in Figure 1. This early life failure was due to increase in leakage current. In the subsequent failure analysis, it was revealed that the anode foil shorted. Figure 6 shows burnt paper separator and shorted anode foil for the early life leakage current failed capacitor C1. Figure 7 shows E-SEM image of the failed anode foil for the same capacitor. In all three tests listed in Table 3, capacitor C1 failed due to drop in capacitance value below 540 μF (20% capacitance drop). The ESR, dissipation factor and leakage current remained stable. The weight of the capacitor dropped as the electrolyte from the capacitors evaporated. Figure 8 shows the average capacitance value during the three tests. It was observed that the

capacitance drop was quickest for the voltage test followed by ripple current test and temperature test. The weight change of the capacitors is shown in Figure 9. The weight loss observed at a particular time in the capacitors from three different tests was about the same which can be seen due to overlapping error bars.

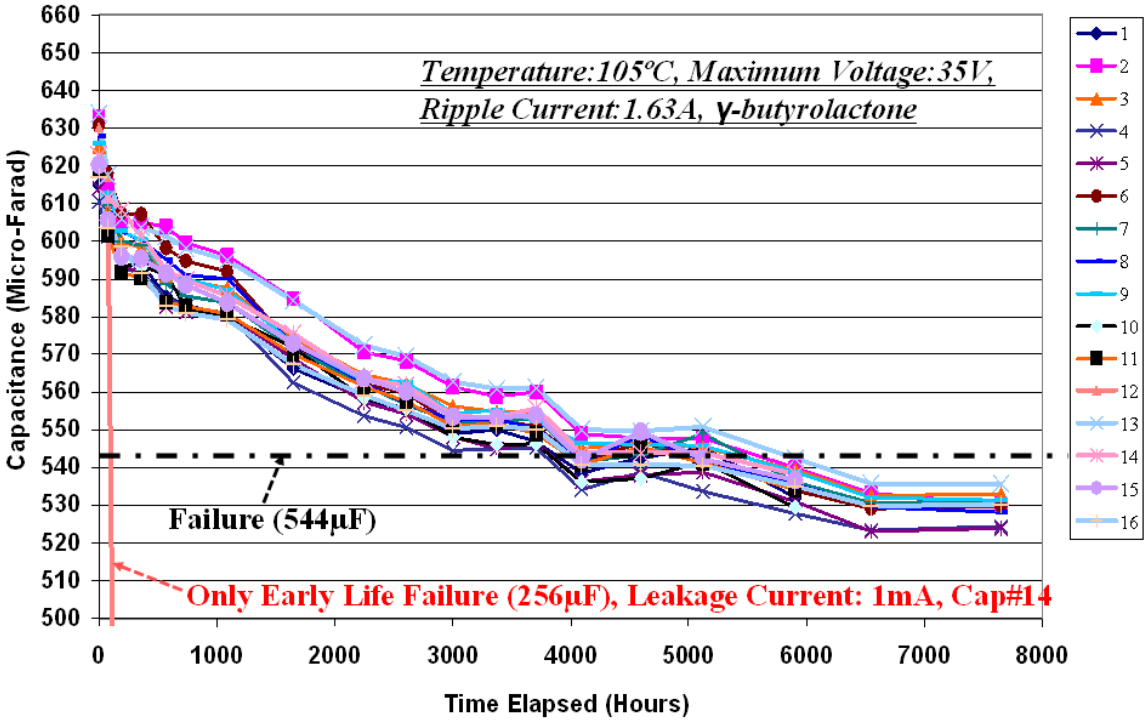

Figure 5: Individual capacitance plot for the ripple current test for C1 capacitors

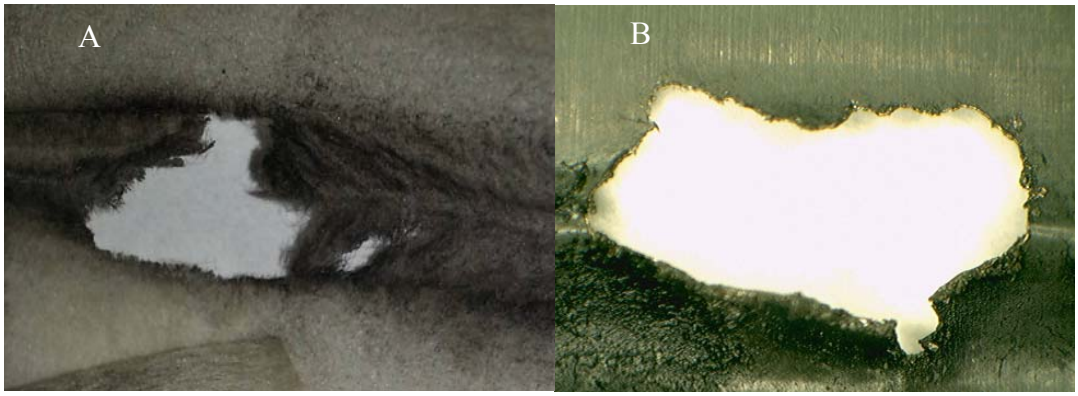

Figure 6: Burnt paper separator (A) and anode foil from the early life leakage current failed capacitor C1

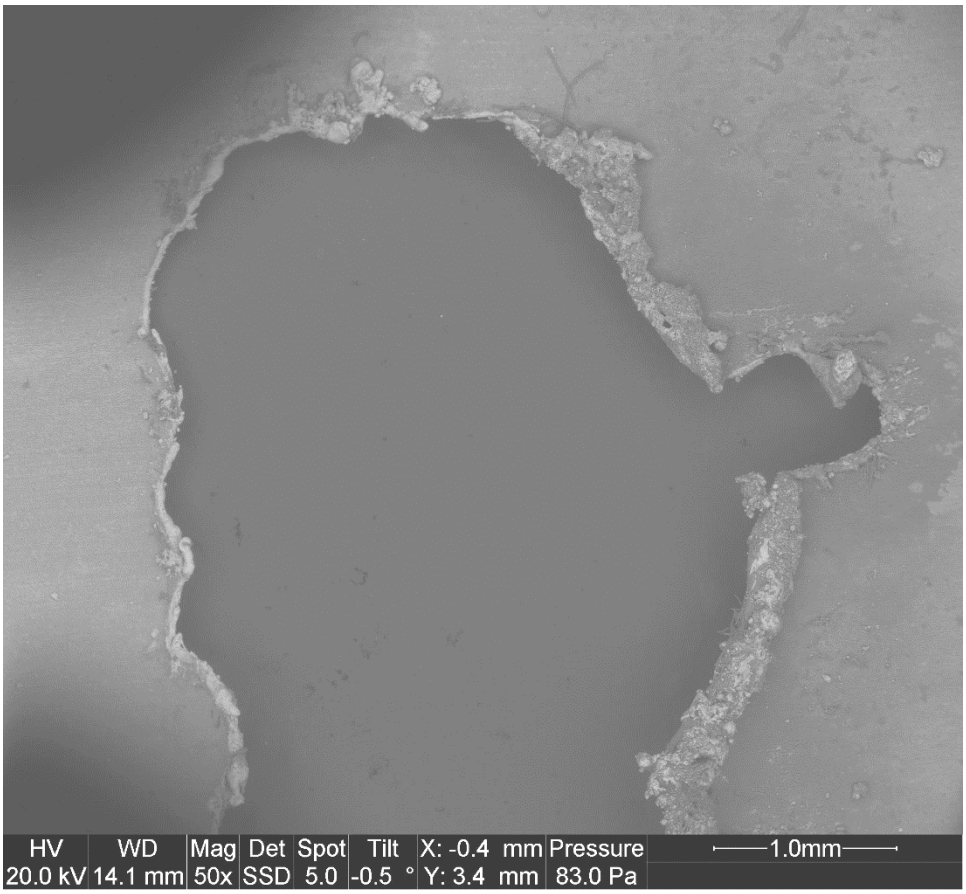

Figure 7: E-SEM image of the shorted anode foil/dielectric layer

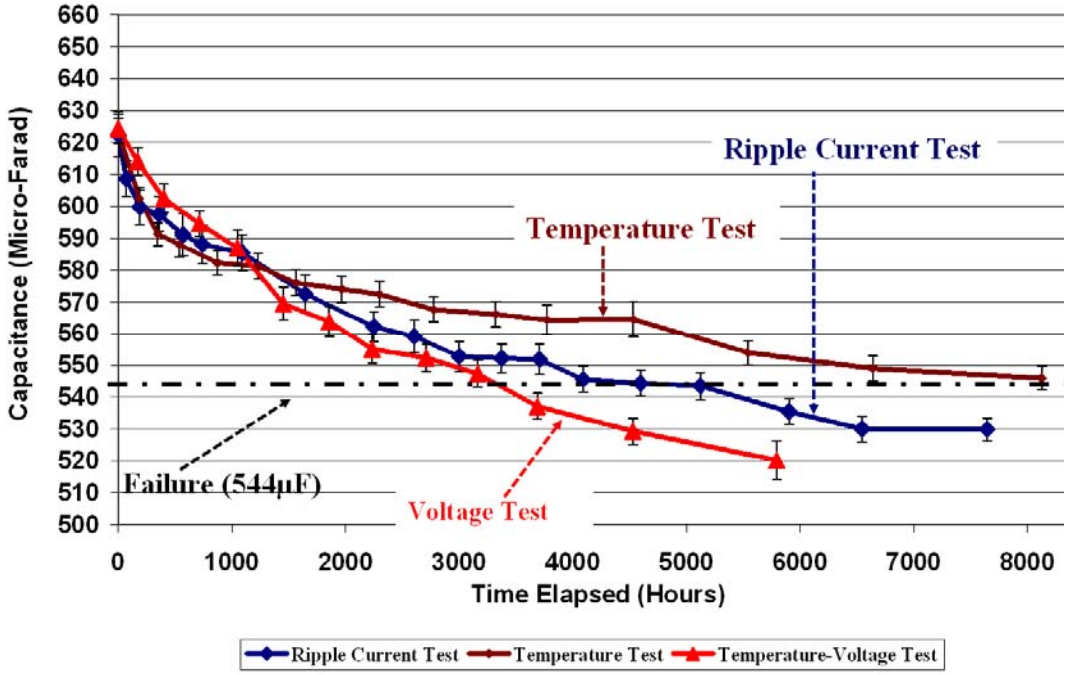

Figure 8: Capacitance plot showing drop in average capacitance for C1

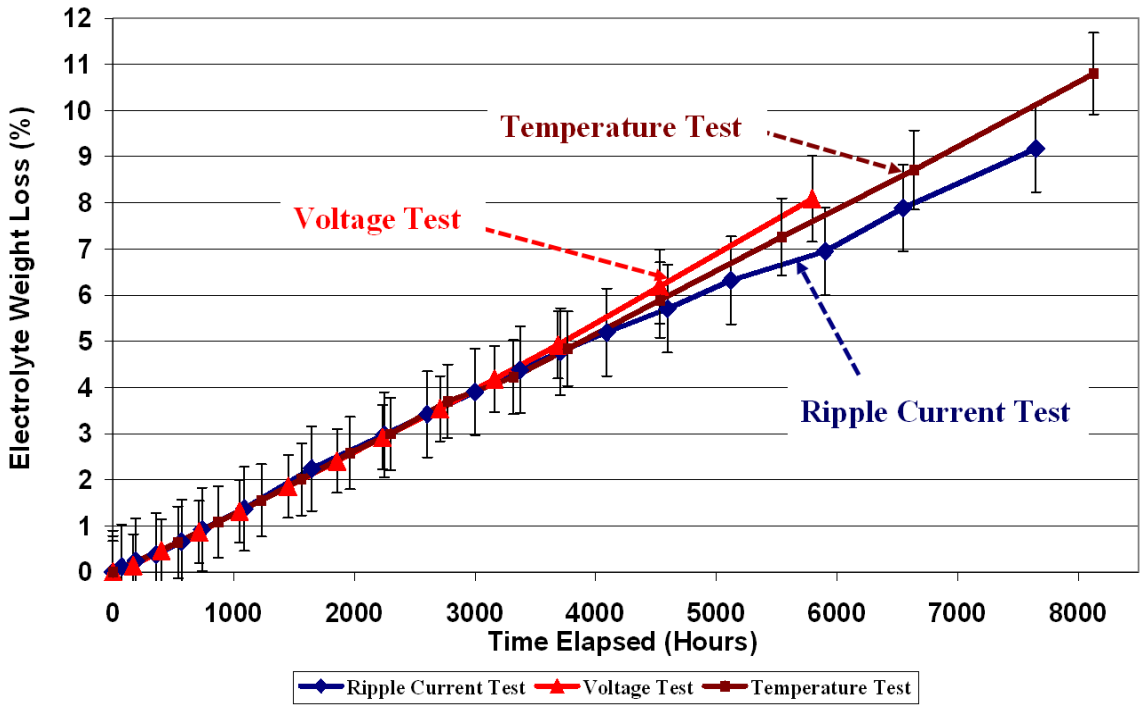

Figure 9: Plot showing electrolyte weight loss during life tests of C1

For capacitor C2 populations undergoing the life tests, capacitance drop and increase in ESR was observed. The capacitors failed first due to increase in ESR value. Figure 10 shows the average ESR plot which shows the increase in average ESR values of the capacitors undergoing the ripple current and voltage test. For C2, ripple current tested samples failed before the voltage tested samples unlike C1 capacitor population. This is due to additional temperature rise due to increase in ESR in C2. Figure 11 shows the capacitance plot which shows drop in capacitance. Capacitance drop in ripple current-tested capacitors is faster than the capacitance drop in voltage-tested samples. Figure 12 shows the average electrolyte weight loss for capacitor C2 population during voltage and ripple current life test. Capacitors under ripple current test exhibited faster electrolyte weight loss than capacitance under voltage test.

Capacitor C3 with ethylene glycol based electrolyte exhibited increase in ESR and very slight decrease in capacitance. The increase in ESR value was faster and the capacitor population failed due to increase in ESR value. Figure 13 shows the average ESR plots for ripple current and voltage tested capacitors showing increase in ESR. The ESR failure threshold was 700mΩ. The capacitor population under ripple current test failed first. Figure 14 shows the capacitance plots for the life tested capacitors which shows a decrease in capacitance value. Figure 15 shows electrolyte weight loss plots for the capacitor populations.

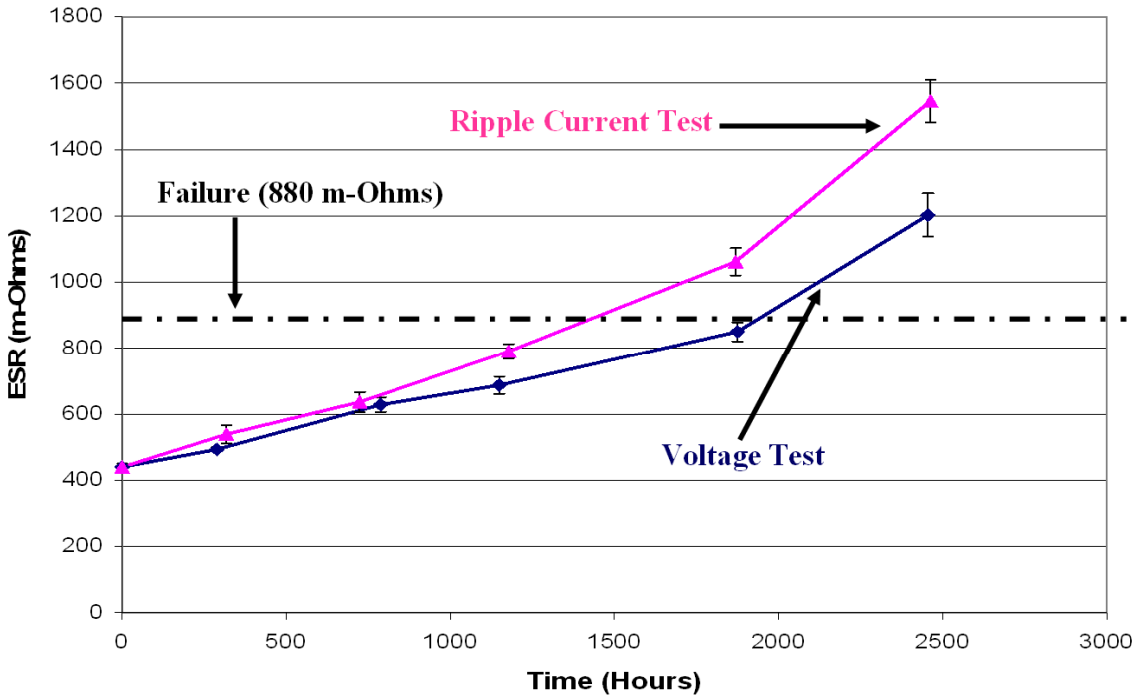

Figure 10: ESR plot showing increase in average ESR for C2 during life testing

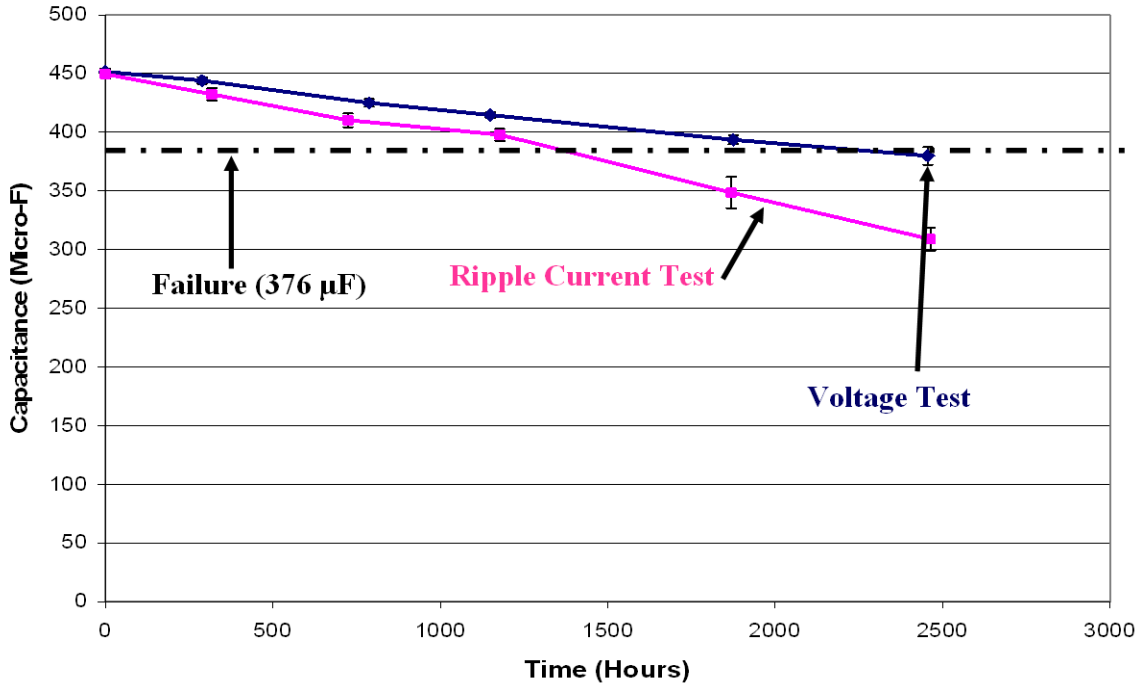

Figure 11: Capacitance plot showing drop in average capacitance for C2

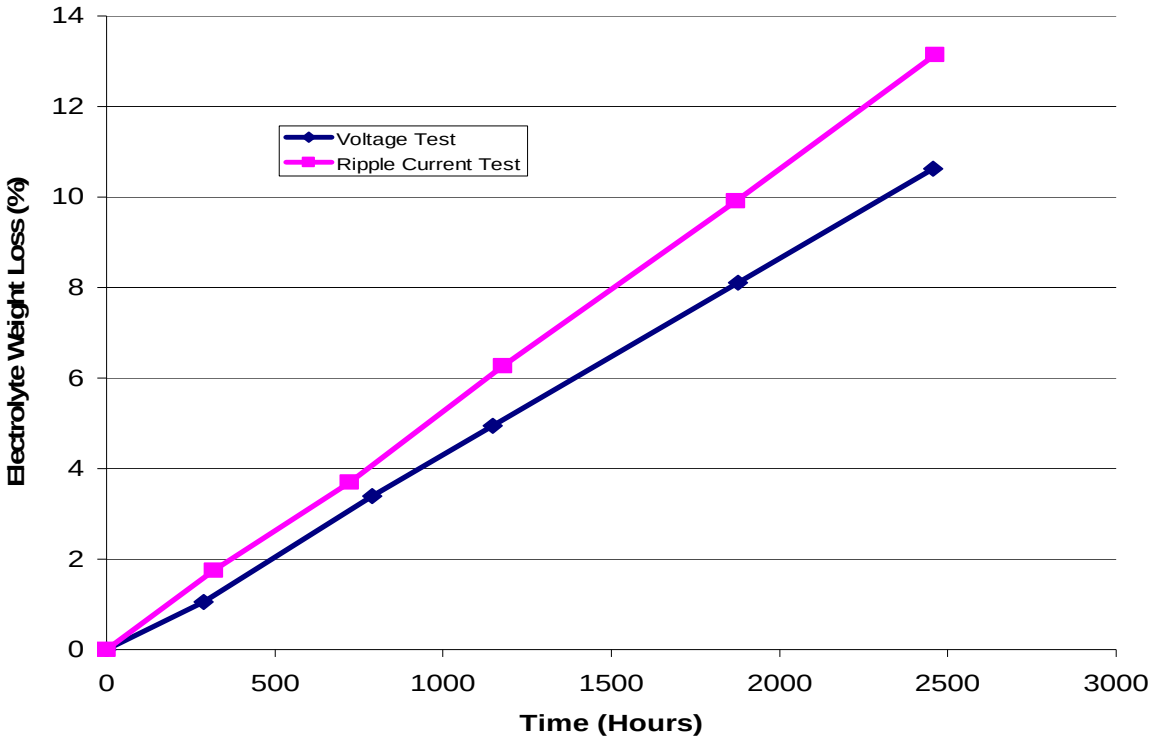

Figure 12: Plot showing average electrolyte weight loss during life tests of C2

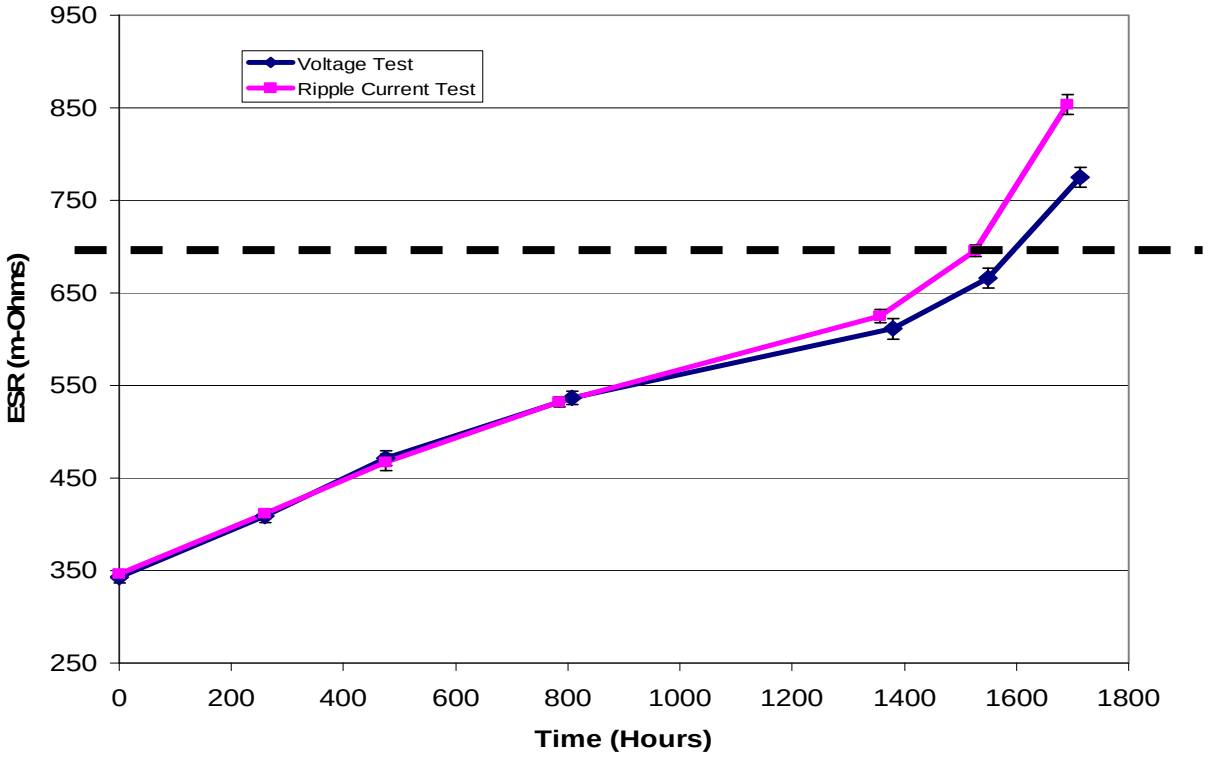

Figure 13: ESR plot showing increase in average ESR for C3 during life testing

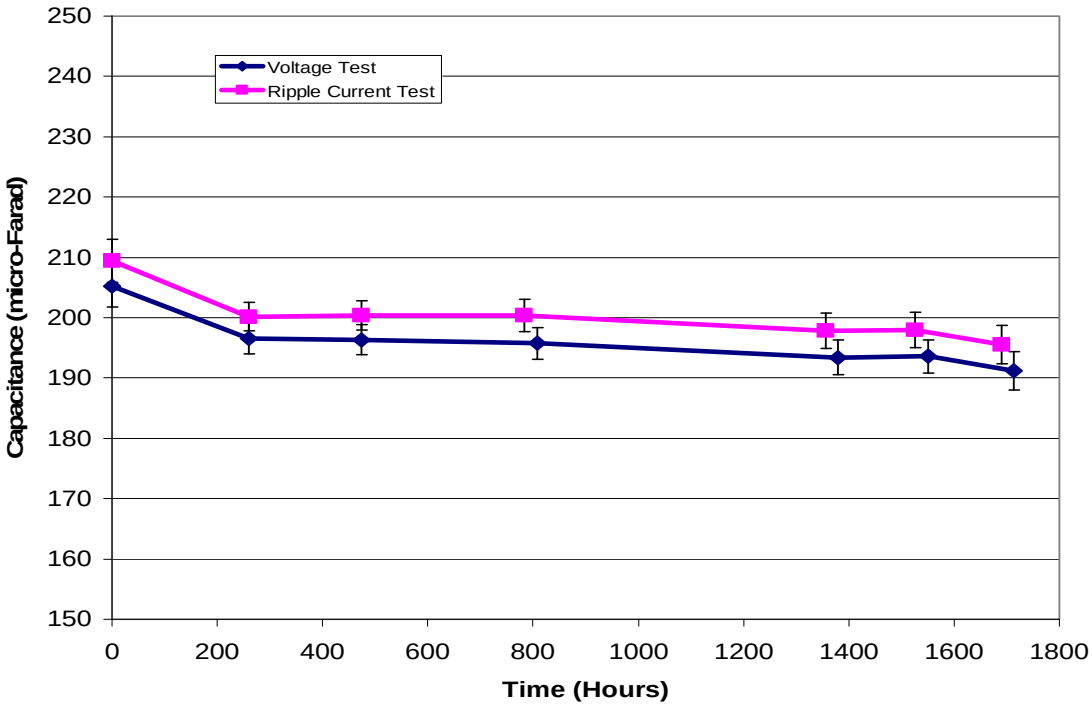

Figure 14: Capacitance plot showing drop in average capacitance for C3

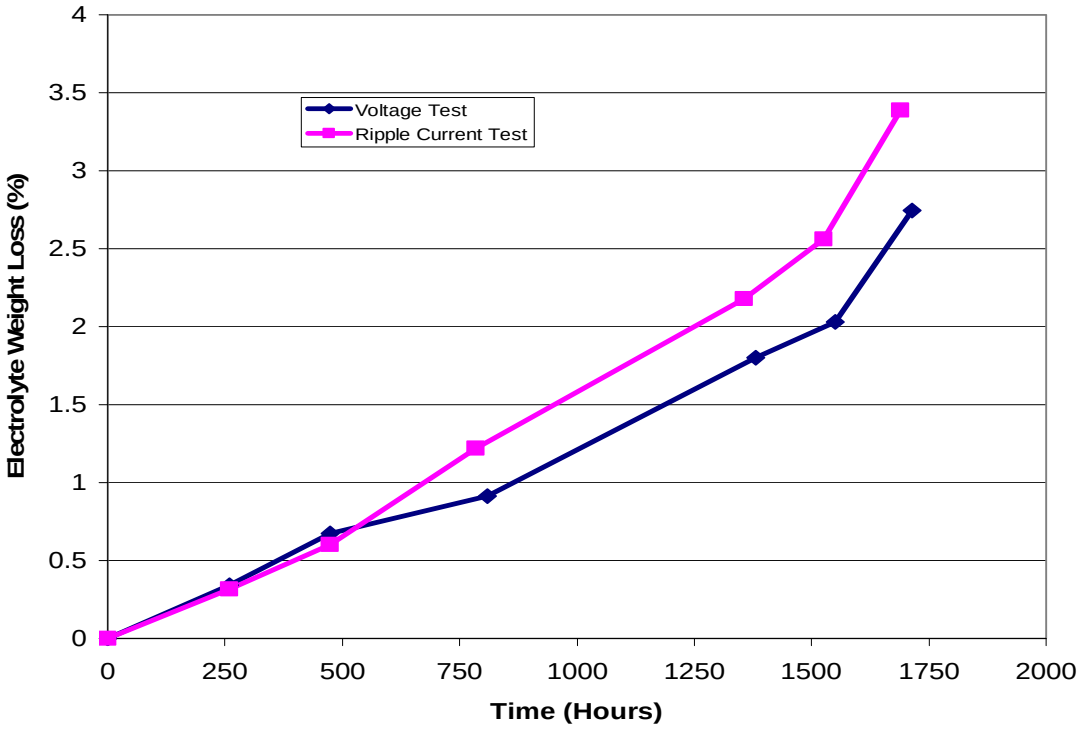

Figure 15: Plot showing average electrolyte weight loss during life tests of C3

In summary, for capacitors C1 (γ-butyrolactone solvent based) which failed due to drop in capacitance, voltage tested (Test 2) capacitors failed first followed by ripple current tested (Test 1) capacitors and finally the temperature tested capacitors failed. For capacitors C2 (γ-butyrolactone solvent based), they failed due to increase in ESR. For C2, the ripple current tested (Test 1) capacitors failed first and then the voltage tested (Test 2) capacitors. Although for both C1 and C2, the liquid electrolyte is γ-butyrolactone solvent based, C1 did not exhibit increase in ESR but C2 did. The answer to this difference in behavior was found in the chemical analysis of the liquid electrolyte by Fourier transform infrared (FTIR) spectroscopy (Refer to section 2.5 "Chemical Analysis of Liquid Electrolyte").

For capacitors C3 (Ethylene glycol solvent based), they failed due to increase in ESR. For C3, again the ripple current tested (Test 1) capacitors failed first and then the voltage tested (Test 2) capacitors.

2.5 Chemical Analysis of Liquid Electrolyte

2.5.1 Objective

The objective of chemical analyses of the liquid electrolyte was to find out if the liquid electrolyte remained chemically stable after the capacitor failed. FTIR analysis can be also used to determine the chemical difference between the γ-butyrolactone based electrolyte from C1 and C2. A process was developed to analyze the liquid electrolyte of the aluminum electrolytic capacitor chemically using FTIR for this work.

2.5.2 Fourier Transform Infrared Spectroscopy (FTIR)

FT-IR stands for Fourier Transform Infrared, the preferred method of infrared spectroscopy. In infrared spectroscopy, IR radiation is passed through a sample. Some of the infrared radiation is absorbed by the sample and some of it is passed through (transmitted). The resulting spectrum represents the molecular absorption and transmission, creating a molecular fingerprint of the sample. Like a fingerprint no two unique molecular structures produce the same infrared spectrum. This makes infrared spectroscopy useful for several types of analysis.

2.5.3 Developed Technique using FTIR to Analyze the Liquid Electrolyte

Fourier transform infrared spectroscopy (FTIR) was used to chemically analyze the liquid electrolyte. FTIR was set up in attenuated total reflectance (ATR) mode, which is a type of internal reflection spectroscopy. ATR allows the analysis of liquid and solid samples without any special preparation. This is very helpful in failure analysis

as it avoids the chances of removal of evidence. In the ATR device, an infrared beam enters into a crystal of high refractive index, while this beam is refracted, strikes the sample one or more times and enter into a monochromator as shown in Figure 16.

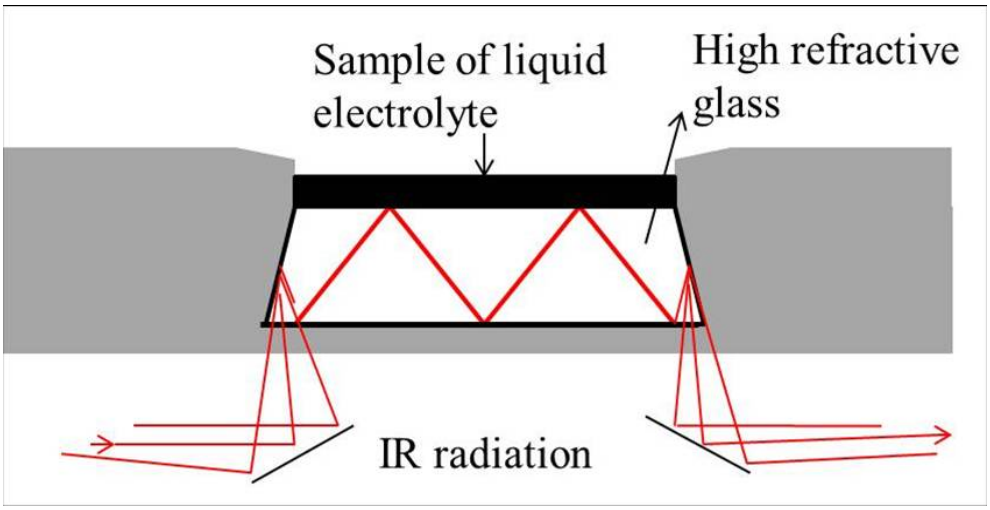

Figure 16: Schematic of Attenuated Total Reflectance (ATR) equipment

The liquid electrolyte in aluminum electrolytic capacitor is absorbed in the paper layer. The steps involved in analyzing the electrolyte are:

a). Remove the top plastic cover from the capacitor body.

b). Cut and remove the top aluminum case to access the internal coiled capacitor structure containing the anode foil, cathode foil and the paper layer which is between cathode and anode foil and holds the liquid electrolyte. There is a tape on top holding the whole coiled structure.

c). Cut the tape holding the capacitor roll containing the anode foil, cathode foil and the paper soaked with electrolyte.

d). Unwind the rolled capacitor structure.

e). Remove both the layers of paper soaked with electrolyte from the unrolled structure.

f). In ATR mode, squeeze the electrolyte out of the paper layer and apply on the glass surface of the FTIR and perform a run.

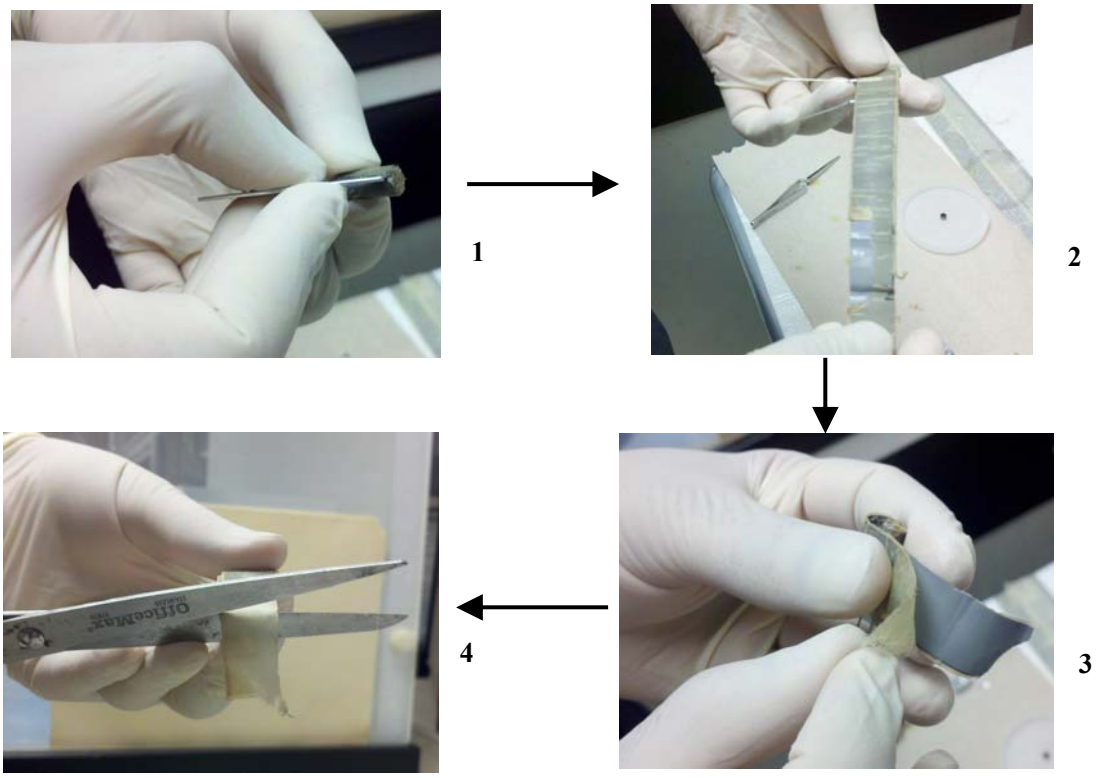

Figure 17: Sample preparation steps

2.5.4 Liquid Electrolyte Comparison of C1 and C2

FTIR comparison of liquid electrolytes of C1 and C2 was performed to determine if there was any difference chemically between the two electrolytes because they showed different behavior in the life tests. In the FTIR spectra comparison, there was only one extra peak which was present in C1 electrolyte which was not there in the C2 electrolyte. All the other peaks in the C1 and C2 electrolytes were the same. Figure 18 shows comparison of FTIR spectra showing a peak around 1620 cm^{-1} which was present in the C1 capacitor electrolyte. This peak was absent in the liquid electrolyte of C2. This peak corresponds to carboxylic acid salts which were added in

C1 electrolyte. Carboxylic acid salts are added in the electrolyte to increase the conductivity of the liquid electrolyte. This explains the difference in ESR behavior of capacitor C1 and C2.

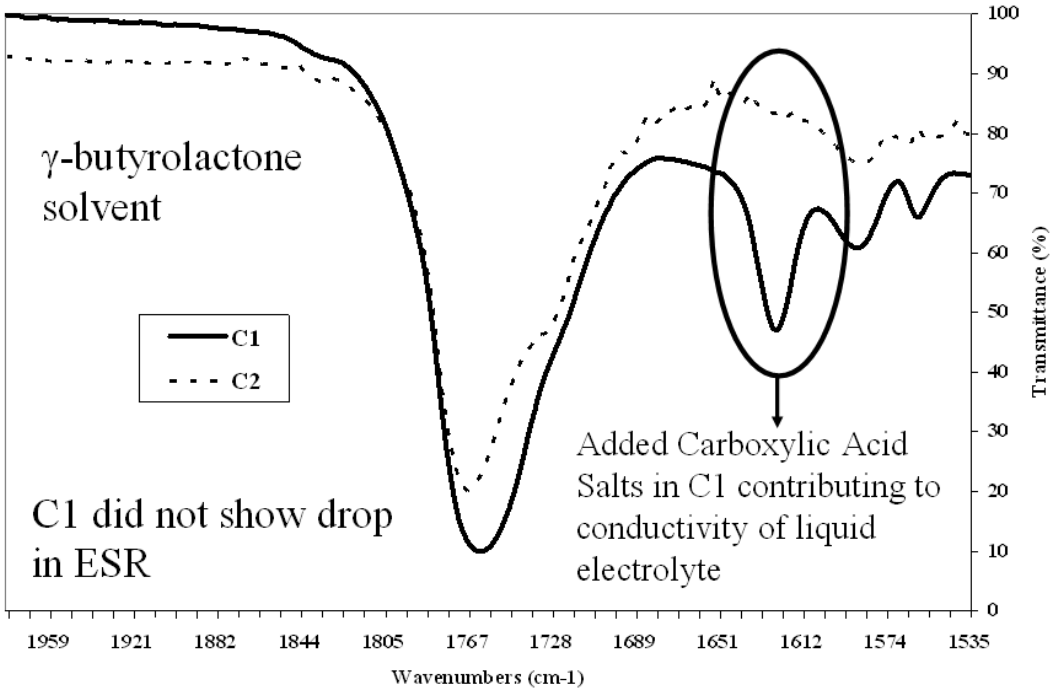

Figure 18: FTIR Spectra comparing liquid electrolyte of C1 and C2

2.5.5 Chemical analysis of liquid electrolyte of tested and untested C1 capacitors

C1 capacitor liquid electrolytes from failed capacitors in temperature test, ripple current test and voltage test were compared to the liquid electrolyte of the unused C1 capacitor to determine the chemical changes in electrolyte after the capacitor failed. Figure 19 shows the comparison of FTIR spectra of the liquid electrolytes from failed C1 capacitors in temperature test, ripple current test, voltage test and unused C1 capacitor. There were no new peaks found in the failed capacitor electrolyte which meant that the chemistry of electrolyte did not change after the capacitors failed. The

only difference which was found was the peaks related to volatiles close to 3500cm^{-1} decreased in concentration.

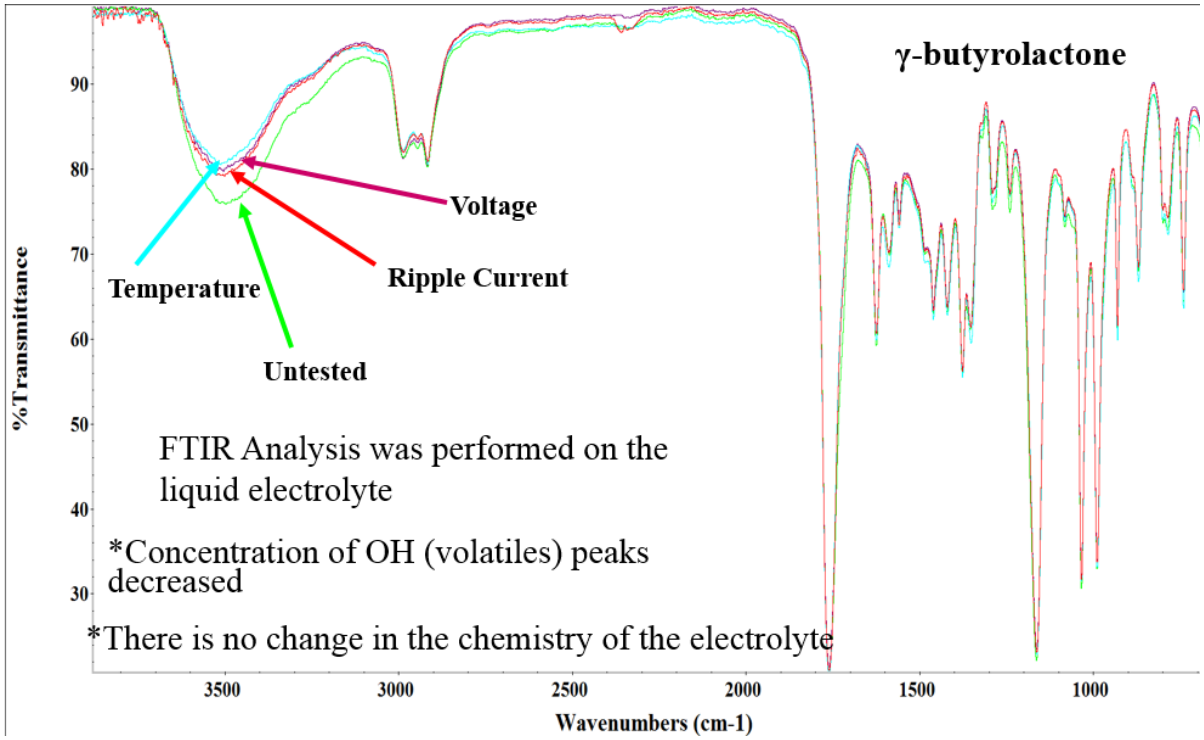

Figure 19: FTIR spectra of failed and unused C1 capacitor electrolyte

2.5.6 Chemical analysis of liquid electrolyte of tested and untested C2 capacitors

C2 capacitor liquid electrolytes from failed capacitors in the ripple current and voltage test were compared to the liquid electrolyte of the unused C2 capacitor to determine the chemical changes in electrolyte after the capacitor failed. Figure 20 shows the comparison of FTIR spectra of the liquid electrolytes from failed C2 capacitors in the ripple current and voltage test and unused C2 capacitor. There were no new peaks found in the failed capacitor electrolyte which meant that the chemistry of electrolyte did not change after the capacitors failed. The only difference which was found was the peaks related to volatiles close to 3500cm^{-1} decreased in concentration.

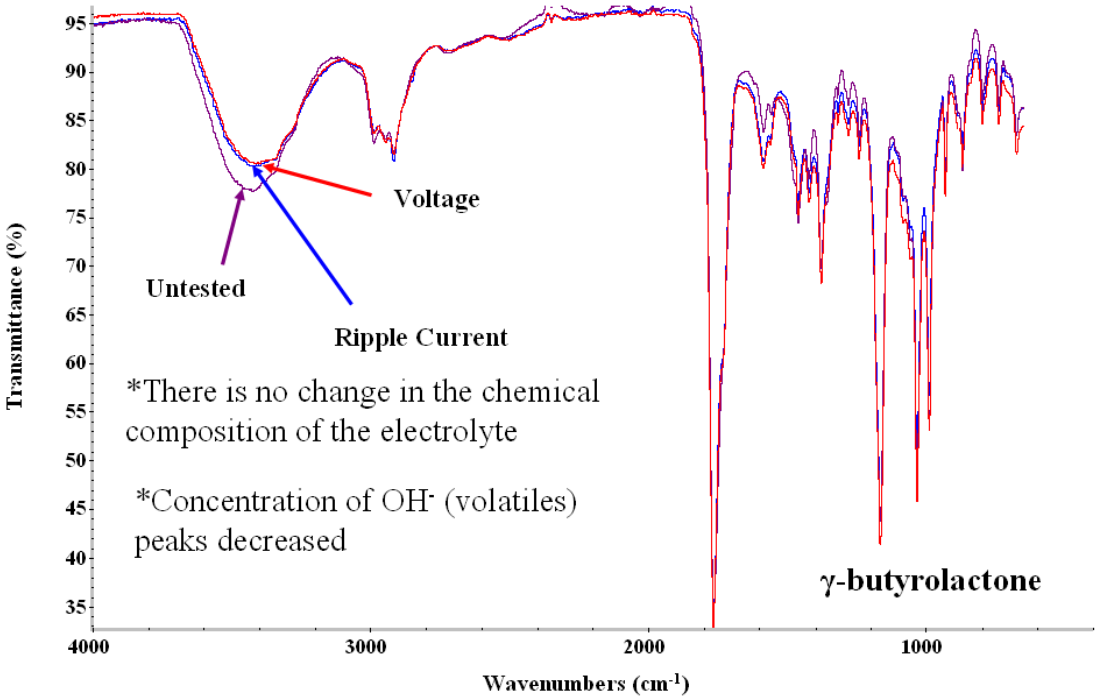

Figure 20: FTIR spectra of failed and unused C2 capacitor electrolyte

2.5.7 Chemical analysis of liquid electrolyte of tested and untested C3 capacitors

C3 capacitor liquid electrolytes from failed capacitors in the ripple current and voltage test were compared to the liquid electrolyte of the unused C3 capacitor to determine the chemical changes in electrolyte after the capacitor failed. Figure 21 shows the comparison of FTIR spectra of the liquid electrolytes from failed C3 capacitors in the ripple current and voltage test and unused C2 capacitor. There were new FTIR peaks found in the ripple current and voltage test failed capacitor electrolyte which meant that the chemistry of electrolyte changed after the capacitors failed. The new FTIR peaks found in the ripple current and voltage test failed capacitor electrolyte corresponded to esters and amides. Another difference was that the FTIR peak corresponding to carboxylic acid salts decreased in the failed capacitor

electrolyte. Formation of ester and amide and decrease in concentration of carboxylic acid salt group decreased the conductivity of the electrolyte of failed capacitors. Below are the chemical equations showing how esters and amides can be formed in liquid electrolyte.

$$\mathbf{R\text{-}COOH + HOCH_2CH_2OH \longrightarrow R\text{-}COOCH_2CH_2OH\ (Ester) + H_2O}$$

$$\mathbf{RCOONH_4 \longrightarrow RCONH_2 + H2O}$$

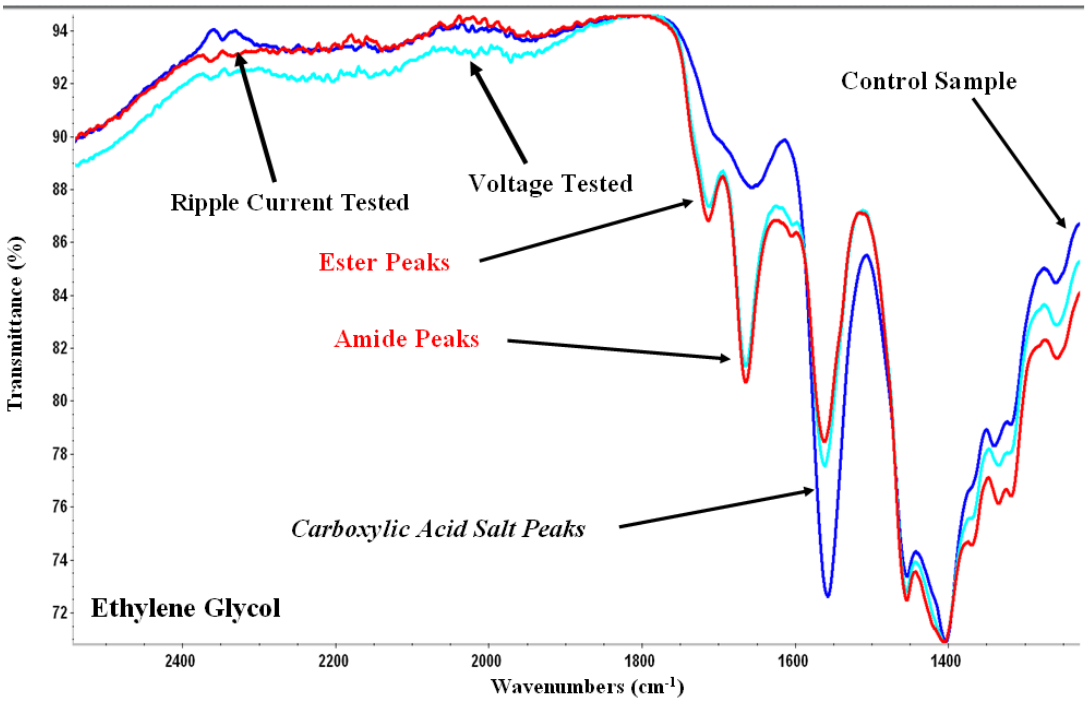

Figure 21: FTIR spectra of failed and unused C3 capacitor electrolyte

2.6 Other Analyses

2.6.1 X-Ray Analysis

X-ray analysis was performed on the capacitors before and after the life testing to look for some obvious or gross anomalies. Expansion of internal coiled structure, damage to the internal tabs and misaligned or bent coiled structure is the kind of

anomalies that X-ray can reveal. No anomalies were found in the X-ray analysis for the life tested capacitors.

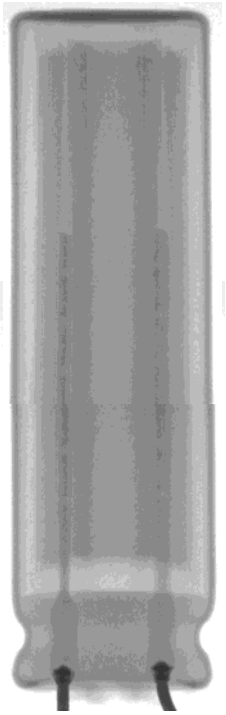

Figure 22: X-ray image of a good untested capacitor (C1)

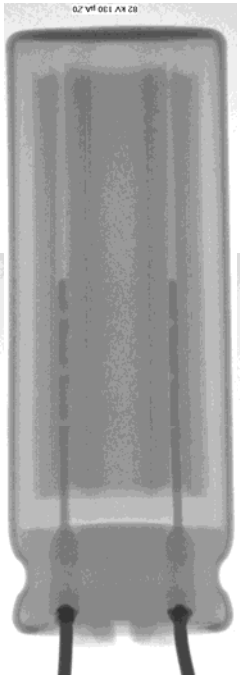

Figure 23: X-ray image of a voltage tested failed capacitor (C1)

Figure 22 shows X-ray image on a good capacitor and figure 23 shows X-ray image of a C1 capacitor that failed in voltage test. No anomalies were observed in this or any other failed capacitors in X-ray analysis.

2.6.2 Cross-Sectioning

Cross-sectioning was performed on the good and failed capacitors to check for changes in oxide layer thickness and to check degradation on the dielectric oxide layer was performed. A hole was made on top of the outer aluminum casing of capacitor using a punch to fill it with a two part epoxy. The capacitor was filled with the two part epoxy in a vacuum chamber. The epoxy was pulled inside the capacitor due to vacuum environment. The epoxy hardens in 8-12 hours and then the cross-sectioning was performed. E-SEM (Environmental Scanning Electron Microscopy) and EDS (Energy Dispersive X-Ray Spectroscopy) analysis was performed on the cross-sectioned samples.

2.6.3 E-SEM/EDS Analysis

Good and failed cross-sectioned capacitors were inspected with E-SEM/EDS. Figure 24 shows cross-section image of an untested C1 capacitors anode foil. Figure 25 shows the dielectric oxide layer on the anode foil of untested C1 capacitor. Figure 26 shows cross-section image of a ripple current test failed C1 capacitors anode foil. Figure 27 shows the dielectric oxide layer on the anode foil of ripple current test failed C1 capacitor. Figure 28 shows cross-section image of a voltage test failed C1 capacitors anode foil. Figure 29 shows the dielectric oxide layer on the anode foil of voltage test failed C1 capacitor. No observable anomalies were observed in the failed capacitors.

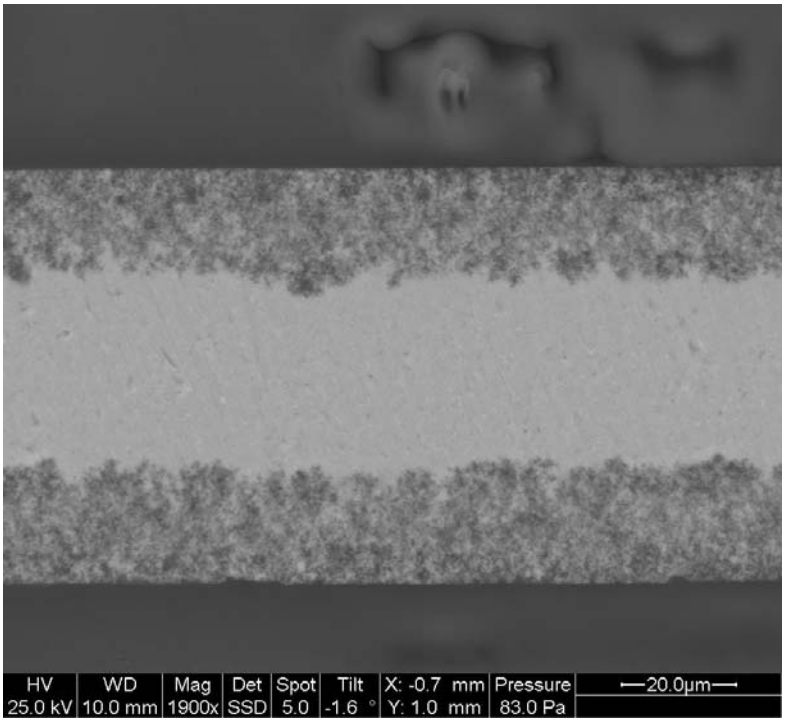

Figure 24: E-SEM image of the anode foil and oxide layer on top of it (Unused Capacitor C1)

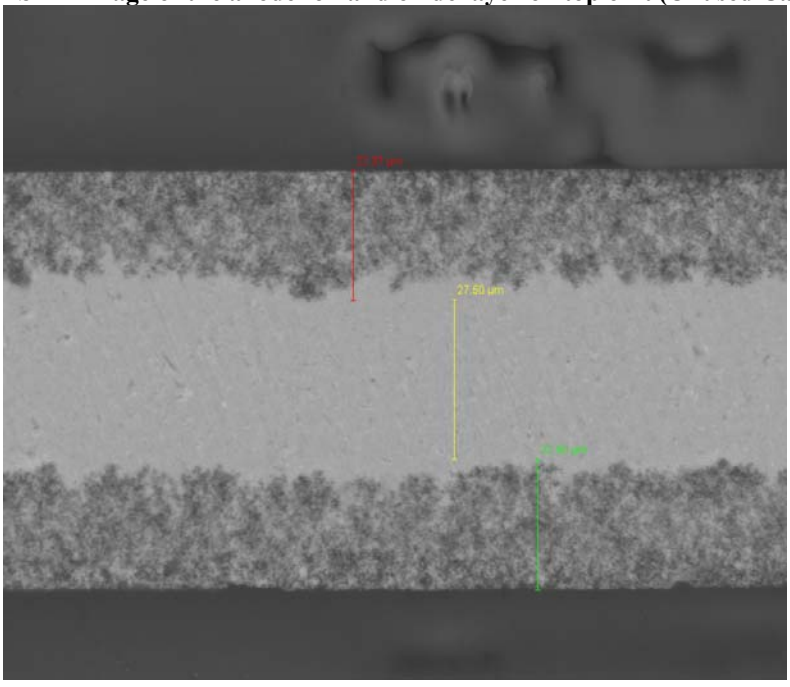

Figure 25: E-SEM image of the anode foil and porous oxide layer (Unused Capacitor C1)

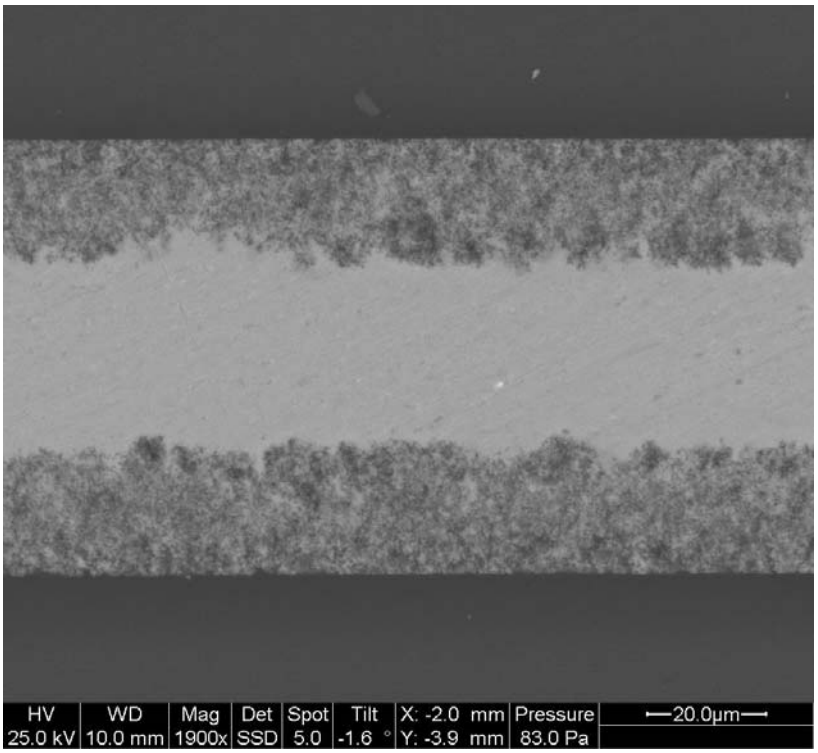

Figure 26: E-SEM image of the anode foil and oxide layer on top of it (Failed Capacitor C1 from Ripple Current Testing)

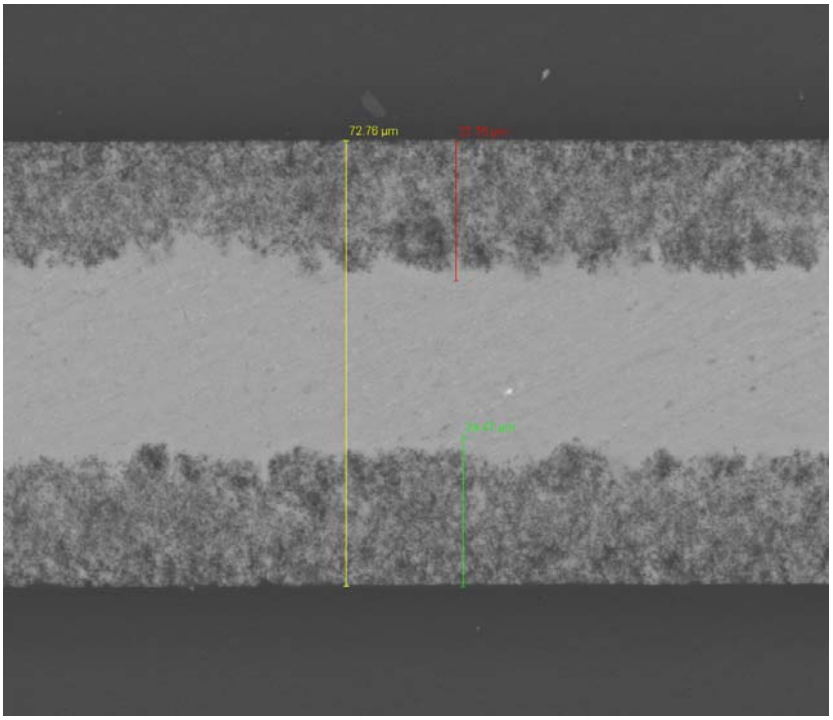

Figure 27: E-SEM image of anode foil and porous oxide layer (Failed Capacitor C1 from Ripple Current Testing)

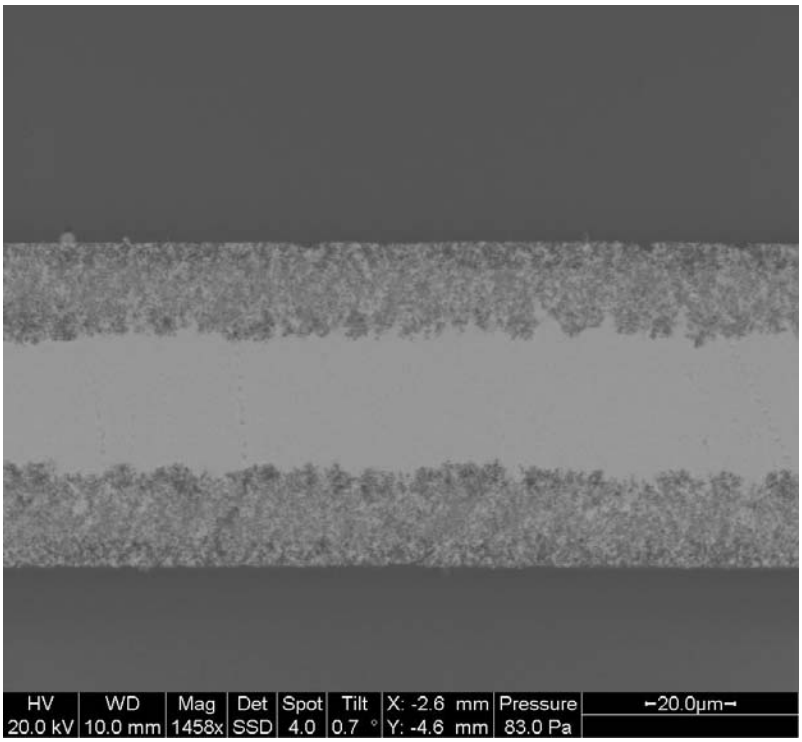

Figure 28: E-SEM image of the anode foil and oxide layer on top of it (Failed Capacitor C1 from Voltage Testing)

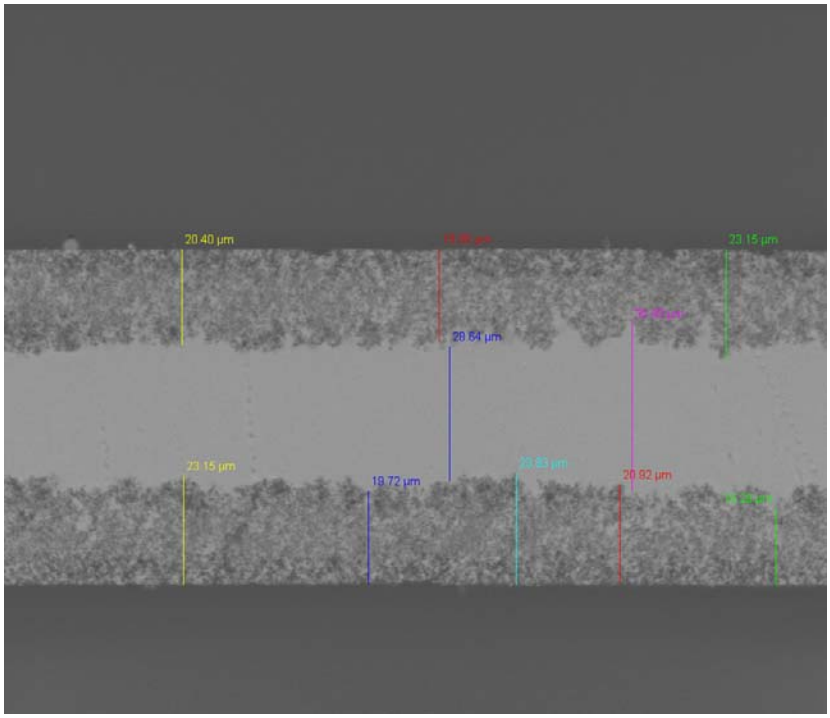

Figure 29: E-SEM image of the anode foil and porous oxide layer (Failed Capacitor C1 from Voltage Testing)

2.7 XPS Analysis

The capacitance value of the capacitor depends directly of the dielectric constant of the dielectric material. In aluminum electrolytic capacitors, aluminum oxide is the dielectric. If there is any change in the chemical composition of the dielectric oxide layer, that will lead to a change in the capacitance value of the capacitor.

Capacitance value is also directly proportional to the overlapping surface area of the electrodes. Any change is surface area affects the capacitance value. In aluminum electrolytic capacitors manufacturing, high purity aluminum (99.9%) is etched to increase (80~100 times) the surface area. The aluminum oxide dielectric is grown electrochemically on the surface of this highly etched aluminum anode foil; the electrochemically grown oxide layer consists of numerous micro pores and appears like a sponge with very high surface area to attain high capacitance value. Change in surface area of the aluminum oxide layer will lead to a change in capacitance value.

Capacitors C1 and C2, in all the three tests (Ripple Current, Voltage and Temperature) exhibited decrease in capacitance value. As we know that the electrolyte weight loss was about the same at a particular test time for the capacitors in the temperature, voltage and ripple current life testing. But, the capacitance drop was fastest in voltage-tested samples followed by ripple current –tested samples and temperature-tested sample. Additional capacitance drop was investigated using XPS analysis on the dielectric aluminum oxide layer of the failed and unused samples to find if there was any chemical compositional change.

X-Ray Photoelectron Spectroscopy (XPS) is one of the most common chemical surface analysis techniques, to determine the elemental composition of surfaces and the electronic configuration of the chemical species present on a surface, and the chemical profile as a function of depth. XPS is based on the photoelectric effect where a photon is bombarded onto the material of study. This phenomenon can be explained by the Equation $E_B = h\upsilon - KE$, E_B is the binding energy of the electron in the atom, h is the Planck constant, υ is the frequency, and KE is the Kinetic energy of the emitted electron and that energy is detected by the XPS spectrometer.

X-Ray Photoelectron Spectroscopy been used to determine the electronic state of the chemical compounds present on the surface of the aluminum oxide, after life tests, capacitors were opened, and anode foil was cut in square approximately of 1 x 1 cm. Samples of anode foil with oxide layer on the surface were cleaned successively in a ultrasonic cleaner with acetone, hexane and isopropyl alcohol to remove the electrolyte residue embedded in the aluminum oxide layer. Samples from all life tests (Temperature, Ripple Current, and Voltage) were analyzed by XPS equipment to determine the compositions on the aluminum oxide surface. No new compounds were detected in aluminum oxide layer. The elements detected in the surface scan were C, O, Al, P and N. Ammonium adipate is used to electrochemically perform primary anodization of the anode foil [81]. The voltage used during the anodization is called forming voltage which is usually 30 to 40% higher than the rated voltage of the capacitor. It is known that heating the anodized aluminum foil at 500C for 2 minutes changes aluminum oxide to amorphous to crystalline [82]. Re-anodization on the oxide layer to repair defects, increase the resistance, and lower the leakage current of

the anodic film is performed. Ammonium dihydrogen phosphate/phosphoric acid are used for re-anodization. Phosphorus provides better hydration resistance to aluminum oxide [81]. If phosphorous containing compound is used only for re-anodization, the phosphorous layer is only adsorbed on the surface. The thickness of the formed dielectric oxide layer on top of high purity (99.99%) anode aluminum foil is 1.3-1.5 nano-meter/volt [11]. The forming voltage is about 30%-40% more than the rated voltage of the capacitors.

During the XPS analysis on the surface of the oxide layers, in the O 1s region, aluminum phosphate/C-O, aluminum oxide and C=O peaks were detected. C=O peaks were from residue of gamma butyrolactone based electrolyte. The maximum C=O concentration was found on the temperature tested sample. The C=O concentration in samples from different tests is shown in Figure 30. Maximum C=O concentration was found in temperature sample and followed by ripple current and voltage tested sample.

		Voltage	**Ripple Current**	**Temperature**
	O1s			
	Binding Energy (eV)	% Area	% Area	% Area
C=O (From Electrolyte)	**533.15**	**4.98**	**7.61**	**17.13**

Figure 30: XPS analysis of failed C1 capacitors showing the C=O concentration

Liquid aluminum electrolytic capacitors have self healing property. Self healing occurs when a voltage is applied to the capacitor. Any localized damage to the aluminum oxide layer is self-healed or reformed by water present in the liquid

electrolyte. Oxygen from the water molecule reacts with aluminum at anode to reform or self heal aluminum oxide. H+ from water forms hydrogen gas at cathode. Self healing process only takes place in presence of voltage. Voltage and ripple current tested samples were tested with voltage and self healing process could have clogged some of the micro-porous aluminum oxide dielectric. Temperature tested sample did not experience voltage; therefore no self healing took place in the temperature sample. The XPS result reflected this; because of no self healing, the temperature sample retained its porous structure and maximum electrolyte residue (C=O) was observed in the O 1s peak of temperature tested sample. Because of the self healing process (formation of aluminum oxide), the porosity of voltage and ripple current tested samples reduced which was reflected by lower C=O electrolyte residue than the temperature sample. Among voltage and ripple current samples, voltage sample had less C=O. This could be due to constant 35V DC voltage. In the ripple current tested sample, the peak of the ripple voltage was 35V and constant 35V was not applied. This could have lead to less self healing that the voltage tested sample and consequently more porous oxide dielectric structure than the voltage sample.

- Capacitance loss in the voltage and RC sample was due to evaporation of electrolyte and self healing of the aluminum oxide layer which caused blockage of pores of the oxide layer leading to reduction in surface area of the oxide layer.
- Capacitance loss in the temperature sample was due to evaporation of electrolyte. There was no self-healing in the temperature sample due to absence of voltage.

- In summary, the total capacitance loss in different tested samples is shown in Table 4.

Temperature	Ripple Current	Voltage
11% electrolyte loss	7.5% electrolyte loss plus reduction in oxide area	5% Electrolyte loss plus reduction in oxide area

Table 4: Summary of total capacitance loss in different tested samples

In summary

- Ripple current tested and voltage tested capacitors failed by same failure mechanisms.
- For γ-butyrolactone based capacitors
  - The capacitance drop was due to evaporation of electrolyte and reduction in anode oxide surface area.
  - The ESR increase was due to evaporation of electrolyte.
- For ethylene glycol based capacitors
  - Increase of ESR was due to evaporation of electrolyte and decease in conductivity of the electrolyte due to formation of esters and amides and decrease in concentration of carboxylic acid salts.

3: Evaluation of Polymer Aluminum Electrolytic Capacitors in Elevated Temperature Humidity Environment

3.1 Objectives

- Determine failure modes and mechanisms of polymer aluminum electrolytic capacitors in elevated temperature humidity environment.
- Develop rapid assessment method for polymer aluminum electrolytic capacitors for elevated temperature and humidity environment.

3.2 Experimental Approach Used in Study

- Procured comparable polymer aluminum electrolytic capacitors from two different manufacturers (A and B), including one set each of SMT (Surface Mount) and through-hole (TH).
- Performed testing at elevated temperature and humidity (85ºC, 85% RH); measured electrical parameters of capacitors at 25°C.
- Performed HAST (110°C, 85% RH) testing using the same capacitors, and compared lifetimes and failure modes and mechanisms to results of 85°C, 85%RH test.
- Electrical parameters (capacitance, dissipation factor, ESR and leakage current) were measured during the tests.

3.3 Test Plan

In the study presented in this paper, winding construction type surface mount and thru-hole PA capacitors from two top-tier manufacturers were exposed to elevated temperature-humidity conditions (85ºC, 85% RH). There are no rapid assessment tests for elevated temperature-humidity evaluation of polymer aluminum capacitors. Therefore, along with elevated temperature-humidity test, HAST (110ºC, 85% RH) test was also performed to evaluate and compare the failure modes and mechanisms of the two tests. Ten samples each of surface mount (SMT) and thru-hole from two manufacturers were exposed to the elevated temperature humidity and HAST testing. Failure analysis of failed capacitors was performed after testing. One set each of 10 surface mount and thru-hole polymer aluminum electrolytic capacitors from two top-tier electrolytic capacitor manufacturers were chosen. The capacitors were opened and Raman spectroscopy was performed on the polymer to confirm that the polymer was PEDOT. Polymer in all the capacitors was found to be PEDOT. Figure 31 shows the Raman spectrograph of the polymer which shows the characteristic peaks of PEDOT shown in the small PEDOT spectrograph image from literature [39]. All the chosen polymer capacitors were rated for 6.3 volts and 220µF. Two tests i.e., elevated temperature-humidity and HAST were performed on the polymer capacitors from the two manufacturers (A & B). Table 5 contains details of test samples and the tests. The electrical properties like capacitance, dissipation factor (DF), leakage current (LC) and equivalent series resistance (ESR) were measured for all the polymer capacitors before the tests started. Periodically, the tests were stopped and capacitors were allowed to cool down to room temperature (25ºC) and electrical

properties measurements were performed. The failure criteria for different electrical parameters from the respective part datasheets is shown in Table 6.

	Manufacturer A	**Manufacturer B**
Surface Mount	Polymer (10 samples per test type) (6.3mm x 6mm)	Polymer (10 samples per test type) (8mm x 7mm)
Through-Hole	Polymer (10 samples per test type) (6.3mm x 10.5mm)	Polymer (10 samples per test type) (6.3mm x 10.5mm)

Table 5: Test Plan, One complete set of samples was subjected to each of the <u>two test conditions</u>: temperature-humidity <u>(85C, 85%RH)</u> and HAST <u>(110°C, 85% RH).</u>

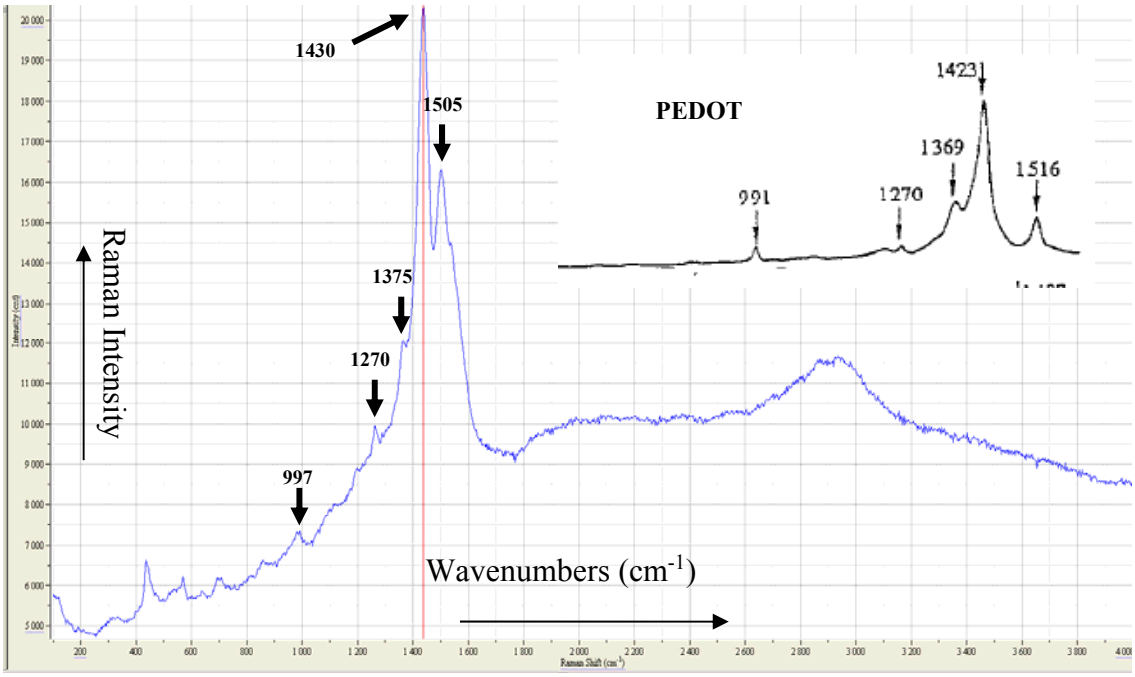

Figure 31: Raman spectrograph of the polymer confirmed the polymer to be PEDOT

	Capacitance (µF) 120 Hz	**DF 120 Hz**	**Leakage Current (µA)**	**ESR (mΩ) 100 KHz**
B (SMT)	<176 or >264	> 0.18	> 277	> 37.5 + 3
A (SMT)	<176 or >264	> 0.18	> 416	> 15 + 3
B (Thru-hole)	<176 or >264	> 0.18	> 277	> 30
A (Thru-hole)	<176 or >264	> 0.12	> 277	> 30

Table 6: Failure Criteria

3.4 Elevated Temperature-Humidity Test

Elevated temperature-humidity test (85ºC, 85%RH) revealed that the dominant failure mode for manufacturer 'A' SMT capacitors was increase in leakage current and all 10 capacitors failed within 2133 hours. The remaining polymer capacitor sets i.e. SMT capacitors from manufacturer B and thru-hole capacitors from manufacturer 'A' and 'B' were tested for 3450 hours. Similar to the manufacturer A SMT capacitors, the manufacturer A thru-hole capacitors also exhibited increase in leakage current. Only 2 thru-hole capacitors from manufacturer 'A' failed due to increase in leakage current but all 10 thru-hole capacitors from manufacturer 'A' showed increase in leakage current behavior. Surprisingly the dominant failure mode for the manufacturer 'B' SMT and thru-hole capacitors was different from the dominant failure mode of Manufacturer 'A' SMT and thru-hole capacitors. 3 failures due to increase in ESR in manufacturer 'B' SMT capacitors were observed. The other 7 non-failed manufacturer 'B' SMT capacitors also exhibited increase in ESR. In 3 thru-hole capacitors from manufacturer 'B', failure due to high ESR was observed, but the rest manufacturer 'B' thru-hole also exhibited increase in ESR. In summary, both manufacturer 'A' and 'B' PA capacitors exhibited different dominant failure modes. Manufacturer 'A' PA capacitors exhibited increase in leakage current and manufacturer 'B' PA capacitor exhibited an increase in ESR. Figure 32 shows average leakage current plot of both manufacturer 'A' and 'B' PA capacitors under elevated temperature-humidity test. Figure 33 shows average ESR plot of both manufacturer 'A' and 'B' PA capacitors under elevated temperature-humidity test. Table 7 shows average capacitance, leakage current and ESR values of the PA

capacitors from both manufacturers before and after elevated temperature humidity testing.

		Average Before Testing	Average After Testing
A SMT	Capacitance (µF)	233.9	230.5
	Leakage Current (µA)	28.7	3539.3
	ESR (mΩ)	9.36	13.2
A Thru-hole	Capacitance (µF)	232.7	231.6
	Leakage Current (µA)	2.94	403.6
	ESR (mΩ)	5.6	17.4
B SMT	Capacitance (µF)	216.4	217.6
	Leakage Current (µA)	5.9	190.2
	ESR (mΩ)	13.7	28.8
B Thru-hole	Capacitance (µF)	224.1	220.3
	Leakage Current (µA)	1.2	10.7
	ESR (mΩ)	7.6	25.7

Table 7: Average Capacitance, Leakage Current and ESR values of the polymer capacitors from both manufacturers before and after elevated temperature-humidity testing

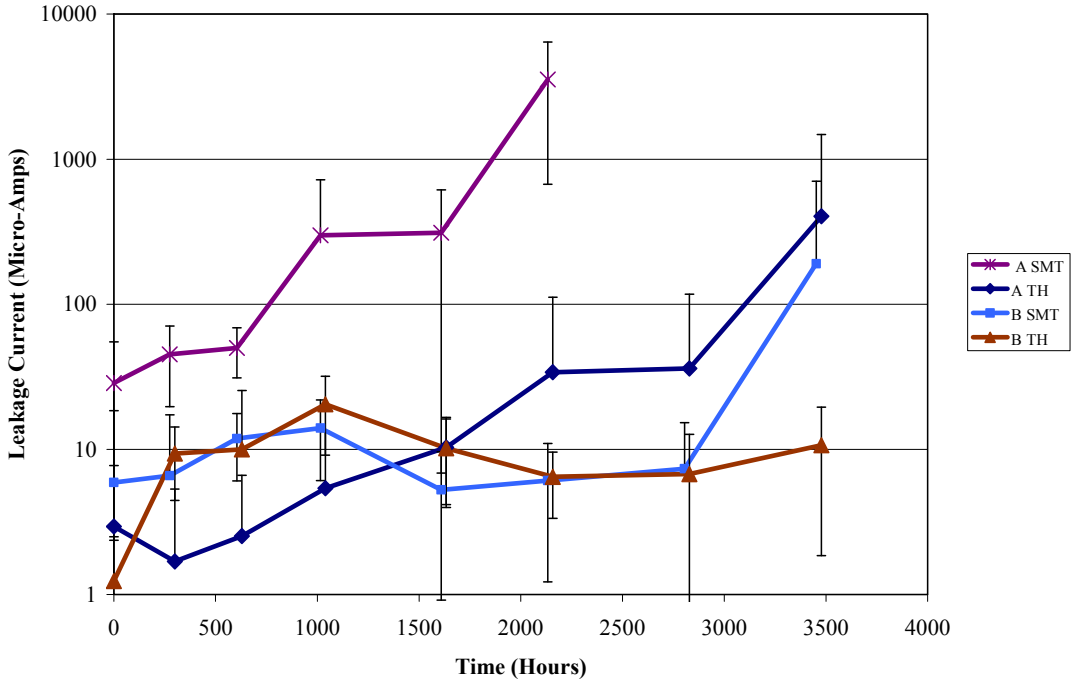

Figure 32: Average leakage current plot of both manufacturer A and B PA capacitors under elevated temperature-humidity test

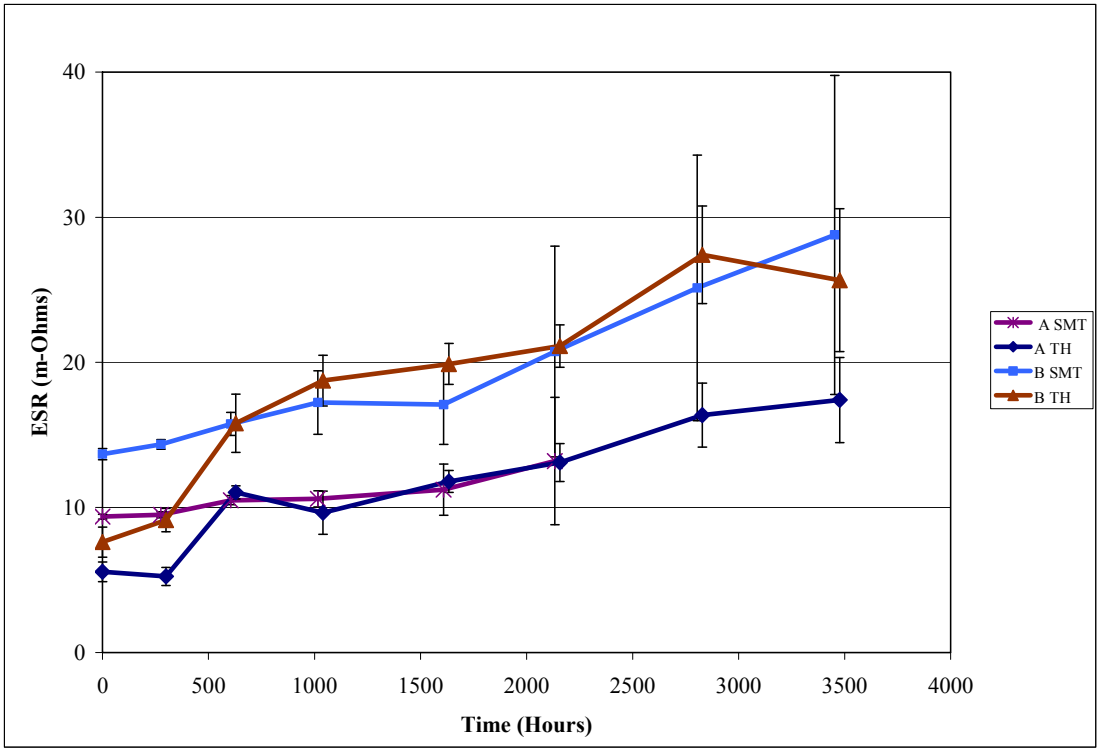

Figure 33: Average ESR plot of both manufacturer A and B PA capacitors under elevated temperature-humidity test

3.5 HAST Test Results

In HAST testing (110ºC, 85% RH), the earliest failures were observed in the SMT PA capacitors from both manufacturers. Among SMT capacitors from manufacturers 'A' and 'B', SMT capacitors from manufacturer 'A' failed earlier than capacitors from manufacturer 'B'. Thru-hole PA capacitors from both manufacturers 'A' and 'B' failed after the respective SMT PA capacitors. Surprisingly, again like the elevated temperature humidity test (85ºC, 85%RH) the dominant failure mode in PA capacitors from both manufacturers was different. Dominant failure mode for capacitors from manufacturer 'A' was increase in leakage current (All 10) and for capacitors from manufacturer 'B', dominant failure mode was increase in ESR (All 10). Figure 34 shows the average leakage current plot for the manufacturer 'A' and

'B' PA capacitors during HAST test, all manufacturer 'A' PA capacitors failed due to increase in leakage current. Figure 35 shows the average ESR plot for the manufacturer 'A' and 'B' PA capacitors during the HAST test, all the manufacturer 'B' PA capacitors failed due to increase in ESR. 6 SMT capacitors from manufacturer 'B' that failed due to increase in ESR, also failed due to increase in leakage current. The other electrical properties remained within datasheet specifications shown in Table 6. 1 thru-hole capacitor from manufacturer 'B' that failed due to increase in ESR, also failed due to increase in leakage current. The other electrical properties remained within datasheet specifications shown in Table 6. Average capacitance, leakage current and ESR values of the PA capacitors from both manufacturers before and after the HAST testing is shown in Table 8.

		Average Before HAST	Average After HAST
'A' SMT	Capacitance (µF)	235	224
	Leakage Current (µA)	73.93	6409.3
	ESR (mΩ)	9.3	13.5
'A' Thru-hole	Capacitance (µF)	234	230.2
	Leakage Current (µA)	22	7220.2
	ESR (mΩ)	5.5	19.6
'B' SMT	Capacitance (µF)	213.7	213.4
	Leakage Current (µA)	7.5	71.5
	ESR (mΩ)	14	226.8
'B' Thru-hole	Capacitance (µF)	223.5	213.5
	Leakage Current (µA)	7.7	75.7
	ESR (mΩ)	8.2	47.2

Table 8: Average Capacitance, Leakage Current and ESR values of the polymer capacitors from both manufacturers before and after the HAST testing

In summary, thru-hole capacitors from both manufacturers performed better than SMT capacitors. Again, like in the elevated temperature humidity test (85ºC,

85%RH), different dominant failure modes were observed in PA capacitors from both the manufacturers. Dominant failure mode for capacitors from manufacturer 'A' was increase in leakage current and for capacitors from manufacturer 'B', dominant failure mode was increase in ESR.

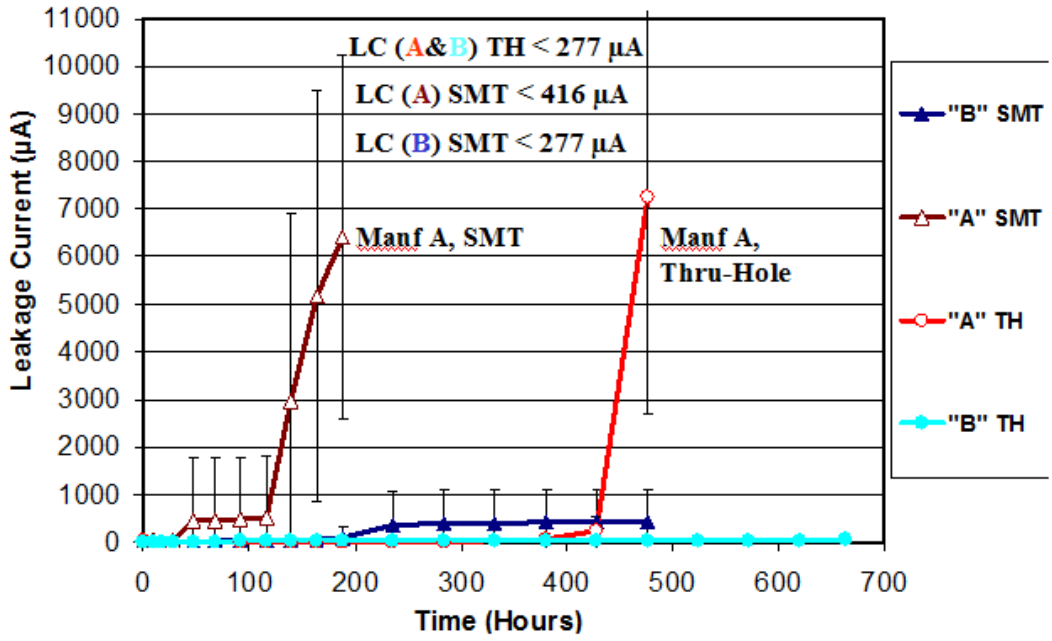

Figure 34: Average leakage current plot of capacitors from manufacturer A under HAST testing

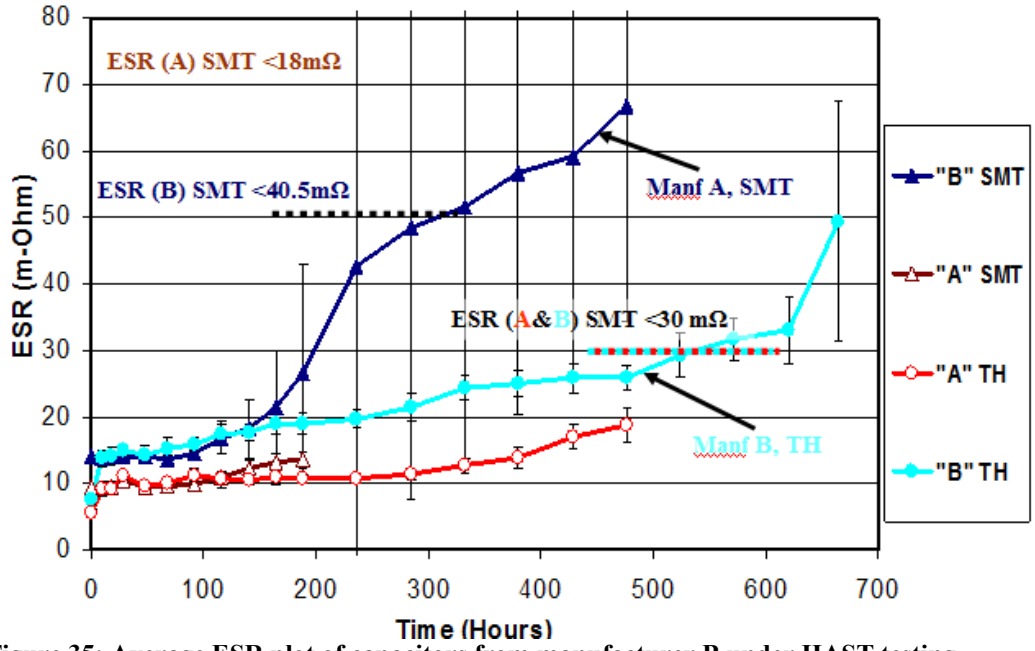

Figure 35: Average ESR plot of capacitors from manufacturer B under HAST testing

3.6 Failure Mechanisms

Failure analysis was performed on the failed PA capacitors to determine the failure mechanisms causing the failures. In elevated temperature-humidity and HAST testing, failed capacitors from manufacturer 'A' exhibited dominant failure mode of increase in leakage current. The PA capacitors were mounted in an epoxy and cross-sectioned and inspected with Environmental scanning electron microscope (E-SEM). E-SEM micrograph of cross-sectioned thru-hole PA capacitor from manufacturer 'A', which failed during the HAST test is shown in Figure 36. Some shiny particles were observed in the porous aluminum oxide dielectric shown in the box in Figure 36. Figure 37 shows E-SEM image of cross-section of SMT HAST tested capacitor from manufacturer 'A'. Energy dispersive X-ray spectroscopy (EDS) mapping of the shiny particles as shown in Figure 40 revealed that the particles consisted of iron. The iron particles provided the electrically conductive path which increased the leakage current of the PA capacitors and caused the failure. Iron particles were found in both manufacturers 'A' & 'B' PA capacitors which failed due to increase in leakage current. No iron particles were found in the untested or new PA capacitors. No iron particles were observed in Figure 39 which shows E-SEM image of cross-section of thru-hole untested capacitor from manufacturer A. No iron particles were observed in the untested PA capacitors.

During the manufacturing of PEDOT PA electrolytic capacitors, the PEDOT polymer is made by a sequential chemical oxidative polymerization where the monomer ethylenedioxithyophene (EDOT) is polymerized by an oxidizer Iron p-toluenesulfonate (Iron (III) salt). During the PEDOT polymerization in the PA

capacitor manufacturing process, an oxidizer solution (Iron p-toluenesulfonate) is applied on the dielectric, followed by application of EDOT [16]. The thickness of the porous dielectric aluminum oxide layer is 1.3~1.5 nano-meter/volt of the forming voltage, which is 30-40% higher than the rated voltage. As the rated voltage for these PA capacitors is 6.3 volts, the thickness of dielectric would be in order of 11~13 nm. During the polymer manufacturing process, the iron (III) salt oxidizes the monomer (EDOT) to polymer (PEDOT) and the iron (III) salt is reduced to iron (II) salt which is supposed to be washed away. If the iron salt is not washed away, it could be sitting on top of the 11~13 nm anode oxide layer. Manufacturer 'B' probably performed a better job than Manufacturer 'A', of washing the iron (II) salt after the sequential polymerization process. This could be the reason that the dominant failure mode in manufacturer 'B' was not increase in leakage current. Another reason could be that Manufacturer 'B' did not use the sequential PEDOT polymerization process. Manufacturer 'B' could have used pre-mixed reactive solutions of EDOT and oxidizer, in such mixtures EDOT and oxidizer can be used in stoichiometric ratio. The residual iron p-toluenesulfonate after the sequential polymerization process in the PA capacitors in elevated humidity environments can react with hydroxyl groups and/or absorbed water on the aluminum oxide surface, to form $Fe(OH)_3$ and p-toluenesulfonic acid (pTSA). The pTSA can cause the defects and the surface dissolution of the dielectric layer. Any damage to the dielectric layer can lead to pores and cracks in the oxide layer. As the iron salts were sitting on top of the oxide layer, the iron particles can get in the oxide layer providing conducting path and increasing the leakage current and thus failing the PA capacitors.

In summary, the failure mechanism for increase in leakage current failures in the PA capacitors was due to iron particles in the dielectric aluminum oxide layer. These iron particles originated from the iron salt used in the PA capacitors manufacturing process.

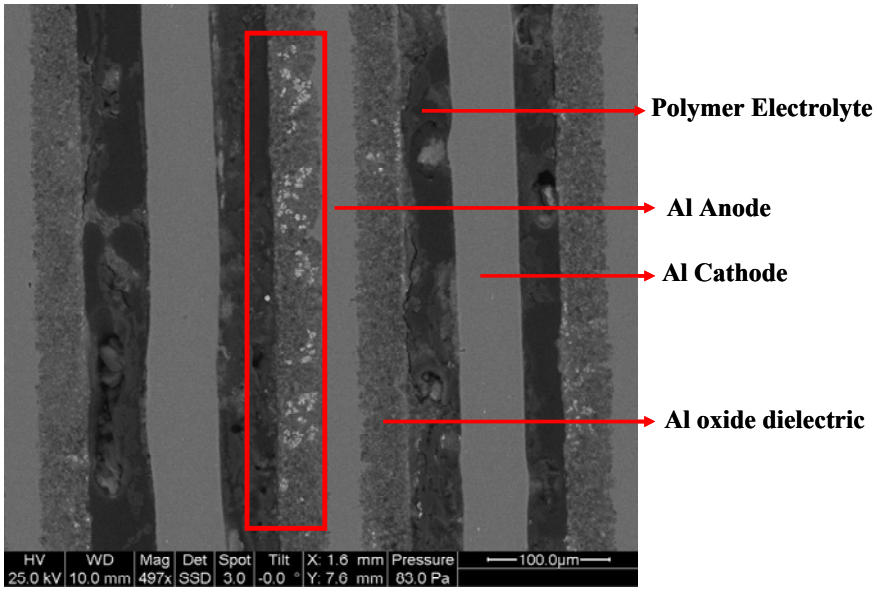

Figure 36: E-SEM image of cross-section of thru-hole HAST tested capacitor from manufacturer 'A'

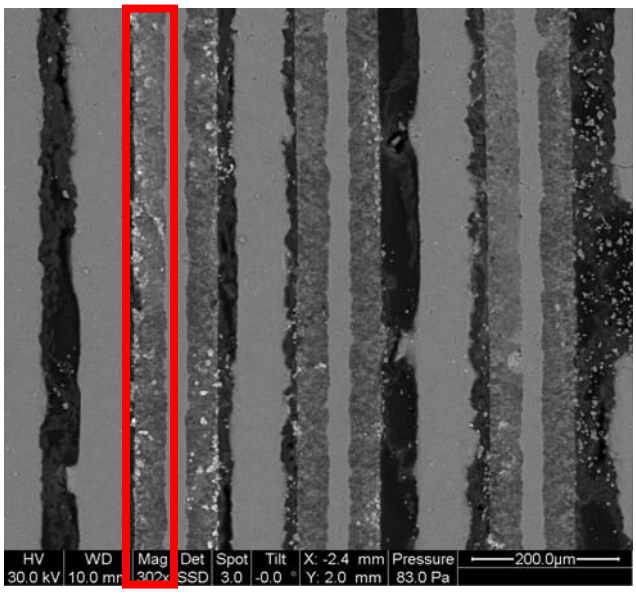

Figure 37: E-SEM image of cross-section of SMT HAST tested capacitor from manufacturer 'A'

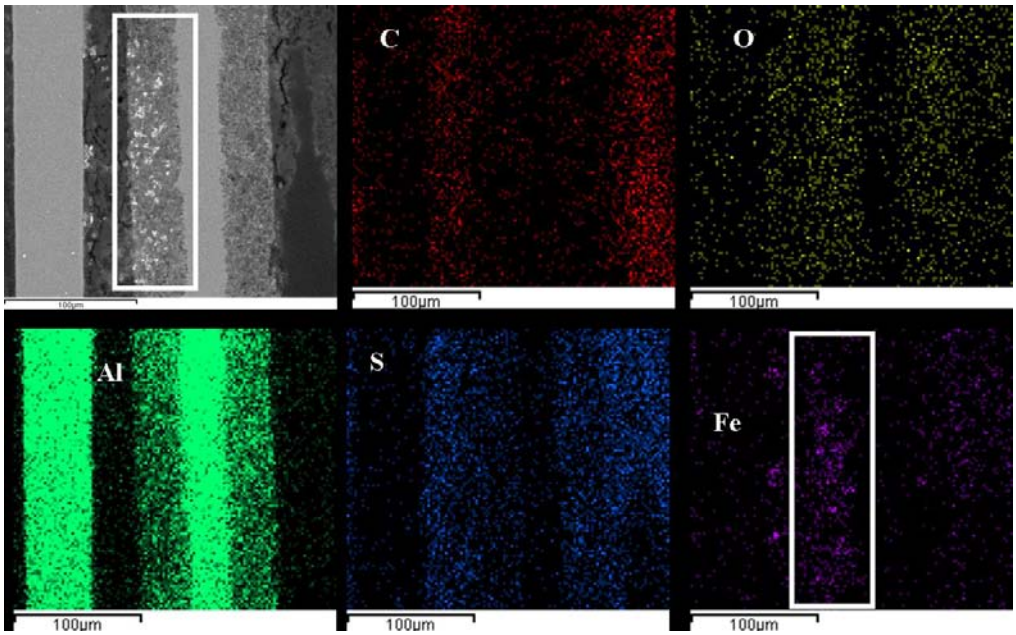

Figure 38: EDS mapping of the shiny particles shows presence of iron particles

Elevated temperature-humidity and HAST tested capacitors from manufacturer 'B' that failed due to high ESR. The charge conduction in PEDOT occurs due to charge hopping [34, 40]. The effect of humidity on PEDOT is to increase the resistivity of the PEDOT. This degradation of PEDOT is spatially inhomogeneous associated with the formation of insulating patches [42]. ESR degradation in the PA capacitors was observed due to degradation of PEDOT polymer causing reduction in conductivity in high humidity conditions.

Surface mount capacitors failed earlier than the thru-hole capacitors for both manufacturers. The rubber seal thickness of SMT PA capacitors was found to be lower than the thickness of the thru-hole PA capacitors. The thickness of Manufacturer 'A' SMT and thru-hole PA capacitors was 1.7 mm and 2.7 mm respectively. The thickness of Manufacturer B SMT and thru-hole PA capacitors was 1.85 mm and 2.7 mm respectively. Better sealing of SMT capacitor can increase the life of SMT PA capacitors in high humidity environments.

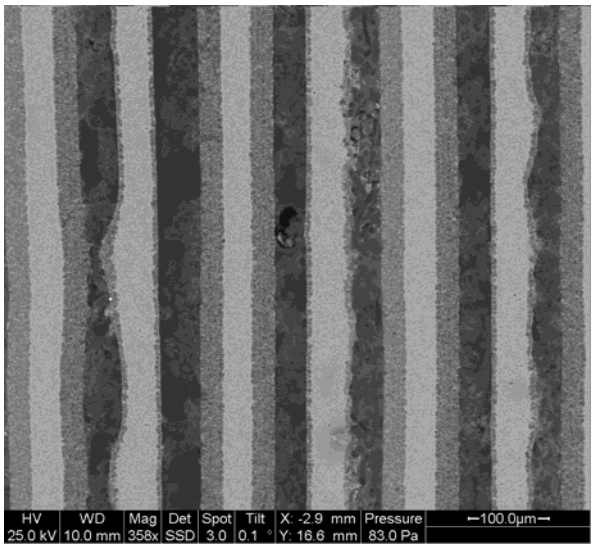

Figure 39: E-SEM image of cross-section of thru-hole untested capacitor from manufacturer A. No shiny iron particles were observed in the untested samples

4: Conclusions

4.1 Liquid Aluminum Electrolytic Capacitors

- Ripple current tested and voltage tested capacitors failed by same failure mechanisms.
- For γ-butyrolactone based capacitors
  - The capacitance drop was due to evaporation of electrolyte and reduction in anode oxide surface area.
  - The ESR increase was due to evaporation of electrolyte.
- For ethylene glycol based capacitors
  - Increase of ESR was due to evaporation of electrolyte and decease in conductivity of the electrolyte due to formation of esters and amides and decrease in concentration of carboxylic acid salts.

4.2 Polymer Aluminum Electrolytic Capacitors

- SMT capacitors failed earlier than the thru-hole capacitors.
  - This could be due to thicker rubber used in sealing the thru-hole capacitors than the SMT capacitors.
- Dominant failure modes in HAST and Temperature-Humidity were identical, involving leakage current failures for Manufacturer 'A' capacitors and ESR increase for Manufacturer 'B' capacitors.
  - HAST can be used as a rapid assessment tool for PA capacitors at elevated temperature-humidity conditions.

- High ESR failures were due to degradation of the polymer PEDOT under elevated humidity.
- High leakage current was due to iron particles in the dielectric layer. During manufacturing, sequential polymerization of EDOT is performed using iron (III) salt as the oxidizer.

5: Contributions

5.1 Liquid Aluminum Electrolytic Capacitors

- Determined the failure mechanisms in liquid aluminum electrolytic capacitors undergoing ripple current and voltage testing.
  - Failure mechanisms observed with and without ripple current were the same.
  - If the ESR does not change and the capacitors fail due to drop in capacitance, it can be due to reduction in surface area of the oxide layer and evaporation of electrolyte.
  - If the capacitors fail due to increase in ESR, it could be due to evaporation of liquid electrolyte or decrease in electrical conductivity of the liquid electrolyte or combination of both these mechanisms.
- Determined failure mechanisms for liquid aluminum electrolytic capacitors based on the solvent used in the capacitor electrolyte.
  - For γ-butyrolactone based capacitors
    - The mechanism of capacitance drop could be due to evaporation of electrolyte and reduction in surface area of the oxide layer.
    - The mechanism of ESR increase could be due to evaporation of electrolyte.

- For ethylene glycol based capacitors
    - The mechanism of increase in ESR could be due to evaporation of electrolyte and decrease in conductivity of the electrolyte due to esters and amides formation and decrease in the concentration of carboxylic acid salts.

5.2 Polymer Aluminum Electrolytic Capacitors

- Identified a new failure mechanism of PA capacitors in elevated temperature and humidity.
    - Increase in leakage current was due to iron particles in the dielectric layer. Iron salts are used in the polymerization process of PEDOT during the capacitor manufacturing process.
- Developed rapid assessment test (HAST) to evaluate performance of PA capacitors in elevated temperature humidity (> 85ºC, 85%RH) performance.

6: Future Work

6.1 Liquid Aluminum Electrolytic Capacitors

The drop in capacitance for C1 capacitors (γ-butyrolactone based) was due to liquid electrolyte evaporation and reduction in surface area of the dielectric aluminum oxide layer in the voltage and ripple current tested capacitors due to self-healing. To quantify the reduction in surface area for the voltage and ripple current tested sample, specific surface area (SSA) analysis should be performed.

6.2 Polymer Aluminum Electrolytic Capacitors

To evaluate the porosity of the aluminum oxide dielectric layer and to find out where the iron salts were inside the porous dielectric layer, Transmission Electron Microscopy (TEM) analysis should be performed.

Current work on elevated temperature-humidity behavior of Polymer Aluminum Electrolytic Capacitors was performed to determine the failure modes and failure mechanisms during the storage condition without application of bias. Follow up work should be performed to determine the failure modes and mechanisms of Polymer Aluminum Electrolytic Capacitors under elevated temperature-humidity and applied voltage environment.

In order to validate if the smaller size of rubber seal was responsible to early failure of SMT PA capacitors, the weight should be monitored and compared as the percentage weight increase of the initial coiled structure. If the size of SMT PA

capacitor is smaller than thru-hole PA capacitor, there will be less polymer electrolyte inside the SMT PA capacitor as compared to thru-hole PA capacitor which will degrade quicker. The thinner rubber seals of the SMT PA capacitors will let the moisture seep inside the SMT PA capacitors body quicker too than the thru-hole PA capacitors as they have thicker seal.

Appendices

During the present on liquid aluminum electrolytic capacitor, for volatility analysis of liquid electrolyte, a TGA (Thermogravimetric Analysis) methodology for volatility analysis was developed. For chemical evaluation of the liquid electrolyte, a FTIR (Fourier Transform Infrared) methodology was developed. The developed TGA & FTIR methodologies can be used for detection of counterfeit liquid aluminum capacitors. These TGA and FTIR techniques were added to be published in the SAE AS1671, "Test Methods Standard; Counterfeit Electronic Parts". Specifics of the standard are:

- SAE AS6171, Test Method VIIj, "Technique for Suspect/Counterfeit EEE Parts Detection by Thermogravimetric Analysis (TGA) Test Method".
- SAE AS6171, Test Method VIIf, "Technique for Suspect/Counterfeit EEE Parts Detection by Fourier Transform Infrared Spectroscopy (FTIR) Test Method".

Below is the detailed text and figures from the standards.

Detection of Counterfeit Electrolytic Capacitor Using Thermo-gravimetric Analysis (TGA) of Electrolyte

The following example illustrates the application of TGA in detection of a counterfeit liquid aluminum electrolytic capacitor. The capacitors in this example had been used in ballasts for arc lamps intended for medical and industrial applications. A contract manufacturer purchased the capacitors from a parts broker because the parts were not available from the authorized distributors or independent

suppliers within the required lead time. Approximately 4000 power supply units were manufactured using the capacitors obtained from the broker. Early failures in the field, and reduced reliability in laboratory tests, led to the suspicion that the capacitors were counterfeit.

To establish the authenticity of the suspect capacitors, known authentic capacitors were obtained from an authorized distributor for comparison. Both the known authentic capacitors and the DUT were opened and the separator paper soaked with liquid electrolyte was removed. Since there was not enough electrolyte to squeeze out of the paper for analysis, the separator paper soaked in the electrolyte was used as the sample. The separator paper close to the core of the capacitor was used since it contained more electrolyte. The weight of the separator paper sample was in the 18-20 mg range. The purge or flow gas used in the analysis was air. The TGA sample holder was made of alumina and the test was run from ambient room temperature (25ºC) to 250ºC. The temperature ramp rate used was 5ºC/minute. A maximum temperature of 250ºC was chosen because temperatures beyond that can cause the paper layer to oxidize and combust.

The results of a TGA measurement are usually displayed as a TGA curve in which weight is plotted against temperature or time. An alternative and complementary way is to use the first derivative of the TGA curve with respect to temperature or time (dm/dT). In this case, it shows the rate at which the electrolyte evaporates and is known as differential electrolyte weight loss or DEWL. The

DEWL curves from electrolytes had to be normalized so that they could be compared. For a particular capacitor electrolyte, the normalized DEFL curve is repeatable like a fingerprint, and can therefore be used for detection of counterfeit capacitors. The normalization process is described below:

$$Wtotal = Wp + Wve + Wnve$$

Where:

W_{total} = Total weight of the TGA sample (Paper separator soaked with electrolyte)

W_P = Weight of the paper

W_{VE} = Weight of the volatile constituents of the electrolyte (up to 250ºC)

W_{NVE} = Weight of the non-volatiles in electrolyte (up to 250ºC)

The volatile component of the TGA sample (WVE) is the portion of interest. To remove the effect of non-volatiles in the electrolyte and the weight of the paper from the analysis of the differential curve (dm/dT), dm/dT was divided by WVE to obtain the fractional differential electrolyte weight loss (FDEWL) curve which is the normalized curve.

$$FDEWL = \frac{dm}{dt} x \frac{1}{WVE}$$

The FDEWL curve in Figure 40 was obtained from electrolytes of two identical known authentic capacitors. Two separate analyses were performed and the FDEWL curve showed good repeatability between the two runs.

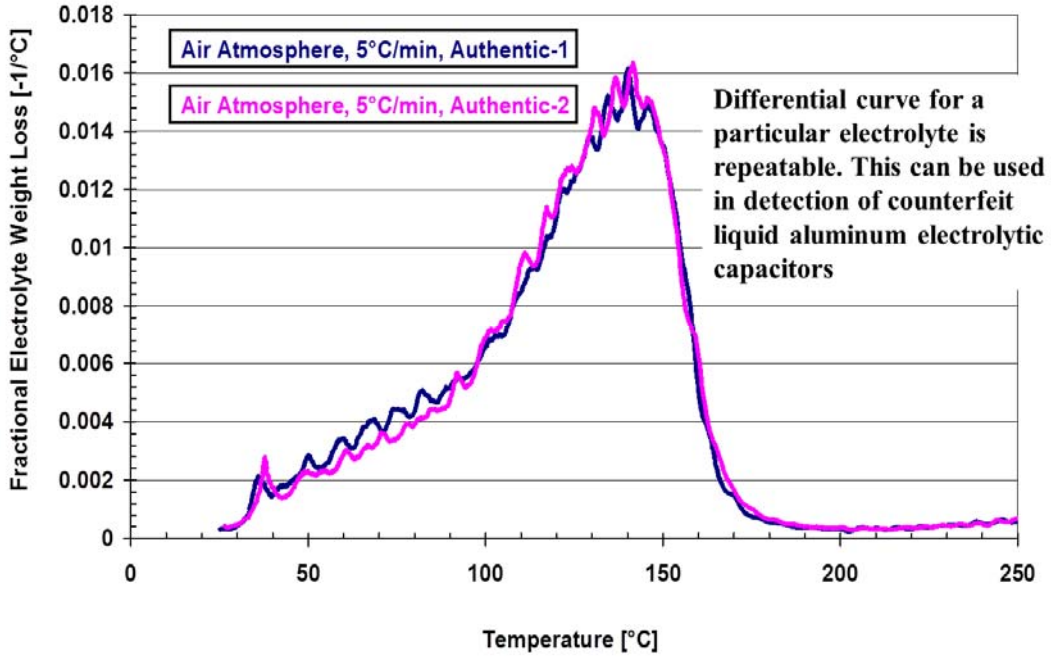

Figure 40: Two Separate FDEWL curves for the electrolytes from two authentic capacitor showing excellent repeatability

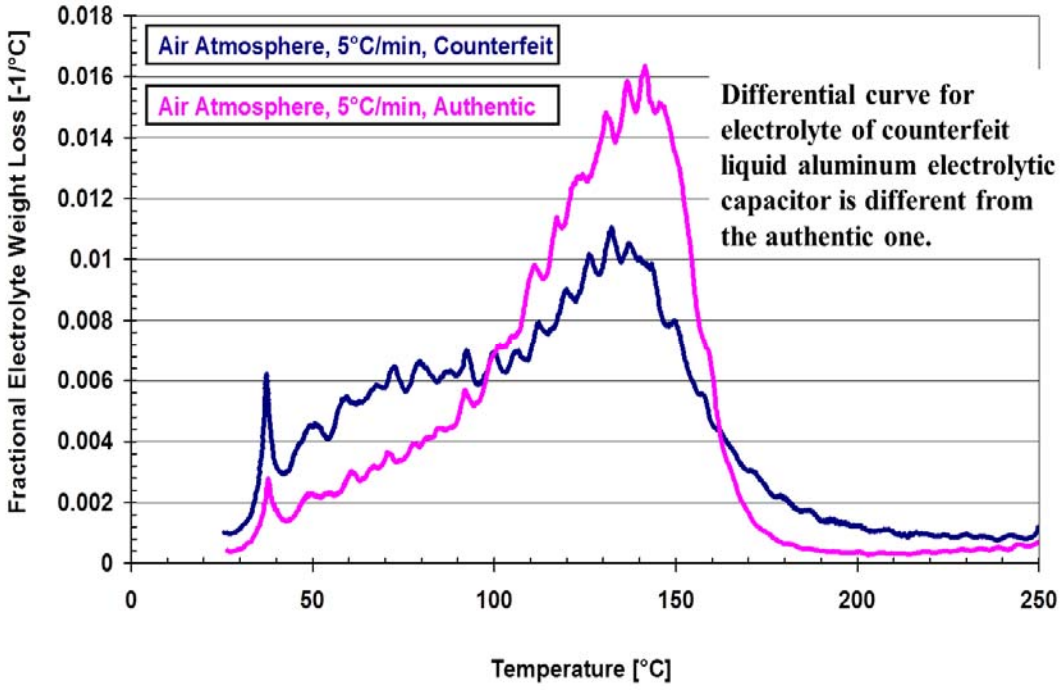

Figure 41: Two FDEWL curves of the electrolytes from the authentic and the counterfeit capacitor

Detection of Counterfeit Electrolytic Capacitor Using FTIR Spectroscopic Analysis of Electrolyte

The following example illustrates the application of FTIR spectroscopy to the detection of a counterfeit liquid aluminum electrolytic capacitor. The capacitors in this example had been used in ballasts for arc lamps intended for medical and industrial applications. A contract manufacturer purchased the capacitors from a parts broker because the parts were not available from the authorized distributors or independent suppliers within the required lead time. Approximately 4000 power supply units were manufactured using the capacitors obtained from the broker. Early failures in the field, and reduced reliability in laboratory tests, led to the suspicion that the capacitors were counterfeit.

To establish the authenticity of the suspect capacitors, known authentic capacitors were obtained from an authorized distributor for comparison. Both the known authentic capacitors and the suspect capacitors were opened and the separator paper soaked with liquid electrolyte was removed. The electrolyte was squeezed out of the paper layer and was transferred to the reflective element of an ATR assembly.

The spectra in Figure 42 were obtained from the electrolyte of the known authentic capacitor. Two separate analyses were performed, and the figure shows that repeatability between the two runs was excellent.

The spectrum obtained from the counterfeit capacitor's electrolyte is compared to that from the known authentic capacitor in Figure 43, and a portion of that spectrum is

shown in greater detail in Figure 44. The FTIR spectra revealed that the main solvent found in the capacitor electrolyte (both authentic and counterfeit) was ethylene glycol, but the corresponding peaks in the spectrum from the counterfeit capacitor have higher percentage transmittance than the peaks from the known authentic capacitor. From the comparison of FTIR peaks of the counterfeit and authentic electrolytes, it was apparent that the concentration of ethylene glycol in the counterfeit electrolyte was lower than that in the authentic electrolyte, and the relative concentration of water to ethylene glycol was higher in the counterfeit electrolyte.

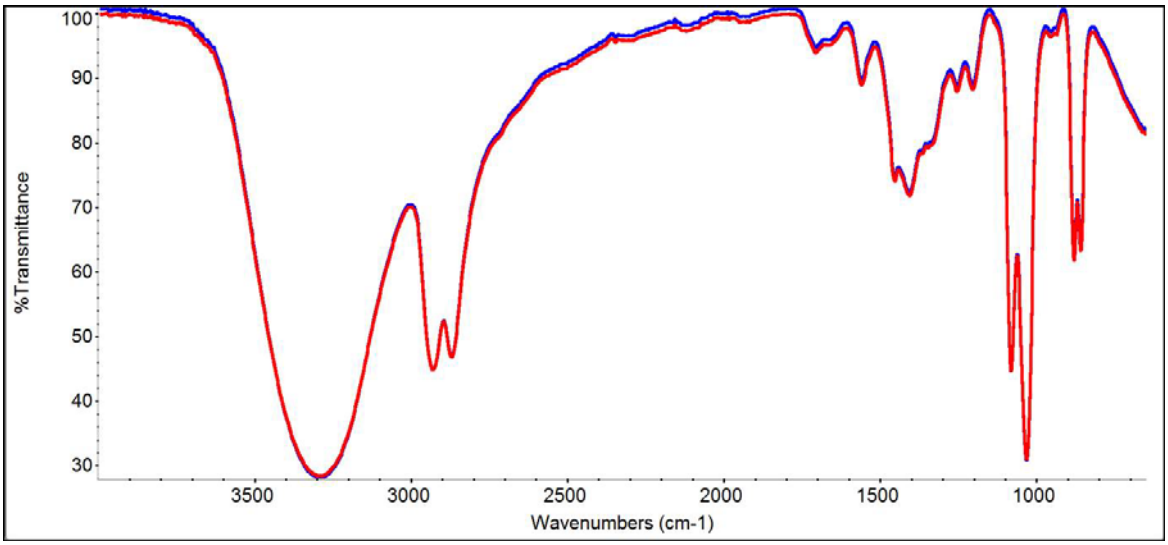

Figure 42: Two FTIR spectra collected from the electrolyte of a known authentic aluminum electrolytic capacitor

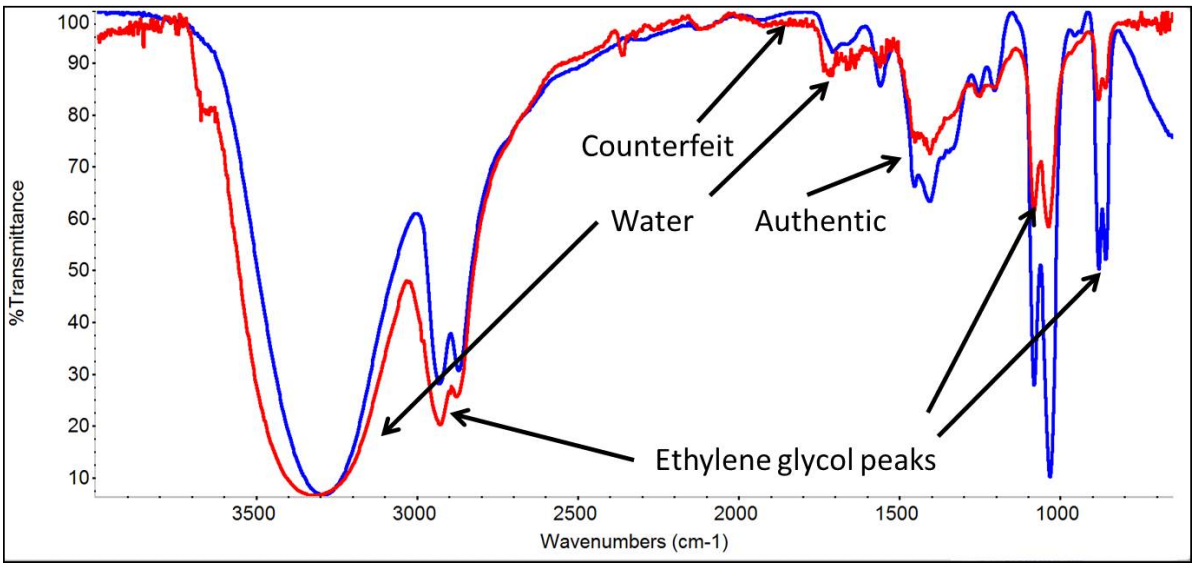

Figure 43: FTIR spectra collected from the electrolytes of a known authentic aluminum electrolytic capacitor and suspected counterfeit capacitor

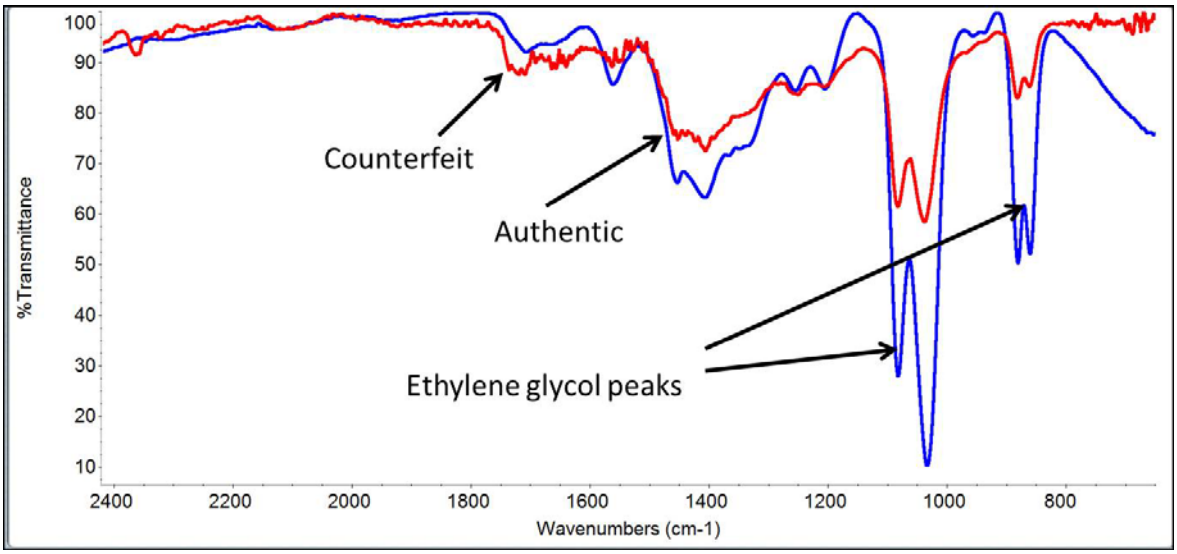

Figure 44: Portion of the FTIR spectra collected from the electrolytes of a known authentic aluminum electrolytic capacitor and a suspected counterfeit capacitor.

Paper published on counterfeit liquid electrolytic capacitor detection using technique developed using FIR analysis for chemical analysis of the liquid electrolyte in *IEEE Transactions on Reliability, June 2014*

TITLE: Detection and Reliability Risks of Counterfeit Electrolytic Capacitors

ABSTRACT

Counterfeit electronics have been reported in a wide range of products, including computers, medical equipment, automobiles, avionics, and military systems. Counterfeiting is a growing concern for original equipment manufacturers (OEMs) in the electronics industry. Even inexpensive passive components such as capacitors and resistors are frequently found to be counterfeit, and their incorporation into electronic assemblies can cause early failures with potentially serious economic and safety implications. This study examines counterfeit electrolytic capacitors that were unknowingly assembled in power supplies used in medical devices, and then failed in the field. Upon analysis, the counterfeit components were identified, and their reliability relative to genuine parts was assessed. This paper presents an offline reliability assessment methodology and a systematic counterfeit detection methodology for electrolytic capacitors, which include optical inspection, X-Ray examination, weight measurement, electrical parameter measurement over temperature, and chemical characterization of the electrolyte using Fourier Transform Infrared Spectroscopy (FTIR) to assess the failure modes, mechanisms, and reliability risks. FTIR was successfully able to detect a lower concentration of ethylene glycol in the counterfeit capacitor electrolyte. In the electrical properties measurement, the distribution of values at room temperature was broader for counterfeit parts than for

the authentic parts, and some electrical parameters at the maximum and minimum rated temperatures were out of specifications. These techniques, particularly FTIR analysis of the electrolyte and electrical measurements at the lowest and highest rated temperature, can be very effective to screen for counterfeit electrolytic capacitors.

INTRODUCTION

Counterfeit electronic components are a problem not only for the electronics industry but also to the society as a whole, which depends on electronics from transportation to home care equipment. Original equipment manufacturers (OEMs) are concerned about counterfeiting because counterfeit parts can compromise the reliability of their final products [43]–45]. Concern about counterfeiting has generally focused on high-cost components, such as integrated circuits. However, less expensive passive components, such as capacitors and resistors, can also cause serious system reliability problems. In the past, counterfeit electrolytic capacitors with faulty electrolytes have resulted in failures of electronic equipment made by big companies like Dell, IBM, HP, and Intel [46]. Electrolytic capacitors are known for their reliability problems, and are often the weakest link in the reliability of power electronics systems [47]–[49]. The most common failure mode for liquid aluminum electrolytic capacitors is the gradual degradation of electrical parameters, including a decrease in capacitance, or an increase in equivalent series resistance (ESR). Electrolytic capacitors can also experience catastrophic failures where there is complete loss of functionality due to a short or open circuit [50], [51]. In this study, we evaluate inexpensive Nichicon electrolytic capacitors that cost about five dollars each. The lead times for these

electrolytic capacitors through authorized distribution channels can be several weeks or months. The 2011 earthquake and tsunami in Japan put additional pressure on the supply chain for capacitor raw materials and parts, further extending lead times. Production at leading capacitor manufacturers, including Nippon Chemi-con, Nichicon, and Rubycon, was disrupted in Japan to varying degrees [52]. OEMs are under pressure to find parts quickly, and many of them purchases part from second- and third-tier suppliers. The unfortunate consequence is that counterfeit capacitors are making their way into the market, and into systems. This was not the first time that Nichicon capacitors were found to be counterfeit. In October 2011, Nichicon posted an alert on their website that counterfeit Nichicon electrolytic capacitors were turning up in the market, and these capacitors could cause early failures in end products [53]. The present study discusses an electrolytic capacitor labeled as Nichicon, 220μF, rated at 400 volts. The part number was LGU2G221MELA. As of April 2014, there were no current advisories under the Government-Industry Data Exchange Program (GIDEP) for this particular Nichicon part. Aluminum electrolytic capacitors were used by a medical electronics company in a power supply. A contract manufacturer for the electronics company purchased aluminum electrolytic capacitors from a parts broker because the parts were not available from the authorized distributors or independent suppliers. Authorized distributors typically obtain parts from the manufacturers and are contractually authorized by the part manufacturers to store, kit, and distribute the parts. Independent suppliers may not be contractually authorized by the part manufacturers to distribute parts, and these suppliers may procure these parts and distribute them from their warehouses. Parts brokers try to fulfill orders by

obtaining parts from wherever they can find them quickly. Around 4000 power supply units were manufactured using the aluminum electrolytic capacitors obtained from a part broker. By the time it was discovered that the capacitors were counterfeit, about 2000 units with counterfeit capacitors had been assembled and shipped to the field. An investigation was performed to assess the reliability of the counterfeit capacitors, estimate how long they are likely to survive, and determine the failure mechanisms. Ten power supplies were returned to the company or identified during production as failures as a result of the failed counterfeit capacitors. The field failure history showed that some of the counterfeit capacitors were failing within just a few months, and exhibiting evidence of venting, low capacitance, high dissipation factor, high ESR, and high leakage current.

A. Initial Analysis

An initial analysis was performed on 10 counterfeit and 2 authentic capacitors. Only 2 authentic Nichicon capacitors were provided for this study as the power supply manufacturer wanted to keep the authentic capacitors to replace the field-failed counterfeit capacitors. External visual and optical information was performed. Fig. 45 shows a counterfeit capacitor (right), and an authentic capacitor (left). The authenticity of a part can be verified by visual inspection of the markings, and comparing the dimensions. These characteristics were compared with datasheet information, and with known authentic parts. Other externally observable characteristics that are different from the authentic part were checked.

When the counterfeit capacitor was compared with an authentic Nichicon capacitor, it was found that the ink from the markings on the counterfeit capacitor was missing

in some regions, shown within the small rectangles in Fig. 45. The text on the counterfeit capacitors was bigger than the text on authentic capacitors. Solder that was observed on the end terminations of the counterfeit capacitors was confirmed to be residue from the removal process. The part datasheet specified the diameter to be a maximum of 25±1 mm, and length specifications were 40±2 mm. Table I shows the measured dimensions of the counterfeit capacitors. All the dimensions of the counterfeit capacitors were observed to be within specifications.

An initial weight measurement of the 10 counterfeit capacitors was performed. The same 10 capacitors were exposed to 10 days of high temperature (110ºC) exposure, and the weight was measured again. Table II shows the details of weight measurement. It can be seen that the weight varied between 24.86 grams and 30.95 grams for the counterfeit capacitors. This variation indicates poor quality control. Variations in weight were perhaps due to varying amounts of electrolyte in the counterfeit capacitors.

The electrical parameters were measured over temperature. Capacitance, dissipation factor, insulation resistance, and leakage current were measured for 10 counterfeit, and 2 authentic electrolytic capacitors at room temperature at the lowest rated temperature (–25ºC), and at the highest rated temperature (105ºC). Table III and Table IV show the measured values of electrical properties of the authentic capacitors, plus the mean, standard deviation, maximum values, and minimum values for the ten counterfeit capacitors at room temperature, and –25ºC, respectively. All measurements at room temperature and at –25ºC were within the specifications provided in the datasheets. However, there was a lot of variation in the measured

insulation resistance, leakage current, and dissipation factor values among the 10 counterfeit capacitors, even at room temperature. Fig. 46 through Fig. 48 show histograms of the measured electrical parameters which show the variation in electrical properties. Table V shows the measured electrical properties of the counterfeit and authentic capacitors at 105ºC. At 105°C, the leakage current and insulation resistance values of 6 of the 10 capacitors were out of specification. Dissipation factor values at –25ºC and 105°C were not provided in the datasheet. The values that were out of specification are shown in bold italic font.

The purity of the aluminum foil should be greater than 98% [54], or else impurities such as copper, magnesium, iron, and zinc can cause hydrogen generation at the cathode. The aluminum foils of the authentic and counterfeit capacitors were analyzed for purity using electron dispersive spectroscopy (EDS). The purity levels of the foils of both the authentic and counterfeit capacitors were found to be more than 99%.

B. Elevated Temperature (110º) Exposure and Analysis

Ripple current is known to increase the core temperature of an electrolytic capacitor by 5–10ºC [13]. To simulate the effect of ripple current on the electrolytic capacitors, we used a temperature of 110ºC (105ºC (Rated Temperature) + 5ºC (Temperature Rise due to ripple current); ten counterfeit capacitors, and one authentic capacitor were exposed to 110°C for 10 days. The second authentic capacitor was used to measure and compare the pH of the electrolyte. Electrical properties including capacitance, dissipation factor, insulation resistance, and leakage current were measured before and after the exposure. Table VI, Table VII, and Table VIII provide

the measurements performed at room temperature, –25°C, and 105°C, respectively, after exposure. The electrical measurements performed at room temperature and at –25ºC were within the specifications provided in the data sheet of the authentic Nichicon capacitor, and the tables for these two temperatures contain the mean, standard deviation, and minimum and maximum values of the measured properties for the counterfeit capacitors. The leakage current values for all the counterfeit capacitors were out of specification at 105°C, as shown in bold italic font in Table VIII. A high leakage current suggests that the electrolyte was not healing the dielectric oxide layer for the counterfeit capacitors. The leakage current of one of the capacitors was not measured due to the crack that formed on the capacitor seal after the 10-day high temperature exposure. There was a chance of the cracked capacitor exploding while charging during leakage current measurement.

The measured dissipation factor value of one capacitor was also found to be higher than the specified value. Upon closer inspection, it was observed that the seal was cracked in the counterfeit capacitor that showed a higher dissipation factor. Most other counterfeit capacitors also showed some bulging. Bulging can happen either due to hydrogen gas generation at the cathode when the electrolytic capacitor is biased with an applied voltage, or if the electrolyte volatility it high and it is not suited for high temperature use. Bulging in counterfeit capacitors after high temperature exposure for just 240 hours suggests that the electrolyte is unstable at elevated temperatures. There was no hydrogen generation in this case because there was no voltage applied in this high temperature exposure. Fig. 49 shows the crack in the seal of the counterfeit electrolytic capacitor.

X-ray inspection of the counterfeit capacitors after 10 days at a high temperature confirmed the bulging. X-ray inspection was carried out to conduct internal inspection on parts to verify the internal attributes of parts such as spacers, terminations, and quality. The X-ray micrograph on the left in Fig. 50 shows the base of an authentic capacitor. The micrograph on the right shows an X-ray image of the base of a counterfeit capacitor, which showed bulging, as shown within the black box. Most of the counterfeit capacitors showed some amount of bulging after exposure to 110ºC for 10 days. Fig. 51 shows an X-ray image of the snap-in leads of a counterfeit capacitor on the left, and the authentic capacitor on the right. Note that due to the crack and a bend in the seal, the snap-in terminals appear bent.

The plastic sleeve of one of the counterfeit capacitors had shrunk and split after the high temperature exposure. This result indicates that the plastic was not of good enough quality to survive at high temperatures. An image of the counterfeit capacitor with the shrunken plastic sleeve is shown in Fig. 52.

The weight measurements were repeated after 10-days of high temperature exposure at 110°C. The average weight loss after 10 days of high temperature exposure for the counterfeit capacitors was 0.2 grams, and the standard deviation was 0.053. The weight loss of the one authentic capacitor was 0.043 grams. This means that the weight loss rate (electrolyte evaporation rate) for the counterfeit capacitor was higher than the weight loss rate of the authentic capacitor.

C. Elevated Temperature (110º), and Rated DC Voltage (400 Volts) Exposure and Analysis

Ten counterfeit capacitors were exposed to 110°C, and biased with 400 Volts of

DC voltage for 10 days. The capacitance, dissipation factor, insulation resistance, and leakage current were measured before, and after the exposure. After the exposure, the seals of two counterfeit capacitors were cracked, and electrolyte leaked. The safety vent of another electrolytic capacitor was found open, and leaking electrolyte. All the electrolytic capacitors showed some bulging. The capacitance, dissipation factor, insulation resistance, and leakage current of the ten counterfeit capacitors shown in Table IX were measured before the high temperature bias exposure. After the exposure, the electrical parameters were again measured, as shown in Table X. The seven capacitors that did not leak had low insulation resistance (high leakage current), and the insulation resistance of the remaining 3 capacitors was not measured due to cracks in the seals or venting issues. The insulation resistance for a good capacitor according to the datasheet of the authentic Nichicon capacitor should be greater than 0.45 MΩ. All seven counterfeit capacitors failed as the value of insulation resistance was below 0.45 MΩ for all of them after the exposure. Fig. 53 shows the insulation resistance values of the seven capacitors before, and after the temperature bias test.

D. Analysis of Seven Failed Counterfeit Capacitors Received from the OEM

Seven failed capacitors were received from the power supply manufacturer for analysis. Four of these were production failures, and the other three were field failures, as shown in Table XI.

The failed capacitors were optically inspected. A capacitor which experienced field failure was vented, as shown in Fig. 54. Fig. 55 shows the left capacitor with the top off, as described by the OEM. The right capacitor has the top on.

X-ray analysis of the failed capacitors was performed. It revealed that the top part of the capacitors looked different from the non-failed counterfeit capacitors. Fig. 56 shows an X-ray image of the tops of 2 failed counterfeit capacitors that look different (in the black box) from the X-ray of the top part of the non-failed counterfeit capacitor shown in Fig. 57. This difference was due to high pressure either due to hydrogen gas formation or unstable electrolyte which resulted in the bulging of capacitors. The electrical properties of the failed capacitors were measured. The leakage current was measured after charging the capacitors at 50 volts, because if it were charged at 400 volts there would be an explosion hazard. The electrical properties of four capacitors were found to be out of specification, as shown in bold italic font in Table XII. For the remaining three capacitors, the electrical properties were within specifications.

E. Chemical Analysis

The composition of capacitor electrolyte is proprietary, so manufacturers usually do not disclose their formulas, and this proprietary feature can be used as an advantage, in the development of methodologies to identify counterfeit electrolytic capacitors based on specific characteristics of chemical compounds. Typically, a capacitor electrolyte consists of solvents, solutes, some additives [56], and less than 5% water by weight [57]. Ethylene glycol and gamma butyrolactone are common examples of solvents. A solute can be a conductive salt which usually is a resultant of the chemical reaction between an acid and a base. Additives added are corrosion inhibitors, depolarizers, hydrogen absorbers, and conductivity enhancers.

FTIR was used to determine the chemical components of the electrolyte of the counterfeit and authentic capacitors. Because capacitor electrolytes are mostly organic, they are easily detected by infrared radiation. Thus infrared spectroscopy becomes a suitable tool to identify and compare the chemical components. FTIR equipment was used to perform infrared spectroscopy on the capacitor electrolyte. FTIR equipment was used in attenuated total reflectance (ATR) mode. ATR allows the inspection of samples directly from the capacitor with a minimal preparation [58], which avoids the removal of evidence in identification of counterfeit electrolytes. In usual transmittance mode, due to sample preparation, some information about the chemical composition may get lost. Nicolet Spectra libraries and the NIST Chemistry WebBook databases were consulted to compare the IR spectra.

In the present work, the electrolyte was directly obtained from the paper layer inside the authentic Nichicon and counterfeit capacitor. The electrolyte was squeezed out of the paper layer, and placed on top of the reflective element of the ATR assembly. In the IR spectrum showed in Fig. 58, organic functional groups from the capacitor electrolytes of this study are shown. The authentic capacitor electrolyte revealed aliphatic hydrocarbon, aliphatic carboxylic acid salt, and primary aliphatic alcohol; nevertheless the counterfeit electrolyte did not contain the peak that corresponds to the aliphatic carboxylic acid salt. The FTIR spectrum revealed that the main solvent found in the capacitor electrolyte (authentic and counterfeit) was ethylene glycol. Also the FTIR peaks of the counterfeit capacitor have a higher percentage transmittance than the peaks of the authentic capacitor. From the comparison of FTIR peaks of counterfeit and authentic electrolyte, it appeared that the concentration of

ethylene glycol in the counterfeit electrolyte was less than that in the authentic electrolyte. To validate this hypothesis, FTIR spectra of different concentrations of ethylene glycol solution varying from 100% to 70% were collected. It was found, as shown in Fig. 59, that as the concentration of ethylene glycol decreased, the transmittance increased. This effect validates the hypothesis that the counterfeit electrolyte has less ethylene glycol and perhaps more water.

F. Failure Time Estimation of Counterfeit Electrolytic Capacitors

The primary failure mechanism of aluminum electrolytic capacitor failures is the loss of electrolyte through and around the seal over the period of its life. Capacitor manufacturers use an electrolyte loss of greater than 30% of the initial electrolyte weight as a rule of thumb to define failure. At that point, the equivalent series resistance (ESR) value of the capacitor increases beyond a safe level, causing too much heat generation in the capacitor, and the capacitance value begins to decrease rapidly with time.

The objective of this test is to provide an approximate evaluation of the failure time of the counterfeit electrolytic capacitors at 45ºC ambient temperature, assuming that the capacitors fail due to evaporation of electrolyte. Failure time is defined as a 30% weight loss in the electrolyte present in the capacitor, the critical degradation number. With the evaporation of electrolyte, the capacitance drops and ESR increases. The electrolyte quantity in the counterfeit capacitors was calculated experimentally by evaporating the electrolyte from the capacitors at high temperature (110°C) until the weight of the capacitor became stable. Electrolyte was found to account for one third the weight of the counterfeit capacitors. Two sets of 10 counterfeit capacitors were

used in this failure time estimation study. An initial weight measurement of all capacitors was performed. After the weight measurement, 10 capacitors were kept in a chamber at 85ºC, and the other 10 were kept at 115ºC. Weight measurement of the capacitors was performed every day for 10 days. For each day, 10 weight readings for each temperature set (85ºC and 115ºC) were taken.

After gathering the weight data for 10 days, the distribution of time to failure of all the capacitors at both temperatures was analyzed using Weibull++ software. The degradation analysis folio was used to perform this analysis for both sets of temperatures (85ºC and 115ºC). Inspection times (in hours), degradation (percentage electrolyte evaporated), and unit ID for the capacitors were entered in the software. The electrolyte weight was found to be one third of the weight of the counterfeit capacitor. The model for extrapolation is chosen as linear because previous CALCE work has shown that the initial 30% loss of electrolyte can be modeled as linear. The values of the lifetime of the capacitors were then extrapolated using the software. The values obtained for all of the capacitors at 85ºC are given in Table XIII. The values of failure times obtained for all the capacitors at 115°C are given in Table XIV.

After obtaining the failure time values from the Weibull++ software, the values were plugged into ALTA 7 software. The "Accelerated Life Data Analysis" portfolio was used in ALTA 7. The failure times obtained, and the temperatures of the test (358.15 K, and 388.15 K) were inserted into ALTA 7, and the model used for running ALTA 7 was Arrhenius. The failure distribution used was Weibull. The ambient temperature in which the counterfeit electrolytic capacitors are normally used is 45ºC. If we add a 5ºC core temperature rise due to ripple current, the maximum temperature

that the capacitors would experience would be 50ºC. Using ALTA 7, the lifetime at 50ºC was predicted. Fig. 60 shows the Weibull plot obtained for 50ºC using the life data from 85ºC and 115ºC. As per the Weibull chart, the failure time of 5% of the population at 50ºC is approximately 11.4 years.

The analysis of weight loss during aging at elevated temperatures indicated that the counterfeit capacitors could survive for many years if they fail by the mechanism of gradual electrolyte evaporation through intact seals. Nevertheless, the field failure history showed that some of the counterfeit capacitors were failing within just a few months, and exhibiting evidence of venting, low capacitance, high dissipation factor, high ESR, and high leakage current. If these failures were due to electrolyte loss, it is likely that their short lifetimes were a result of imperfect or degraded seals or other quality defects, or due to electrical stresses experienced in the circuit. Also, the capacitors tested with the high temperature bias test exhibited venting, seal cracking, low capacitance, high ESR, and high leakage current, which suggests that there could be other failure mechanisms acting along with the electrolyte evaporation mechanism.

There may be competing causes of failure other than electrolyte evaporation. These causes may include poor formulation of electrolyte (Liquid electrolyte reheal dielectric (Aluminum Oxide) layer, when voltage is applied to the capacitor) causing the electrolyte to be unable to heal localized damage to the dielectric layer; or degradation of electrolyte (decrease in ionic conductivity), leading to an increase in ESR and dissipation factor. Deterioration and degradation of the electrolyte can also cause an internal pressure rise which leads to venting or leakage. Electrolyte formulation is frequently a problem in low quality or counterfeit electrolytic

capacitors, and evidence has already been presented in this report that the electrolyte was not formulated properly for use at the rated operating conditions.

DISCUSSION

In the FTIR spectra, it was observed that there are differences between counterfeit capacitor and authentic capacitor electrolyte. There was no carboxylic acid salt in the counterfeit capacitor electrolyte; and the concentration of ethylene glycol, which is the main solvent in the electrolyte, was lower. The concentration of water was higher in the counterfeit capacitor electrolyte. The chemical differences between the authentic and counterfeit electrolytes can explain the observed failure modes like venting, drop in capacitance, increase of ESR, and leakage current in the counterfeit capacitors.

As the boiling point of ethylene glycol, and water is 197°C, and 100°C respectively, the lower concentration of ethylene glycol, and higher concentration of water in the counterfeit electrolyte will decrease the boiling point of the counterfeit electrolyte, and increase the counterfeit electrolyte volatility. Higher volatility of the counterfeit electrolyte can increase the pressure inside the capacitor body. This pressure can cause bulging of capacitor at high temperatures, resulting in venting failures. Increased pressure inside the capacitor can increase the spacing, thus reducing the overlap area between cathode and anode foils. This increased spacing causes a decrease in capacitance, and an increase in ESR value. The increased pressure can also cause damage to the dielectric oxide layer, resulting in higher leakage current.

It was observed in the tests that more counterfeit capacitors failed due to high leakage current after the high temperature bias test than after the high temperature exposure test alone. This failure is due to higher stresses on the dielectric oxide layer of counterfeit capacitors, when rated voltage was applied along with high temperature. Usually the authentic electrolyte heals the dielectric oxide layer when a voltage bias is applied. But, because of the faulty composition of the counterfeit electrolyte, it was not able to heal the oxide layer, thus causing more leakage current failures in temperature and voltage tests than just temperature testing.

CONCLUSIONS AND RECOMMENDATIONS

Counterfeit electrolytic capacitors cause grave concern to original equipment manufacturers, and have resulted in millions of dollars in losses to companies like Dell, Apple, HP, and Intel in the past. Undetected counterfeit electrolytic capacitors can increase the risk of failure, and thus reducing the reliability of power electronics.

To validate the authenticity of the capacitors electrolytes, FTIR was used to compare the chemical composition of the authentic and counterfeit electrolytes. We found that the counterfeit electrolyte has a lower concentration of solvent (ethylene glycol), and lacked of carboxylic acid salt, which made the counterfeit electrolyte unstable at high temperatures. This problem led to early failures of the counterfeit electrolytic capacitors.

To evaluate the electrical parameters of counterfeit electrolytic capacitors, the electrical properties were measured at room temperature before using them in the power supply. Though all the electrical properties were determined to be within

specifications as per the datasheet of the authentic capacitors at room temperature, the distribution of values at room temperature was broader for counterfeit parts than for the authentic parts, and some electrical parameters at the maximum and minimum rated temperatures were out of specifications. If the capacitors do not fail due to the inferior quality of the electrolyte, or due to defective seals, then they are expected to fail due to gradual evaporation of the electrolyte through intact seals. In such cases, 5% of the population at 50ºC is predicted to fail within approximately 11.4 years in the field.

Original equipment manufacturers, and other industry members that use capacitors in power supplies, should perform measurements of electrical parameters at the maximum and minimum rated temperatures, and chemical analysis of the electrolyte. One way to perform chemical analysis of the capacitor electrolyte is to dissemble the capacitor and use a spectroscopy technique like FTIR with an ATR assembly. The application of these methods will reduce failures due to counterfeit capacitors. In view of the prevalence of counterfeit parts in the supply chain, it is recommended that lot acceptance procedures be adopted that are tailored to the risk of counterfeiting, as well as the likelihood and criticality of failures associated with each component. FTIR technique can be applied for other chemical or residue analysis in failure analysis, and reliability studies. Counterfeiting is an ongoing problem. A systematic methodology like the one developed can be applied to other electronic components.

TABLE I
DIMENSIONS OF 10 COUNTERFEIT CAPACITORS

	Diameter	Height
Mean	25.17 mm	40.83 mm
Standard Deviation	0.06	0.62
Minimum	25.07 mm	39.85 mm
Maximum	25.25 mm	41.58 mm
Specifications Limit	25 +1 (mm)	40± 2(mm)

TABLE II
WEIGHT OF COUNTERFEIT CAPACITORS BEFORE AND AFTER 10 DAYS OF HIGH TEMPERATURE EXPOSURE

	Weight before (grams)	Weight after (grams)
1	28.5192	28.3067
2	26.5516	26.3585
3	27.761	27.5542
4	24.8551	24.6582
5	24.9737	24.7194
6	27.1063	26.9171
7	27.4954	27.1913
8	27.7758	27.6013
9	26.4153	26.3096
10	30.9511	30.7885
Mean	*27.2405*	*27.0405*
Standard Deviation	*1.76*	*1.77*
Minimum	*24.8551*	*24.6582*
Maximum	*30.9511*	*30.7885*

TABLE III
ELECTRICAL PROPERTIES AT ROOM TEMPERATURE

	120Hz	120Hz		
	Capacitance (μF)	Dissipation Factor	Insulation Resistance (M-ohm)	Leakage Current (μA)
Authentic-1	188.68	0.0580	5.48	73
Authentic-2	188.36	0.0603	6.67	60
Mean	*195.06*	*0.0400*	*2.72*	*165*
Standard Deviation	*1.92*	*0.01*	*0.91*	*64.52*
Maximum	*198.21*	*0.0649*	*4.49*	*314*
Minimum	*192.22*	*0.0297*	*1.27*	*89*
Specifications	*220 ±20%*	*<0.15*	*>0.45M Ohms*	*<880 μA*

TABLE IV
ELECTRICAL PROPERTIES AT –25°C TEMPERATURE

	120Hz	120Hz		
	Capacitance (µF)	Dissipation Factor	Insulation Resistance (M-Ohm)	Leakage Current (µA)
Authentic-1	180.35	0.4061	7.14	56
Authentic-2	180.33	0.3755	7.30	45
Mean	*189.82*	*0.23*	*5.05*	*80.80*
Standard Deviation	*1.49*	*0.09*	*0.74*	*11.75*
Maximum	*191.75*	*0.3984*	*6.15*	*98*
Minimum	*187*	*0.1306*	*4.08*	*65*
Specifications	*N.A.*	*N.A.*	*>0.45M Ohms*	*<880 µA*

TABLE V
ELECTRICAL PROPERTIES AT 105°C TEMPERATURE
(THE VALUES IN BOLD ITALIC FONT ARE OUTSIDE THE SPECIFICATIONS)

	120Hz	120Hz		
	Capacitance (µF)	Dissipation Factor	Insulation Resistance (M-ohm)	Leakage Current (µA)
Authentic-1	196.3	0.0265	1.40	286
Authentic-2	198.69	0.0257	1.60	371
Counterfeit 1	208.02	0.0305	***0.20***	***1960***
2	204.57	0.0268	***0.38***	***1060***
3	205.34	0.025	0.71	560
4	201.57	0.0261	0.47	850
5	202.8	0.0345	***0.24***	***1702***
6	207.4	0.0246	***0.39***	***1020***
7	209.04	0.0243	***0.19***	***2080***
8	201.46	0.0239	0.55	725
9	205.85	0.0356	1.11	359
10	206.93	0.0254	***0.11***	***3702***
Mean	205.30	0.03	0.44	1401.80
Standard Deviation	2.67	0.00	0.30	998.54
Maximum	209.04	0.0356	1.11	3702
Minimum	201.46	0.0239	0.11	359
Specifications	N.A.	N.A.	>0.45M Ohms	<880 µA

TABLE VI
ELECTRICAL PROPERTIES AT ROOM TEMPERATURE AFTER 10 DAYS OF HIGH TEMPERATURE EXPOSURE

	120Hz	120Hz		
	Capacitance (μF)	Dissipation Factor	Insulation Resistance (M-ohm)	Leakage Current (μA)
Good-2(Nichicon)	185.86	0.0595	5.97	67
Mean	*193.53*	*0.06*	*1.54*	*338.67*
Standard Deviation	*2.17*	*0.04*	*0.99*	*158.57*
Maximum	*196.98*	*0.1564*	*3.81*	*562*
Minimum	*190.25*	*0.031*	*0.71*	*105*
Specifications	*220 ±20%*	*<0.15*	*>0.45M Ohms*	*<880 μA*

TABLE VII
ELECTRICAL PROPERTIES AT -25°C AFTER 10 DAYS OF HIGH TEMPERATURE EXPOSURE

	120Hz	120Hz		
	Capacitance (μF)	Dissipation Factor	Insulation Resistance (M-ohm)	Leakage Current (μA)
Authentic-2	178.33	0.3756	9.30	43
Mean	*182.45*	*0.48*	*4.13*	*121.67*
Standard Deviation	*14.24*	*0.36*	*1.52*	*85.61*
Maximum	*189.72*	*1.4197*	*6.15*	*341*
Minimum	*142.63*	*0.1462*	*1.17*	*65*
Specifications	*N.A.*	*N.A.*	*>0.45M Ohms*	*<880 μA*

TABLE VIII
ELECTRICAL PROPERTIES AT 105°C AFTER 10 DAYS OF HIGH TEMPERATURE EXPOSURE
(THE VALUES IN BOLD ITALIC FONT ARE OUT OF SPECIFICATION)

	120Hz	120Hz		
	Capacitance (μF)	Dissipation Factor	Insulation Resistance (M-ohm)	Leakage Current (μA)
Authentic-2	197.94	0.0278	0.98	410
Counterfeit-1	204.59	0.0376	***0.05***	***7375***
Counterfeit-2	203.7	0.0254	***0.06***	***6421***
Counterfeit-3	206.62	0.0235	***0.08***	***5156***
Counterfeit-4	199.3	0.0256	***0.14***	***2950***
Counterfeit-5	204.24	0.0454	(cracked seal)	(cracked seal)
Counterfeit-6	205.25	0.0258	***0.04***	***8971***
Counterfeit-7	203.64	0.0242	***0.23***	***1720***
Counterfeit-8	198.34	0.0216	***0.31***	***1303***
Counterfeit-9	203.41	0.0378	***0.45***	***885***
Counterfeit-10	205.78	0.0267	***0.30***	***1350***
Mean	*203.49*	*0.03*	*0.18*	*4014.56*
Standard Deviation	*2.67*	*0.01*	*0.14*	*3033.10*
Maximum	*206.62*	*0.0454*	*0.45*	*8971*
Minimum	*198.34*	*0.0216*	*0.04*	*885*
Specifications	*N.A.*		*>0.45M Ohms*	*<880 μA*

TABLE IX
ELECTRICAL PROPERTIES AT ROOM TEMPERATURE BEFORE 10 DAYS OF HIGH TEMPERATURE BIAS EXPOSURE

	120 Hz	120 Hz	
	Capacitance(μF)	DF	IR (M-Ohm)
Counterfeit-1	200.36	0.0498	0.4762
Counterfeit-2	201.18	0.0637	0.4902
Counterfeit-3	193.84	0.0694	0.4587
Counterfeit-4	206.19	0.0427	0.5435
Counterfeit-5	200.82	0.0587	0.5263
Counterfeit-6	198.32	0.077	0.5618
Counterfeit-7	239.62	0.0738	0.4902
Counterfeit-8	201.49	0.0368	0.5319
Counterfeit-9	202.8	0.041	0.5000
Counterfeit-10	203.13	0.0415	0.6410
Mean	204.775	0.05544	0.5220
Standard Deviation	12.662	0.015	0.053
Maximum	239.62	0.077	0.6410
Minimum	193.84	0.0368	0.4587
Specifications	220±20%	<0.15	>0.45MΩ

TABLE X
ELECTRICAL PROPERTIES AT ROOM TEMPERATURE AFTER 10 DAYS OF HIGH TEMPERATURE BIAS EXPOSURE

	Capacitance(μF)	DF	IR (M-Ohm)	Status
Counterfeit-1	198.67	0.0695	*0.0525*	
Counterfeit-2	204.19	0.0738		*Seal Cracked/Electrolyte Leak*
Counterfeit-3	193.05	0.113	*0.0572*	
Counterfeit-4	244.41	0.0907	*0.1515*	
Counterfeit-5	199.8	0.0642	*0.1969*	
Counterfeit-6	165.71	1.095		*Seal Cracked/Electrolyte Leak*
Counterfeit-7	196.29	0.0643	*0.1449*	
Counterfeit-8	195.15	0.0917	*0.3448*	
Counterfeit-9	0.094	0.5655		*Vent Open*
Counterfeit-10	209.28	0.0606	*0.0986*	
Mean	*180.6644*	*0.229*	*0.1495*	
Standard Deviation	*66.3014*	*0.341*	*0.1008*	
Maximum	*244.41*	*1.095*	*0.3448*	
Minimum	*0.094*	*0.0606*	*0.0525*	
Specifications	*220±20%*	*<0.15*	*>0.45MΩ*	

TABLE XI
DETAILS OF SEVEN FAILED CAPACITORS RECEIVED FROM THE COMPANY

S/N	Failure Mode	Power Supply Type
24845	Field failure - leaked from bottom of cap	150W
7411	Production failure - top bubbled	300W
24535	Field failure - low capacitance	300W
24912	Field failure - vented	150W
7207	Production failure - top bubbled	300W
7188	Production failure	300W
Top off	Production failure - bubbled	300W

TABLE XII
PROPERTIES MEASURED AT ROOM TEMPERATURE (VALUES IN BOLD ITALIC FONT ARE OUT OF SPECIFICATION)

	Capacitance (μF)	DF	ESR (m-Ohm)	Leakage Current (μA)	Weight (Grams)
Authentic part	186.77	0.0521	217.97	12	
24825(Field Failure)	196.55	0.0309	97.57	56	32.5185
7411	200.88	0.1305	493.27	***536***	26.0208
24535(Field Failure)	***0.0696***	***2.2815***	***7.7512 k ohm***	40	29.8912
24912(Field Failure)	***13.29***	***1.7935***	***23121***	***151650***	23.8299
7207	213.51	0.1078	259.66	***2380***	26.4477
7188	191.55	0.037	155.51	16	33.4325
Top off	174.99	0.0564	214.2	18	29.2433

TABLE XIII
EXTRAPOLATED FAILURE TIMES OF THE CAPACITORS AT 85°C

Capacitor Serial No.	Failure Time (Hours)
1	23433
2	15713
3	44190
4	26269
5	21166
6	38581
7	15377
8	21826
9	50948
10	32050

TABLE XIV
EXTRAPOLATED FAILURE TIMES OF THE CAPACITORS AT 115°C

Capacitor Serial No.	Failure Time (Hours)
1	3313
2	2255
3	4775
4	8667
5	2387
6	7309
7	1197
8	7180
9	3178
10	943

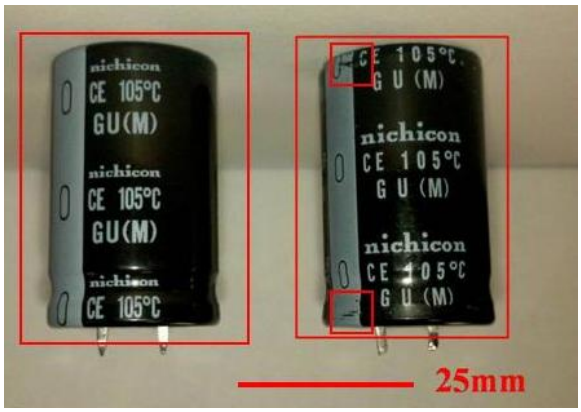

Fig. 45. Image showing the counterfeit capacitor on the right in the red rectangle. The capacitor on the left is an authentic Nichicon capacitor.

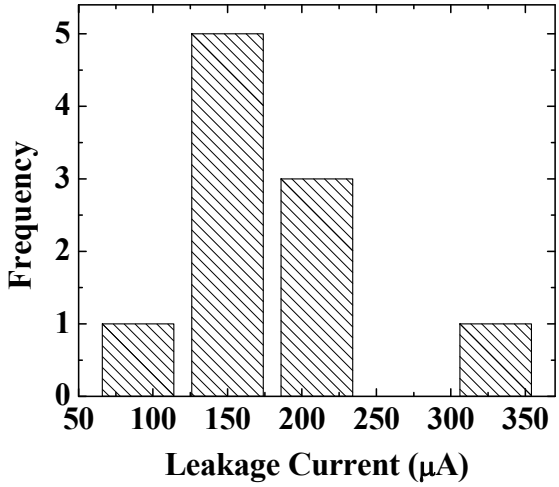

Fig. 46. Histogram showing variation in leakage current values of the ten counterfeit capacitors at room temperature.

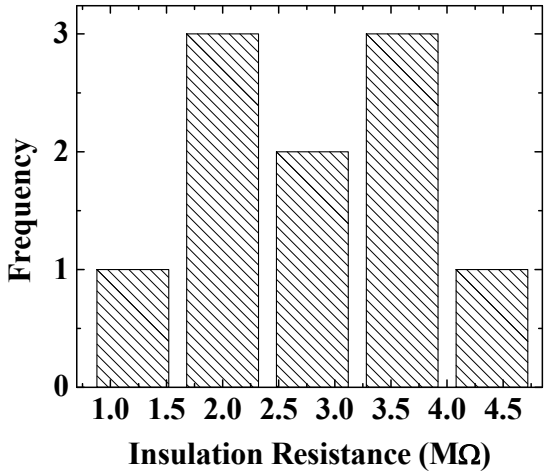

Fig. 47. Histogram showing variation in insulation resistance values of the ten counterfeit capacitors at room temperature.

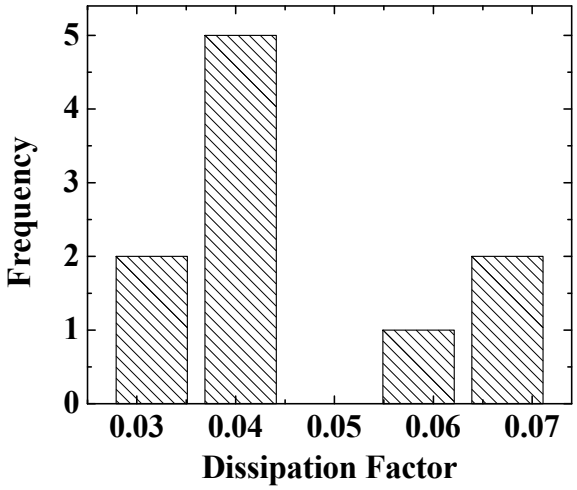

Fig. 48. Histogram showing variation in dissipation factor values of the ten counterfeit capacitors at room temperature

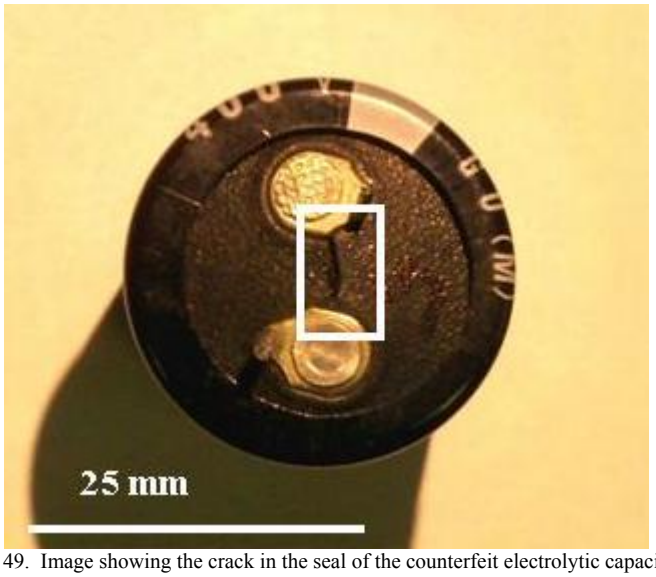

Fig. 49. Image showing the crack in the seal of the counterfeit electrolytic capacitor.

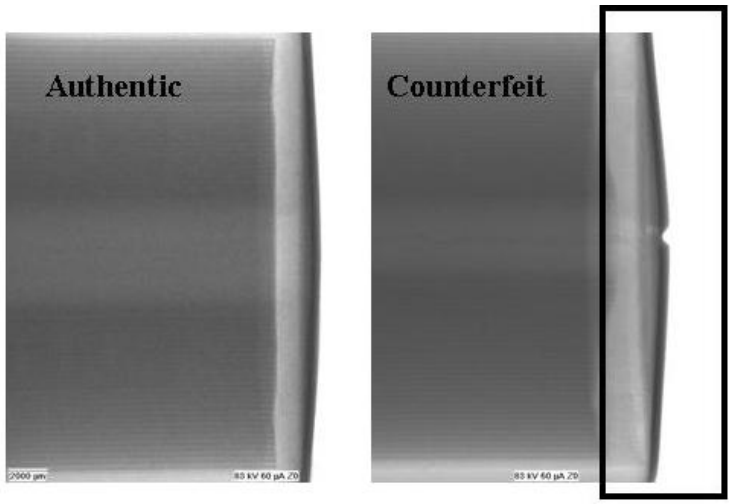

Fig. 50. X-ray of the base of an authentic and a counterfeit electrolytic capacitor.

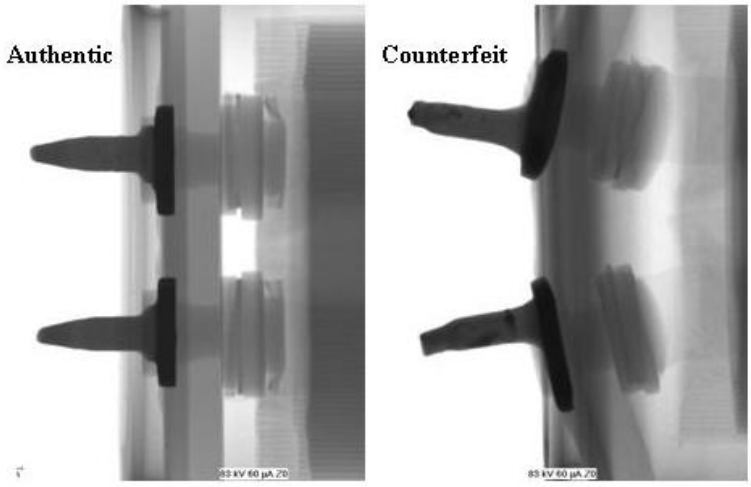

Fig. 51. X-ray image of the snap-in leads of an authentic capacitor and a cracked counterfeit capacitor.

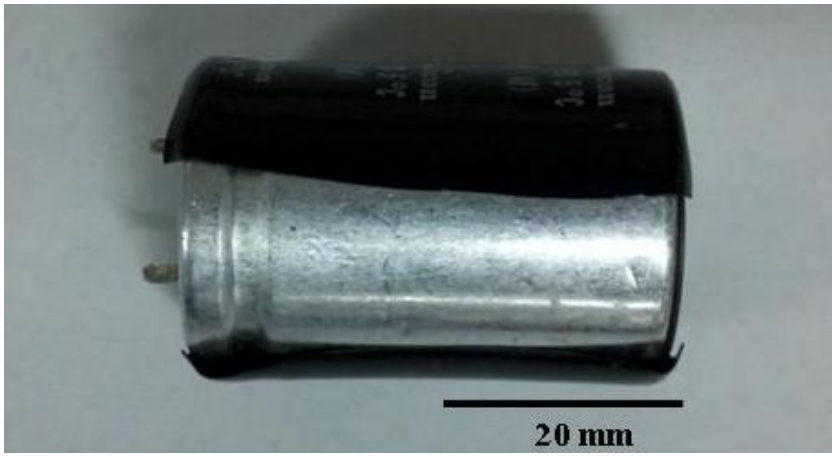

Fig. 52. A counterfeit capacitor with a shrunken plastic sleeve

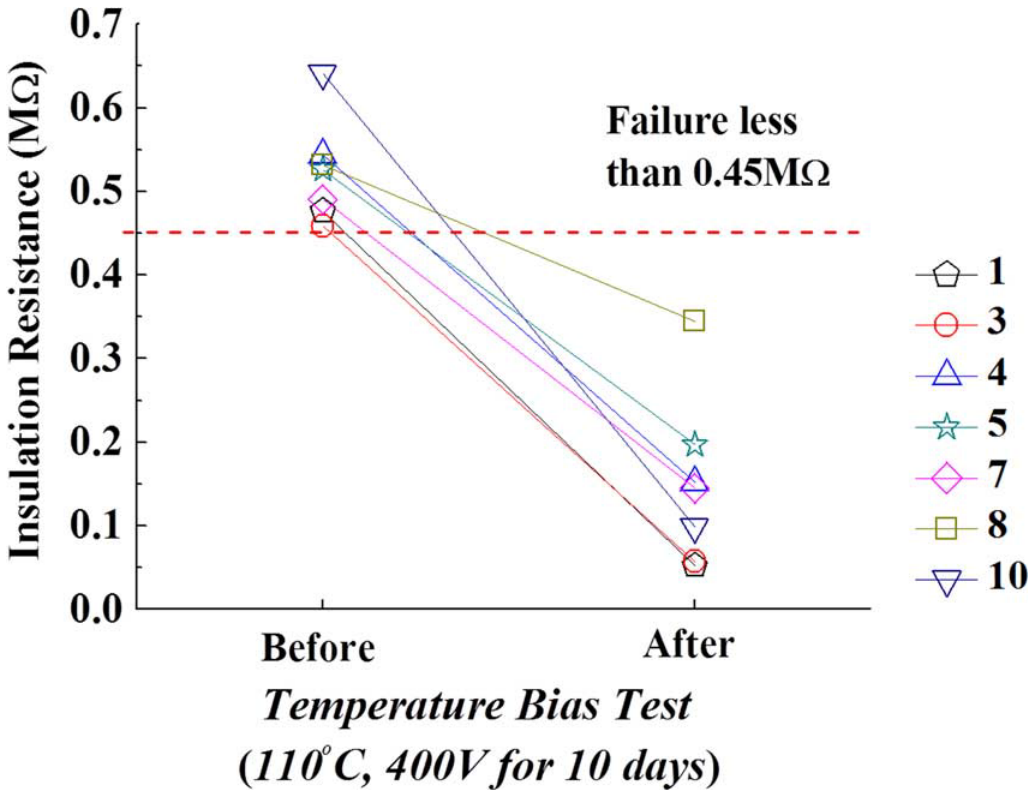

Fig. 53. Plot showing that seven counterfeit capacitors failed due to a decrease in insulation resistance after temperature bias test. The other three capacitors failed because the seal ruptured, and they were not charged for insulation resistance measurement.

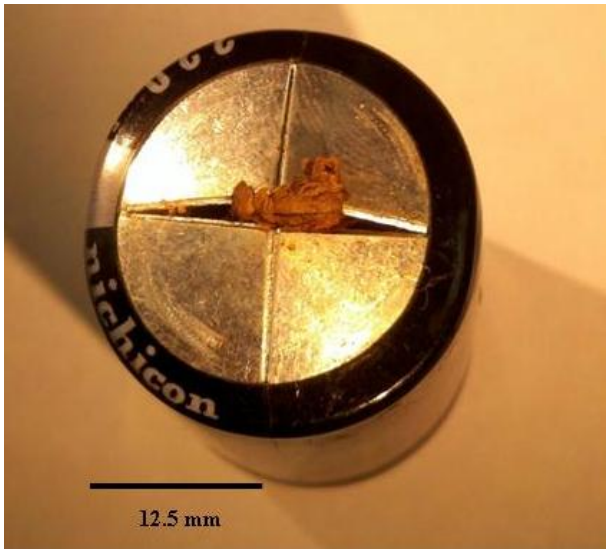

Fig. 54. Field-failed capacitor showing venting.

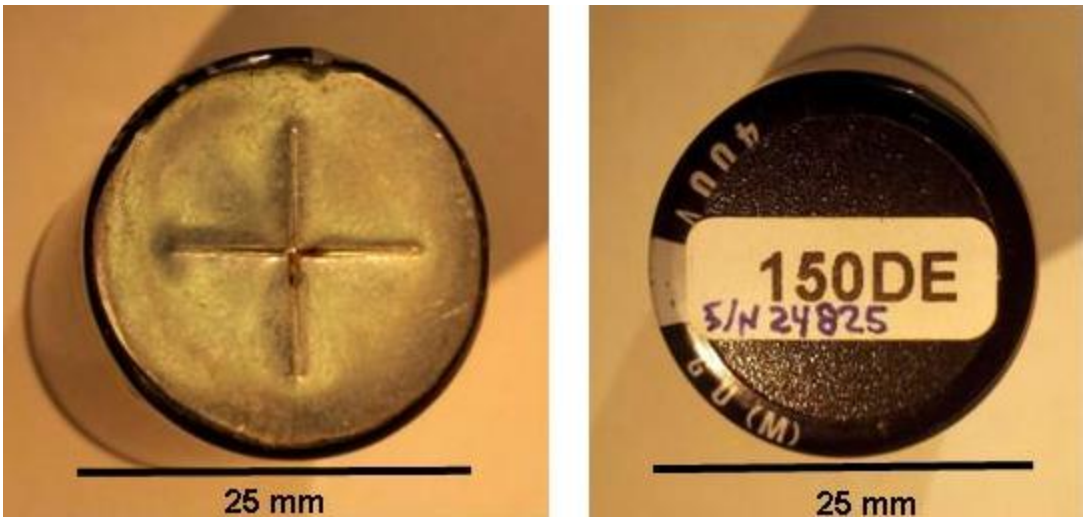

Fig. 55. Capacitor with top-off shown in the left image. Right image shows the normal counterfeit capacitor with top-on.

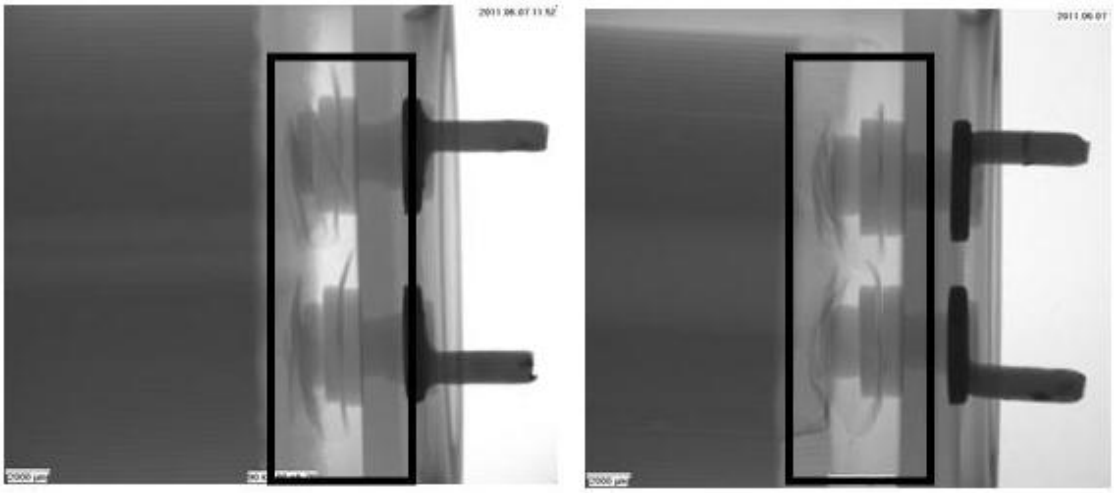
Fig. 56. X-ray image of top part of the failed capacitors.

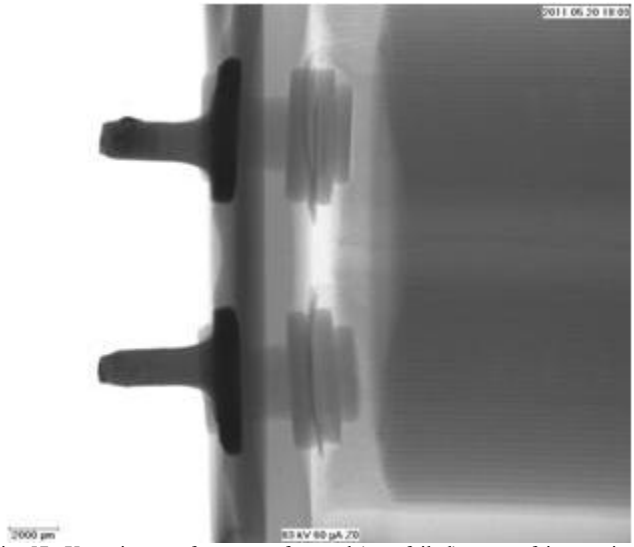
Fig. 57. X-ray image of top part of a good (non-failed) counterfeit capacitor.

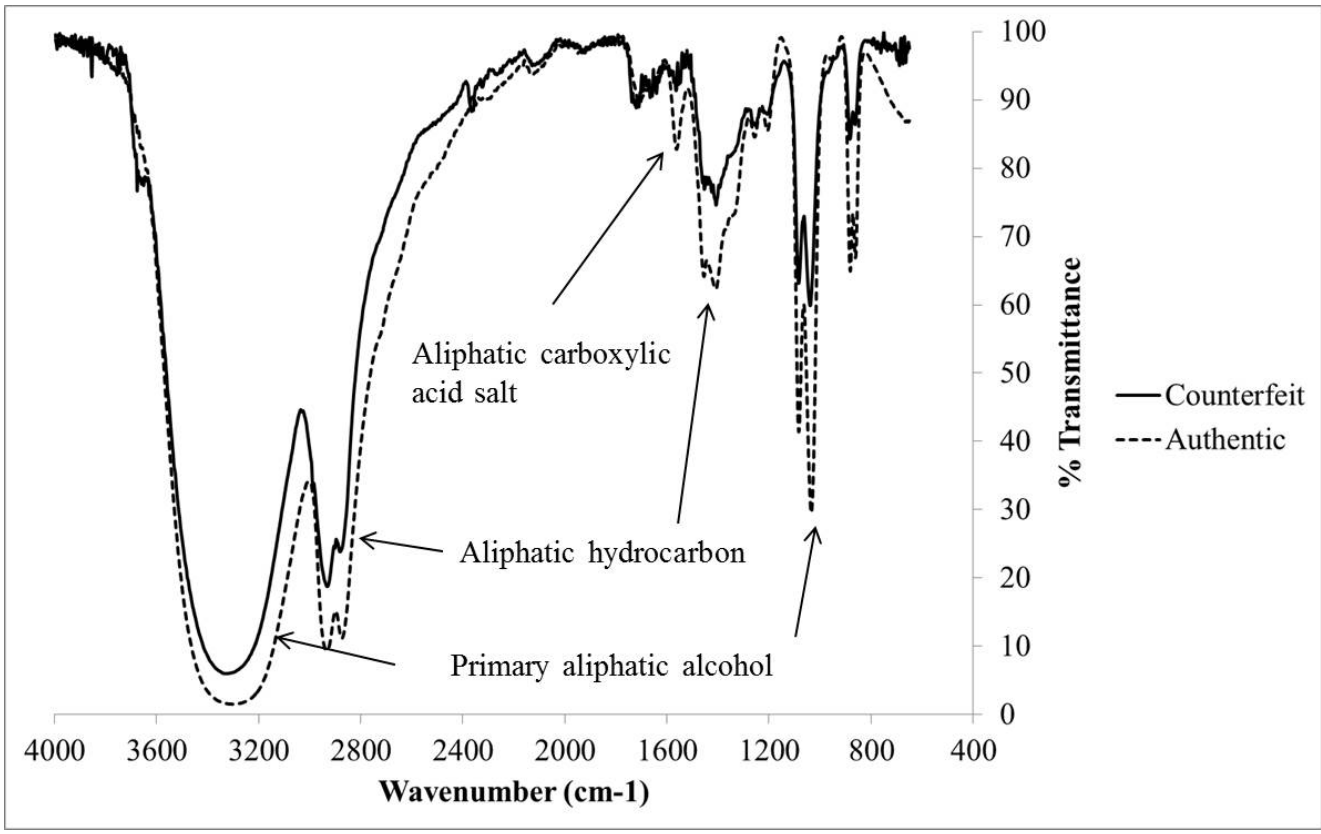

Fig. 58. Comparison of FTIR spectra between an authentic Nichicon electrolyte and counterfeit electrolyte.

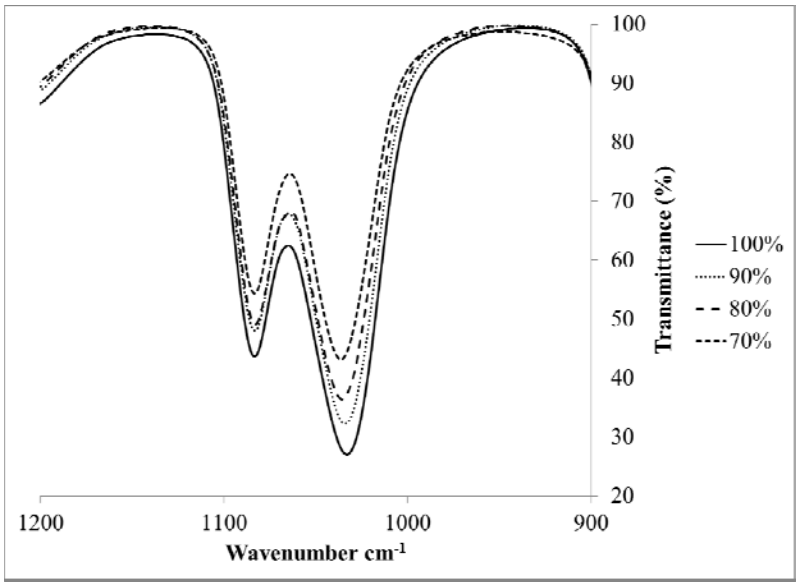

Fig. 59. Comparison of FTIR spectra between different solutions of water and ethylene glycol.

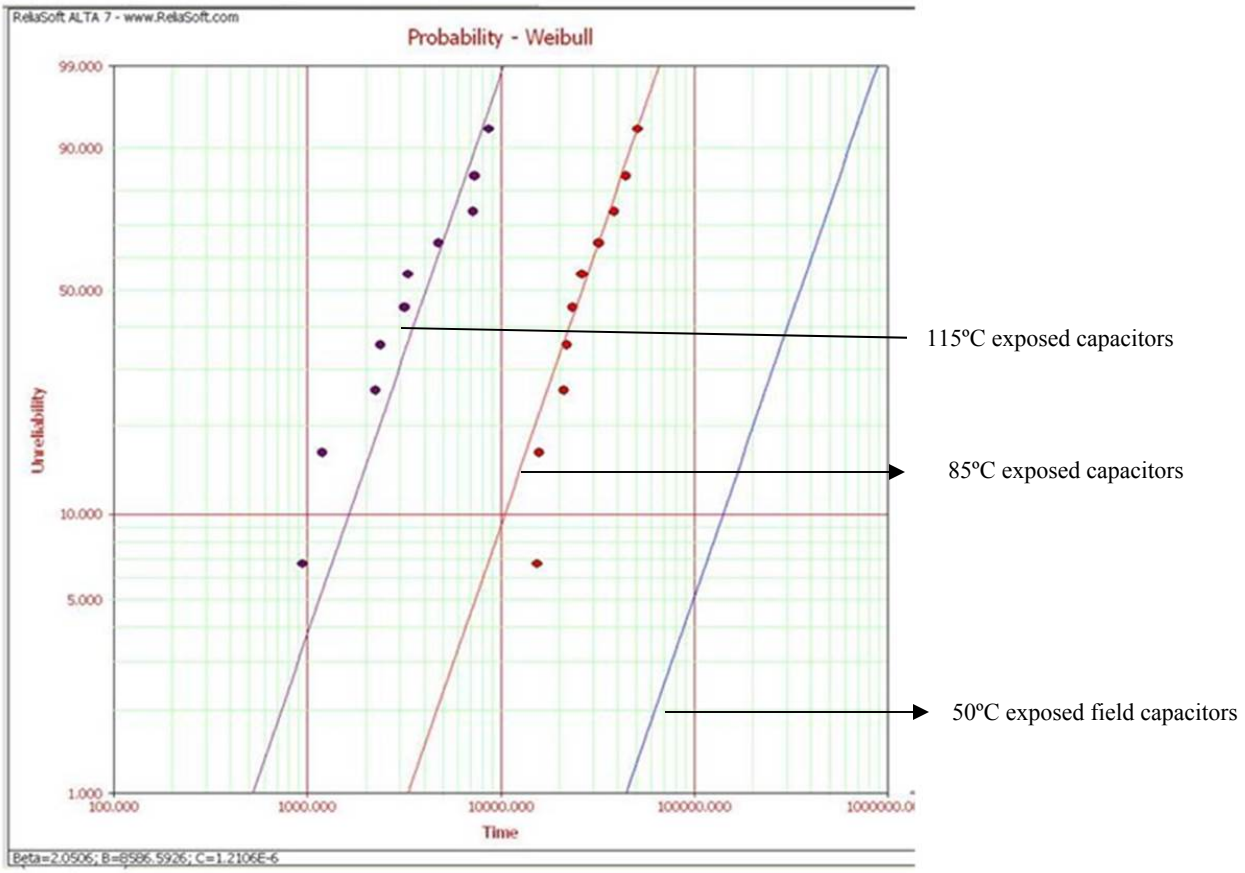

Fig. 60. Weibull plot obtained from ALTA 7.

References

1. C. A. Harper, “Passive Electronic Component Handbook,” McGraw-Hill Professional, 2nd edition, June 1, 1997
2. Cornell Dubilier, “Aluminum Electrolytic Capacitor Application Guide,” Accessed on September 6, 2014
3. Epcos, “General Technical Information of Al Electrolytic Capacitors,” Dec 2010, Accessed on June 3, 2014
4. ELNA America, Introduction to aluminum electrolytic capacitors (2012), http://www.elna-america.com/tech_al_principles.php. Accessed on 18 October 2014
5. T. Morimoto, Y. Hamatani, M. Yoshitake and H. Yamada, US Patent 4831499, 1979
6. C. Gómez-Aleixandre, J. M. Albella, and J. M. Martínez-Duart, “Gas Evolution in Aluminum Electrolytic Capacitors,” Journal of Applied Electrochemistry, Vol. 131, No. 3, pp. 612-614, 1984
7. T. Ebel, F. Stippich, J. Behm, O. Magnussen and S. Lauterborn, US Patent 6942819, 2005
8. B. K. Bose and D. Kastha, “Electrolytic Capacitor Elimination in Power Electronic System by High Frequency Active Filters,” IEEE/IAS Annual. Meet. Conf. Rec., pp. 869-878, 1991
9. A. Lahyani, P. Venet, G. Grellet, and P. Viverge, “Failure prediction of electrolytic capacitors during operation of a switchmode power supply,”*IEEE Transactions on Power Electronics*, vol. 13, pp. 1199–1207, Nov 1998.

10. V. Vorperian., “Simplified analysis of pwm converters using model of pwm switch continuous conduction mode.” *IEEE Transactions on Aerospace and Electronic Systems*, p. 490496, May 1990.
11. Nichicon, “General Descriptions of Aluminum Electrolytic Capacitors,” http://www.nichicon.co.jp/english/products/pdf/aluminum.pdf, (Accessed on May 15, 2012)
12. K. Bruder, M. Intelmann, A. Ishikawa, U. Merker, A. Sautter, T. Suzuki, K. Wussow, “Conductive Polymer Dispersions for Aluminum Capacitors,” CARTS Europe, November 10-11, 2010, Munich, Germany
13. G.D. Rawlings, “New Family of Conductive Polymers For Solid Electrolyte Aluminum Capacitors,” CARTS Asia, October 9-13, 2006, Taipei, Taiwan
14. H. Yamamoto, M. Oshima, M. Fukuda, I. Isa, K. Yoshino, “Characteristics of Aluminium Solid Electrolytic Capacitors Using a Conducting Polymer,” Journal of Power Sources, Volume 60, Number 2, pp. 173-177, June 1996
15. Y. Kudoh, A. Akami, and Y. Matsuya, “Solid Electrolytic Capacitor with Highly Stable Conducting Polymer as a Counter Electrode,” Synthetic Metals, 102(1–3), pp. 973–974, 1999
16. A. Elschner , S. Kirchmeyer , W. Lövenich , U. Merker and K. Reuter, “ PEDOT: Principles and Applications of an Intrinsically Conductive Polymer,” CRC Press 2010, Print ISBN: 978-1-4200-6911-2, eBook ISBN: 978-1-4200-6912-9

17. B. K. Bose and D. Kastha, “Electrolytic Capacitor Elimination in Power Electronic System by High Frequency Active Filters,” IEEE/IAS Annual. Meet. Conf. Rec., pp.869-878, 1991
18. A. Lahyani, P. Venet, G. Grellet, and P. Viverge, “Failure prediction of electrolytic capacitors during operation of a switchmode power supply,”*IEEE Transactions on Power Electronics*, vol. 13, pp. 1199–1207, Nov 1998.
19. M.L. Gasperi, “Life Prediction Model for Aluminum Electrolytic Capacitors,” IEEE Industry Applications Conference, pp. 1347-1351, vol.3, 1996
20. A. Albertsen, “Electrolytic Capacitor Lifetime Estimation,” Jianghai Europe, Jan 2010
21. A. Zanobini, G. Iuculano and A. Falciani, “Automatic-Test Equipment for the Characterization of Aluminum Electrolytic Capacitors,” IEEE Transactions on Instrumentation and Measurement, vol. 55, pp. 682-688, April 2006
22. W. D. Greason and J. Critchley, “Shelf-life Evaluation of Aluminum Electrolytic Capacitors,” IEEE Trans. Components, Hybrids, and Manufacturing Technology, vol. 9, no. 3, pp. 293-299, September 1986
23. J. R. Celaya, C. Kulkarni, S. Saha, G. Biswas, K. Goebel, “Accelerated Aging in Electrolytic Capacitors for Prognostics,” Reliability and Maintainability Symposium (RAMS) Proceedings, pp. 1-6, 23-26 Jan. 2012
24. A. Dehbi, W. Wondrak, Y Ousten, Y. Danto, “High Temperature Reliability Testing of Aluminum and Tantalum Electrolytic Capacitors,” Microelectronics Reliability, Vol. 42, Issue 6, pp. 835–840, June 2002

25. A. Berduque, J. Martin, Z. Dou, R. Xu, “Low ESR Aluminum Electrolytic Capacitors for Mid-to-High Voltage Applications,” CARTS USA 2011
26. Z. Dou, R. Xu, A. Berduque, “The Development of Electrolytes in Aluminium Electrolytic Capacitors for Automotive and High Temperature Applications,” CARTS Europe 2008, 20-23 October
27. V. A. Sankaran, F. L. Rees, C. S. Avant, “Electrolytic Capacitor Life Testing and Prediction,” IEEE Industry Applications Conference, vol.2, pp. 1058 – 1065, 1997
28. M. Ue, M. Takeda, Y. Suzuki, S. Mori, “Chemical Stability of γ-Butyrolactone-Based Electrolytes for Aluminum Electrolytic Capacitors,” Journal of Power Sources, 1996
29. I. Szaraz, W. Forsling, “Interaction Between a Capacitor Electrolyte and γ-Aluminum Oxide Studied by Fourier Transform Infrared Spectroscopy”, vol. 57, pp. 622-627, June 2003
30. D. Liu, “Physical and Electrical Characterization of Aluminum Polymer Capacitors,” NASA Electronic Parts and Package Program, 2009
31. L. L. Macomber, “Solid Polymer Aluminum Capacitor Chips in DC-DC Converter Modules Reduce Cost & Size & Improve High-Frequency Performance,” Proceeding for the PowerSystems World Conference held in Rosemont, IL, September 2001
32. U. Merker, K. Wussow, W. Lovenich, “New Conducting Polymer Dispersions for Solid Electrolyte Capacitors,” 17-20 Oct 2005, CARTS Europe 2005

33. S. Garreau, G. Louarn, S. Lefrant, J. P. Buisson, and G. Froyer, “Optical Study and Vibrational Analysis of the poly(3,4-ethylenedioxythiophene) (PEDT),” Synth Met 101(1–3):312–313, 1999
34. A. Elschner, S. Kirchmeyer, W. Lövenich, U. Merker, K. Reuter, PEDOT Principles and Applications of an Intrinsically Conductive Polymer, CRC Press, Taylor and Francis Group, LLC, 2011
35. Conductive Polymer Aluminum Solid Capacitors OS-CON, Panasonic Technical Note
36. J. D. Prymak, Replacing MnO2 with Conductive Polymer in Tantalum Capacitors, CARTS Europe 1999
37. K. Bruder, M. Intelmann, A. Ishikawa, U. Merker, A. Sautter, T. Suzuki, K. Wussow, “Conductive Polymer Dispersions for Aluminium Capacitors,” 10-11 November Munich, Germany, CARTS Europe 2010
38. J. Lewis, Considerations for Polymer Capacitors in Extreme Environments, KEMET, 2013
39. S. Garreau, G. Louarn, J. P. Buisson, G. Froyer, and S. Lefrant, “In Situ Spectroelectrochemical Raman Studies of Poly(3,4-ethylenedioxythiophene) (PEDT), Macromolecules, 32 (20), pp 6807–6812, 1999
40. A. M. Nardes, On the conductivity of PEDOT:PSS thin films, Masters Thesis, Technische Universiteit Eindhoven, 2007
41. K. Nogami, K. Sakamoto, T. Hayakawa, M. Kakimoto, “The effects of hyperbranched poly(siloxysilane)s on conductive polymer aluminum solid electrolytic capacitors,” Journal of Power Sources, pp. 584–589, 2007

42. K. Kawano, R. Pacios, D. Poplavskyy, J. Nelson, D. D. C. Bradley, J. R. Durrant, "Degradation of Organic Solar Cells Due to Air Exposure," Solar Energy Materials and Solar Cells, pp. 3520-3530, vol. 90, December 2006
43. K. Chatterjee, D. Das, and M. Pecht, "Solving the Counterfeit Electronics Problem," Proceedings of Pan Pacific Microelectronics Symposium (SMTA), pp. 294-300, Hawaii, Jan 30-Feb 1, 2007
44. M. Pecht and S. Tiku, "Bogus: Electronic Manufacturing and Consumers Confront a Rising Tide of Counterfeit Electronics," IEEE Spectrum Vol. 43, No. 5, pp. 37 – 46, May 2006
45. B. Sood, D. Das and M. Pecht, "Screening for Counterfeit Electronic Parts," Journal of Materials Science: Materials in Electronics, Vol. 22, No. 10, pp. 1511-1522, 2011
46. Capacitor Plague, http://en.wikipedia.org/wiki/Capacitor_plague#cite_note-Feb2003Spectrum-8 (Accessed on August 2, 2013)
47. B. K. Bose and D. Kastha, "Electrolytic Capacitor Elimination in Power Electronic System by High Frequency Active Filters," IEEE/IAS Annual. Meet. Conf. Rec., pp. 869-878, 1991
48. A. Lahyani, P. Venet, G. Grellet, and P. Viverge, "Failure prediction of electrolytic capacitors during operation of a switchmode power supply,"*IEEE Transactions on Power Electronics*, vol. 13, pp. 1199–1207, Nov 1998.
49. V. Vorperian., "Simplified analysis of pwm converters using model of pwm switch continuous conduction mode," *IEEE Transactions on Aerospace and Electronic Systems*, p. 490496, May 1990.

50. A. M. R. Amaral, A. J. M. Cardoso, “A Simple Offline Technique for Evaluating the Condition of Aluminium-Electrolytic Capacitors,” IEEE Transaction on Industrial Electronics, Vol. 56, No. 8, pp. 3230-3237, August, 2009.
51. C. Kulkarni, G. Biswas, X. Koutsoukos, J. Celaya and K. Goebel, “Integrated diagnostic/prognostic experimental setup for capacitor degradation and health monitoring,” IEEE Autotestcon, pp. 1-7, 13-16 Sept 2010
52. “Quake contributes to higher prices and longer leadtimes for some components,” Digikey Corporation, April 28, 2011, http://www.digikey.com/us/en/purchasingpro/articles/conditions/quake-contributes-to-higher-prices-longer-leadtimes.html?WT.z_pp_page_sec=WH (Accessed on July 28, 2013)
53. Nichicon Technical Notes, “General Descriptions of Aluminum Electrolytic Capacitors”.
54. R. Dapo, “Electrolyte containing a novel depolarizer and an electrolytic capacitor containing said electrolyte,” U.S. Patent 5,175,674, December 29, 1992
55. A. Albertsen, “Electrolytic Capacitor Lifetime Estimation,” Jianghai Europe, Jan 2010,
56. G. Behrend - US Patent 5055975, 1991
57. T. Morimoto, Y. Hamatani, M. Yoshitake and H. Yamada, US Patent 4831499, 1979

58. A.D. Cross, R.A. Jones, An introduction to practical infra-red spectroscopy, 3rd edn. (Butterworths Scientific Publications, USA, 1969

59. M. R. Alexander, G. E. Thompson and G. Beamson, "Characterization of the Oxide/Hydroxide Surface of Aluminium using X-ray Photoelectron Spectroscopy: a Procedure for Curve Fitting the O 1s Core Level," Surface and Interface Analysis, pp. 468–477, 2000

60. C. A. Harper, "Passive Electronic Component Handbook," McGraw-Hill Professional, 2nd edition, June 1, 1997

61. Epcos, "General Technical Information of Al Electrolytic Capacitors," Dec 2010, Accessed on June 3, 2010

62. P. M. Deeley, FaradNet, http://www.faradnet.com/, Electrolytic Capacitors, Accessed on June 3, 2010

63. Cornell Dubilier, "Aluminum Electrolytic Capacitor Application Guide," Accessed on September 6, 2011

64. J. L. Stevens, J. S. Shaffer, and J. T. Vandenham, "The Service Life of Large Aluminum Electrolytic Capacitors: Effects of Construction and Application," IEEE Trans. Ind. Appl., Vol. 38, No. 5, Sep./Oct. 2002, pp. 1441-1446

65. M. Gasperi, "Life Prediction Model for Aluminum Electrolytic Capacitors," 31st Annual Meeting of the IEEE-IAS, Vol. 4, October, 1996, pp. 1347-1351

66. M. Gasperi, "A method for predicting the expected life of bus capacitors," in Conference Rec. IEEE-IAS Annual Meeting, Oct. 1997, pp. 506–512

67. S. G. Parler Jr., "Deriving Life Multipliers for Electrolytic Capacitors," IEEE Power Electronics Society Newsletter, Vol. 16, No. 1, Feb. 2004, pp. 11–12

68. United Chemi-Con Inc., “Understanding Aluminum Electrolytic Capacitors,” Second Edition, Rosemont, IL, 1995

69. J. A. Lauber, “Aluminum electrolytic capacitors—Reliability, expected life and shelf capability,” Sprague Elect., West Adams, MA, Sprague Technical Paper TP83-9, 1985

70. Philips Components Catalog PA01-A, Philips N.V., Eindhoven, The Netherlands, 1994, pp. 125–128

71. J. M. Albella, C. Gomez-Aleixandre, J. M. Martinez-Duart, “Dielectric characteristics of miniature aluminum electrolytic capacitors under stressed voltage conditions,” Journal of applied electrochemistry, Volume 14, Number 1,1984, pp. 9-14

72. A. Zanobini, G. Iuculano and A. Falciani, “Automatic-Test Equipment for the Characterization of Aluminum Electrolytic Capacitors,” in IEEE Transactions on Instrumentation and Measurement, vol. 55, April 2006, pp. 682-688.

73. V. A. Sankaran, F. L. Rees, C. S. Avant, “Electrolytic Capacitor Life Testing and Prediction,” IEEE Industry Applications Conference, vol.2., 1997, pp. 1058 - 1065

74. W. D. Greason and J. Critchley, “Shelf-life Evaluation of Aluminum Electrolytic Capacitors,” IEEE Trans. Components, Hybrids, and Manufacturing Technology, vol. 9, no. 3, Sep. 1986, pp. 293-299

75. M.L. Tsai, Y.F. Lu, J.S. Do, “High-performance electrolyte in the presence of dextrose and its derivatives for aluminum electrolytic capacitors,” Journal of Power Sources, 2002, pp. 643-648

76. M. Ue, M. Takeda, Y. Suzuki, S. Mori, "Chemical Stability of Gamma-Butyrolactone-Based Electrolytes for Aluminum Electrolytic Capacitors," Journal of Power Sources, vol. 60, June 1996, pp. 185-190
77. L. J. Hart, D. Scoggin, "Predicting Electrolytic Capacitor Lifetime," Power Techniques Magazine, pp. 24-29, October 1987
78. Z. Dou, R. Xu, A. Berduque, "Low ESR Aluminum Electrolytic Capacitors for Mid-to-High Voltage Applications," CARTS USA 2011
79. Z. Dou, R. Xu, A. Berduque, "The Development of Electrolytes in Aluminium Electrolytic Capacitors for Automotive and High Temperature Applications," CARTS Europe 2008
80. R. Xu, A. Berduque, Z. Dou, "Further Electrolyte Development for High Temperature Aluminum Electrolytic Capacitors," CARTS USA 2009
81. J. K. Chang, C. M. Liao, C. H. Chen and W.T. Tsai, "Material Characteristics and Capacitive Properties of Aluminum Anodic Oxides Formed in Various Electrolytes," Journal of Materials Research, Vol. 19, Issue 11, 2004
82. J. K. Chang, C. M. Lin, C. M. Liao, C. H. Chen and W.T. Tsai, "Effect of Heat-Treatment on Characteristics of Anodized Aluminum Oxide Formed in Ammonium Adipate Solution," Journal of Electrochemical Society, vol. 151, 2004
83. O. Klug, A. Bellavia, "High Voltage Aluminum Electrolytic Capacitors: Where is the Limit?," Technical Paper, Evox Rifa, 2001